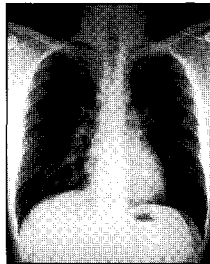


i/55x

Pattern recognition in diagnostic imaging

Peter Corr

MChB, FFRad (D) SA, FRCR
Professor of Radiology
Nelson R Mandela School of Medicine
University of Natal,
Durban
South Africa



In collaboration with

*Wilfred Peh, Wong Siew Kune, Leonie Munro, William Rae, Fei Ling Thoo, Lai Peng Chan,
Lesley A. Goh, Lawrence Hadley, Malai Muttarak, Swee Tian Quek.*

Medical Artist: Merle Conway

Photography: NV Chetty, S Ezekiel



Diagnostic Imaging and Laboratory Technology
Essential Health Technologies
Health Technology and Pharmaceuticals
WORLD HEALTH ORGANIZATION
GENEVA

WHO Library Cataloguing-in-Publication Data

Pattern recognition in diagnostic imaging / Peter Corr ; in collaboration with Wilfred Peh ... [et al.]

1.Diagnostic imaging - methods 2.Pattern recognition 3.Radiography, Thoracic -methods 4.Musculoskeletal system - radiography. 5.Radiography, Abdominal-methods 6.Manuals I.Corr, Peter II.Peh, Wilfred.

ISBN 92 4 154632 8

(NLM classification: WN 180)

This publication is a reprint of material originally distributed as WHO/DIL/01.2

© World Health Organization 2001

Reprinted 2003 (Twice)

All rights reserved. Publications of the World Health Organization can be obtained from Marketing and Dissemination, World Health Organization, 20 Avenue Appia, 1211 Geneva 27, Switzerland (tel: +41 22 791 2476; fax: +41 22 791 4857; email: bookorders@who.int). Requests for permission to reproduce or translate WHO publications - whether for sale or for noncommercial distribution - should be addressed to Publications, at the above address (fax: +41 22 791 4806; email: permissions@who.int).

The designations employed and the presentation of the material in this publication do not imply the expression of any opinion whatsoever on the part of the World Health Organization concerning the legal status of any country, territory, city or area or of its authorities, or concerning the delimitation of its frontiers or boundaries. Dotted lines on maps represent approximate border lines for which there may not yet be full agreement.

The mention of specific companies or of certain manufacturers' products does not imply that they are endorsed or recommended by the World Health Organization in preference to others of a similar nature that are not mentioned. Errors and omissions excepted, the names of proprietary products are distinguished by initial capital letters.

The World Health Organization does not warrant that the information contained in this publication is complete and correct and shall not be liable for any damages incurred as a result of its use.

Designed by minimum graphics in New Zealand
Typeset by Best-set in Hong Kong
Printed in Malta By Interprint Ltd.

Contents

-- JAN 2004

Preface	v
Foreword	vii
Definitions	x
<hr/>	
Part 1. Technique, quality control and radiation protection	1
Chapter 1. Image quality optimisation and control	3
Chapter 2. Radiation protection in radiological practice	16
Chapter 3. Contrast media in imaging	21
Chapter 4. Digital imaging and telemedicine	23
<hr/>	
Part 2. Chest imaging patterns	27
Chapter 5. The normal chest radiograph	29
Chapter 6. Pulmonary infection	34
Chapter 7. Lung cancer	40
Chapter 8. Pulmonary hypertranslucency and cystic lungs	45
Chapter 9. Pleural and extra pleural disease	51
Chapter 10. Rib lesions	56
Chapter 11. Chest trauma	59
Chapter 12. Pulmonary AIDS	65
Chapter 13. Paediatric chest	68
Chapter 14. Cardiac disease	73
Chapter 15. Mediastinal masses	77
Chapter 16. Diaphragm lesions	79
Chapter 17. Pneumoconiosis	80
<hr/>	
Part 3. Musculoskeletal patterns	83
Chapter 18. Approach to focal bone lesions	85
Chapter 19. Periosteal reactions	91
Chapter 20. Extremities trauma	99
Chapter 21. Fractures—classification, union, complications	114
Chapter 22. Spinal trauma	124
Chapter 23. Facial and pelvic trauma	133
Chapter 24. Bone infections	141

Part 4. Gastrointestinal and urinary tract patterns	147
Chapter 25. Plain abdominal radiographs	149
Chapter 26. The acute abdomen	151
Chapter 27. Gastrointestinal contrast studies	159
Chapter 28. Paediatric abdomen	178
Chapter 29. Urinary tract imaging	183
Acknowledgements	205

Preface

As modern, high technology based diagnostic imaging is moving increasingly into therapeutic medicine, and molecular imaging is becoming daily routine, it is important to remember that thousands of hospitals and medical institutions worldwide do not even have possibilities to perform the most basic examinations. Today, few other areas of medicine experience such a rapidly growing gap between what might be technically possible, e.g., what can be done in highly developed, rich countries compared to what is the reality in many less fortunate areas of the world.

As the ultimate target for the World Health Organization is to provide *Health For All*, it is with great pleasure and sincere gratitude to Professor Corr, his staff and co-authors that this book on Pattern Recognition in Diagnostic Imaging is now being published and distributed. It aims in a simple, but precise way at assisting medical professionals doing a tremendous work to save lives and reduce suffering in countries where diagnostic imaging has not yet reached the stage of molecular imaging.

We would warmly recommend that this book should not be put on a shelf or into a locker, but be used by everybody whose obligation it is to prescribe, perform, or interpret simple, but often life-saving diagnostic imaging procedures especially in locations where the presence of qualified and fully trained specialists would be a rare exception.

The book is developed and published as a WHO Document under the umbrella of the Global Steering Group for Education and Training in Diagnostic Imaging. For further information, please contact:

Team for Diagnostic Imaging and Laboratory Technology,
World Health Organization
20, Avenue Appia
CH-1211 GENEVA 27, SWITZERLAND

Fax: +41 22 791 4836; e-mail: ingolfsdotting@who.int

Geneva, 30 June 2001
Harald Ostensen, MD

Foreword

Imaging is currently being performed and interpreted by radiographers/technologists and primary care physicians/hospital medical officers in many developing countries. Many primary care physicians have had little or no training in the interpretation of images, both radiographic and sonographic. Radiographers are trained in producing images but often do not have the background in medicine to interpret images with confidence. This book seeks to bridge this gap by providing images of common pathologies seen in many developing countries in a pattern format. The pattern recognition format has been used successfully by both national and international radiographic societies to educate and train radiographers working in regions where radiology advice or services are unavailable.

We hope this book serves you well in your daily work which involves imaging.

Peter Corr

Durban 2001

Authors

Lai Peng Chan MBBS, FRCR

Registrar, Department of Diagnostic Radiology, Singapore General Hospital, Singapore

Peter Corr MBChB, FFRad (D) SA, FRCR

Professor of Radiology, Nelson R Mandela School of Medicine, University of Natal,
Durban, South Africa

Lesley A Goh MBBS, FRCR

Registrar, Department of Diagnostic Imaging, Tan Tock Seng Hospital, Singapore

Lawrence Hadley MBChB, FRCS (Edin)

Professor of Paediatric Surgery, Nelson R Mandela School of Medicine, University of
Natal, Durban, South Africa

Wong Siew Kune MBChB, FRCR

Associate Consultant, Department of Diagnostic Radiology, Singapore General Hospital,
Singapore

**Leonie Munro Nat Dip Radiography (D), MA (Unisa), Dip Public Admin-postgrad
(UDW), Cert for trainers (Unisa)**

Chief Tutor School of Radiography, King Edward VIII Hospital, Durban, South Africa

Malai Muttarak MD

Professor of Radiology, Department of Radiology, Chiang Mai University Medical
School, Chiang Mai, Thailand

Wilfred C G Peh MBBS, MD, FRCR, FRCPE, FRCPG

Senior Consultant, Department of Diagnostic Radiology, Singapore General Hospital,
Singapore

Swee Tian Quek MBBS, FRCR

Consultant, Department of Diagnostic Imaging, National University of Singapore,
Singapore

William Rae MBChB (Wits) PhD (OFS)

Senior Medical Physicist, Addington Hospital, Durban

Fei Ling Thoo MBBS, FRCR

Consultant, Department of Radiology, Changi General Hospital, Singapore

Definitions

ALARA keeping radiation dose 'as low as reasonably achievable'

AP anteroposterior means patient is facing the X-ray tube/beam (see PA)

Atelectasis radiographic pattern to describe (i) incomplete expansion of lungs at birth, or (ii) collapse of adult lung usually with limited re-expansion

Baud number of bytes transmitted in one second in telemedicine

Bit smallest unit of digital information

Byte a group of 8 bits used to transmit a value of character

Collapse radiographic pattern of partially or completely airless lung due to some form of obstruction

Consolidation a region of lung opacification following pneumonia with air bronchograms. Strictly a pathological term for lobar pneumonia.

CTR cardio-thoracic-ratio is the ratio of the measurement of widest transverse diameter of the heart on a chest radiograph versus the widest transverse ratio of the thoracic cage

Decubitus view patient lying on either left or right side and radiograph is taken using a horizontal X-ray beam at right angles to the cassette placed either behind the patient (PA decubitus) or in front of patient (AP decubitus)

DICOM a standard allowing interfacing of digital imaging devices with other digital devices

Digitise process to convert analogue data or images into digital data

Effusion fluid in a cavity, e.g. pleural cavity

FFD focal film distance, i.e. distance from source of X-ray beam to the film

Horizontal beam/shoot-through film taken using horizontal X-ray beam at right angles to the cassette; patient can be supine, prone, semi-erect, lateral

ISDN integrated system digital network

IVU intravenous urography

KUB plain-film-radiograph of abdomen; i.e. kidneys to bladder region

Lossless compression there is no alteration of original image after reconstruction in digital imaging

Osteopaenia decreased bone density on a radiograph.

PA posteroanterior view with X-ray beam entering from behind the patient and emerging through anterior part because patient is positioned facing cassette

Sclerosis increased bone density or opacity on the radiograph

PART 1



TECHNIQUE, QUALITY CONTROL AND RADIATION PROTECTION



CHAPTER 1

Image quality optimisation and control*Leonie Munro***Introduction**

What is pattern recognition in imaging and what are the factors that impact on this recognition? Pattern recognition may be defined as being able to recognise normal anatomical and physiological appearances on an image and those variations of appearances, which may indicate pathology. This implies that certain criteria should be met, to be competent in pattern recognition. Firstly a person who performs pattern recognition should have a fair amount of expertise in medical imaging and knowledge of radiographic anatomy and normal variants so as to identify variations that may indicate pathology. This is the overarching aim of this book hence the many aspects of pattern recognition are fleshed out in the other chapters. This chapter concentrates on factors that impact on image quality. It is not easy to clearly define optimal image quality. In theory optimal image quality allows one to make accurate diagnosis. This is an ideal as we also should consider dose to patients in keeping with the ALARA principle (as low as reasonably achievable). There are times when an image is suboptimal but not unacceptable. In other words slight deviations in image quality may not have a significant impact for pattern recognition. Unacceptable images may cause one to miss a fracture or a destructive lesion. To repeat or not to repeat depends on the reasons for the examination and whether one can confidently perform pattern recognition to make a diagnosis. Such a decision is usually based on experience and a set procedure when evaluating images. Examples of unacceptable radiographs are included in this chapter to highlight the importance of optimal image quality. If an image is unacceptable then the radiation received by the patient has no benefit. Thus there are some important factors and/or basic tests that should be considered at all times.

It would be difficult to confidently perform pattern recognition if the image quality of a dynamic image or hard copy is not of an acceptable standard. There is consensus that optimal image quality entails meeting medico-legal requirements, such as each image to contain the patient's details, date of examination, anatomical marker, and adequate visualisation of radiographic anatomy/signs. This means that patient positioning should be correct for each projection, that the images are not blurred and that optimal image density is visualised. Image quality thus depends on correct radiographic techniques being used for each projection, correct selection of exposure factors and use of suitable imaging systems which are of an optimal standard. Just to mention that it is usually necessary to do two projections/views, usually at right angles. The patient/area of interest should be in accordance with recommended projections to ensure that all relevant anatomical parts are visualised (fig 1.1a). For example in skull radiography the patient's head should be straight to allow one to comment of symmetry of the skull bones (fig 1.1b). Chest radiographers should always be exposed on full inspiration to prevent incorrect diagnosis due to unacceptable radiography (fig 1.2). Apart from positioning criteria the following are considered to have an impact on image quality.

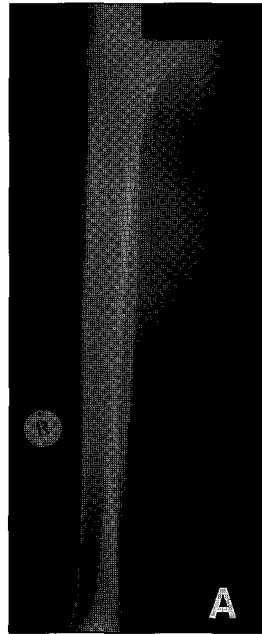


Fig 1.1a
 Poor radiographic technique.
 Ankle and knee joints not on
 film.

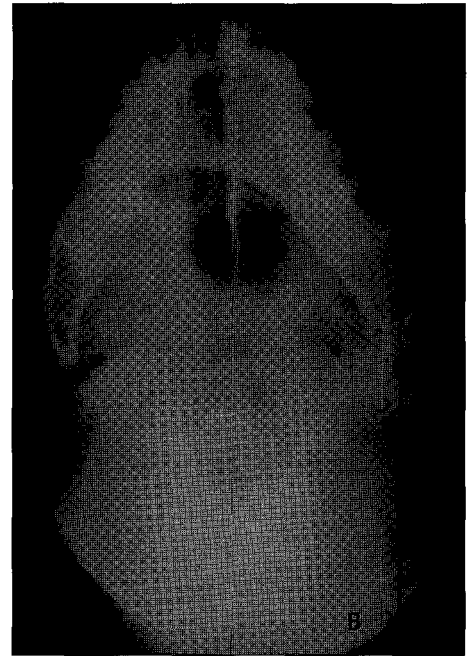
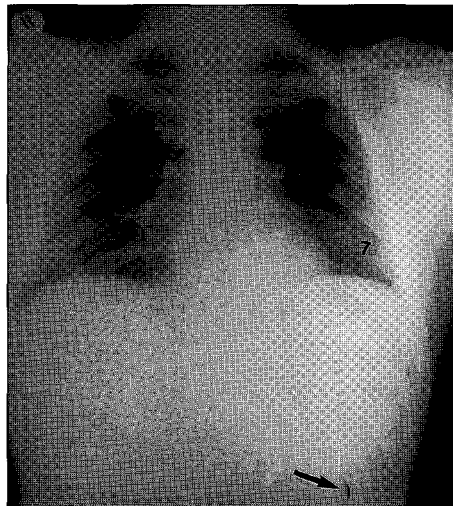


Fig 1.1b
 Poor patient positioning as skull rotated.

Fig 1.2
 Poor inspiration PA
 chest as only shows
 7 ribs. Arrow points
 to crimp mark
 caused by poor film
 handling (fingernail
 pressure).



Care and maintenance of imaging equipment and accessories, and some QA tests

Care and maintenance of imaging equipment is normally being promoted by national authorities to ensure that staff, patients, and members of the public do not receive unnecessary radiation doses. Well maintained equipment benefits service delivery because repeat radiographs, due to malfunctioning units, poorly calibrated generators, and so forth, decrease. This means that unnecessary dose to patients is also reduced. Many checks can be done by radiographers whilst others require sophisticated test tools which are usually expensive and/or require the expertise of physicists (Borras, 1997). Reject

analysis should be carried out regularly to determine reasons for poor quality radiographs. Some basic tests can be done to minimise rejects.

Safelight tests

Unwanted film blackening is fog which reduces radiographic contrast. It is important that darkroom safelighting does not fog unexposed and/or exposed films. Safelight tests should be done at least every six months to ensure that safelights are in proper working order.

Equipment for the tests

An acceptable film/screen light-tight cassette; black paper one-half the size of the cassette (2 sheets of black paper needed), clock/timer with second hand, box of unopened radiographic film, and general X-ray unit capable of selection of low mAs.

Step 1: Switch off all lights in the darkroom and cover lights on the processor. In total darkness place an unexposed film in the light-tight cassette containing intensifying screens.

Step 2: Expose the loaded cassette to radiation to obtain approximately 1 density. Suggested exposure factors—half mAs of finger exposure (see Annexure 2—these factors are appropriate for use with 400 speed system. Should a slower system be used then mAs adjustments to be made.) Working tip: If it is not possible to select low mAs then increase FFD using the inverse square law principle to determine mAs as per FFD changes.

Step 3: In total darkness in the darkroom open the cassette and using the black paper block off half of the exposed film. NB this section of the film to remain covered during the test. The density of the covered part of the film is used to see if the safelights are functioning correctly. Place the other sheet of paper on the other half of the film and move the paper down to uncover part of the unexposed film. Switch on a safelight and expose the uncovered film portion for 60 seconds. Move this sheet of paper off the film and expose the remaining uncovered film half to a further 60 seconds.

Step 4: Process the film which has half exposed to radiation only and the other half to radiation plus light from the safelight.

Step 5: Check the density of the film (fig 1.3). The film- half that was covered throughout the test should have a density of approximately 1. Acceptable density limits when comparing the half not exposed to the safelight and the side exposed to the safelight should not exceed 0,02 for 60 seconds (Barber & Thomas, 1983: 176).

The above steps to be repeated to check each safelight in each darkroom. Should there be unacceptable density/fogging then check safelight position: correct height from working surface should not be less than 120 centimeters. Safelight filters and wattage of safelight bulbs to be checked so that the fault is then corrected. The indicator light on the processor should be checked as per the above steps. Indicator light to be uncovered and safelights switched on. Density should not exceed 0,05 for a 2 minute exposure to indicator light plus safelights.

Careful film-handling and film storage

Note that exposed film is more sensitive to light thus care should be taken when handling film. Crimp marks from excessive handling may be of concern. A problem that has recently surfaced is that of darkroom personnel/radiographers using cell phones whilst handling film in the darkroom (fig 1.4).

Film should always be handled with clean hands and in a dust free environment. Film to

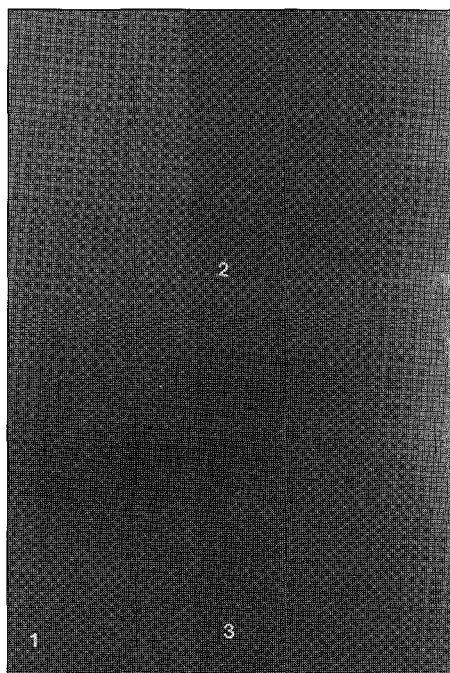


Fig 1.3

*Safelight test:
1 = film-half only
exposed to
radiation to obtain
approximately
density 1. Sections
2 & 3 = film
exposed to safelight
plus radiation.
Section 2 exposed
to safelight for 2 ×
60 seconds, section
3 for 60 seconds.
Both also exposed
to radiation.
Obvious increased
density due to safe-
light; this exceeds
0,02 density limit
compared to 1.*

Fig 1.4
Example of film-fogging caused by LED of cell phone in a darkroom.

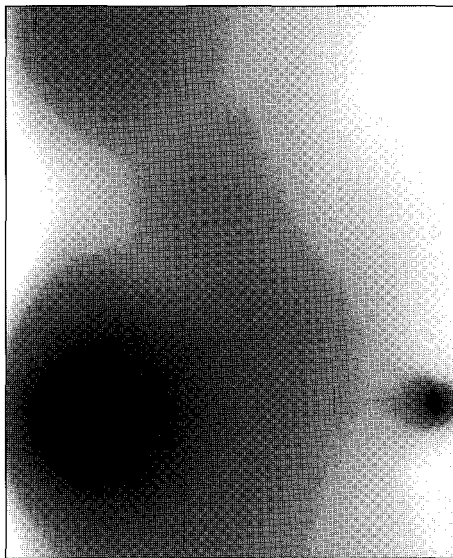
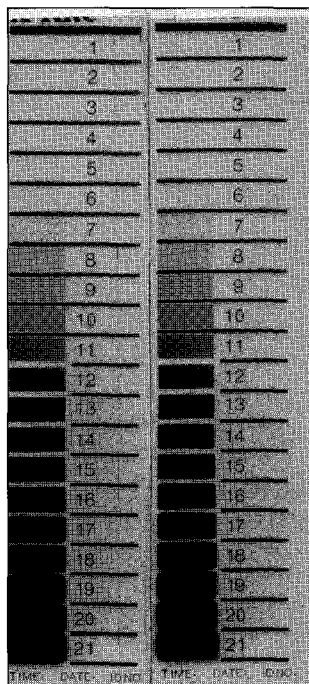


Fig 1.5
Sensitometric strips showing steps 1 to 21.



readings to be recorded to check with thermometer readings. This is done to ensure that the gauge is accurate.

Step 3: Process exposed film.

Step 4: Using a densitometer read densities of each step.

Step 5: The sensitometric step with the density closest to 1, 20 (mid-density) to be used to determine speed index. If sensitometric step 9 has density closest to 1,20 (including base fog) then all subsequent readings for speed index to be at this sensitometric step (ie step 9) for all future films used for processor control.

Step 6: On chart record temperature, date and base fog reading.

Step 7: Plot position for speed index obtained in the above step.

be stored in boxes in cool room with good air circulation. Boxes of film must never to be stacked on top of each other as this will cause marks on the films.

Processor control

This quality control method should be done for all processors to reduce unnecessary repeats caused by processing factors, such as exhausted chemistry, incorrectly mixed chemistry, and incorrect replenishment. Monitoring film quality due to processing factors means that assessment of film contrast, film speed and base fog is done based on an objective method.

Equipment required

A sensitometer to expose film to different light intensities in steps (fig 1.5); a densitometer to measure optical density of selected sensitometric steps, a non-mercury thermometer to manually check the temperature of the chemistry, and a box of unexposed film and sheets of processing control charts or graph paper.

Step 1: Under safelight conditions expose one film to the sensitometer. It is important that blue light be used for monochromatic (blue sensitive film) and green light for orthochromatic film. Select appropriate switch on the sensitometer. Note that some sensitometer only produce blue light thus can only be used with blue sensitive film. Process film after checking temperature of chemistry as per step 2.

Step 2: Temperature of chemistry to be taken using the thermometer. Temperature gauge

PROCESSOR PERFORMANCE LOG

MONTH: _____

PROCESSOR TYPE: _____

PROCESSOR LOCATION: _____

DAY

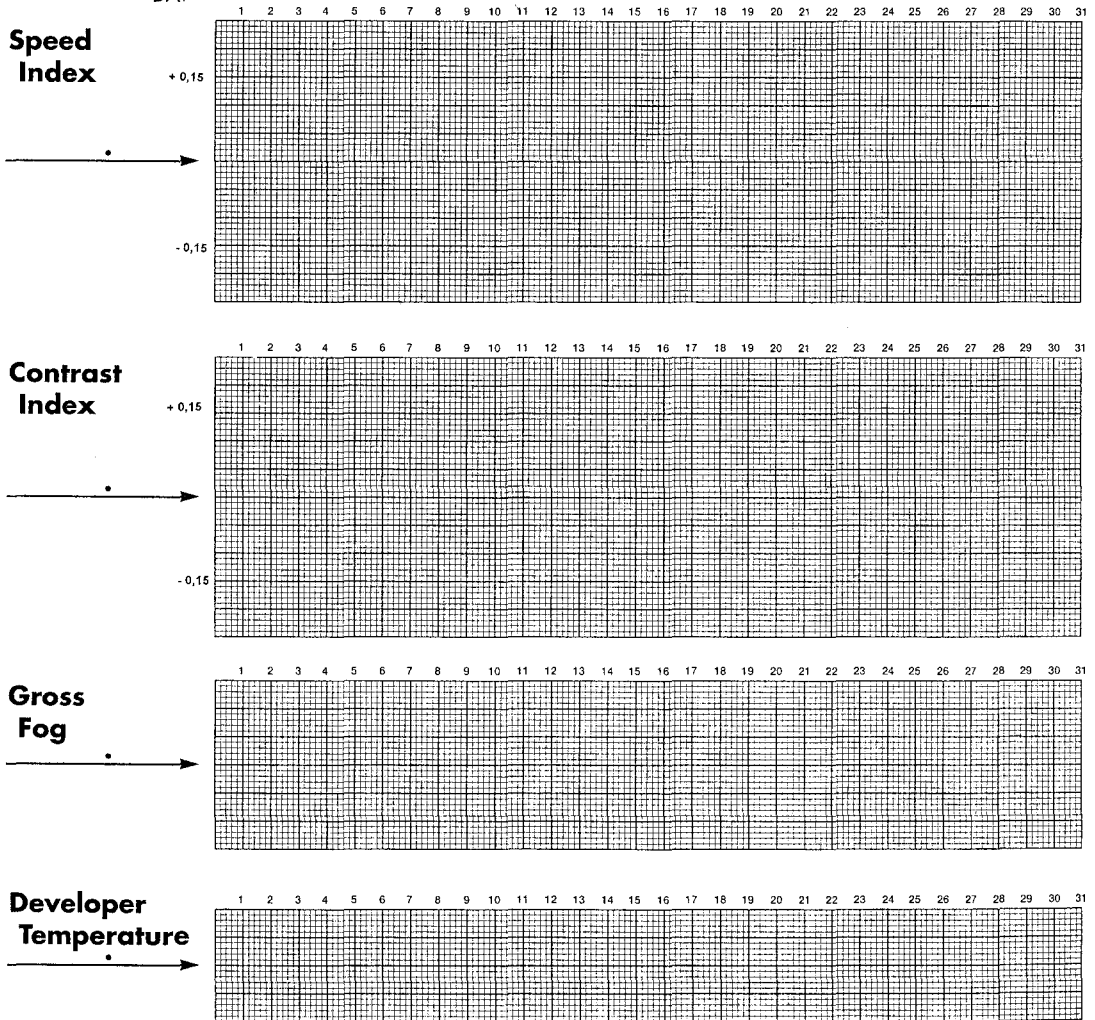


Fig 1.6a
Example of blank graph paper for processor monitoring.

Steps for the test

Place the cassette on the table and centre primary beam to center of cassette. Open light-beam diaphragms to set measurements—suggest 30×30 cms (note readings on the scale). Ensure FFD is at 100 cms or higher. Record this measurement. Place a coin in each corner of the light square and place a metal corner clip/allan key exactly at the edge of each corner. Position L or R marker at center of beam. Expose the cassette: suggest 50 kVp and 4 mAs for 200 speed system. Process the film (fig 1.8). The suggested performance criterion is $\pm 2\%$ of source to image distance. If FFD is 100 cms then upper limits of difference between light field edges and edges of primary beam radiation visualised on the film should not exceed 2% of 100 cms .ie 2 cms (Borras, 1997: 253). This will entail measuring the area of light beam based on position of the

Step 8: For 5 consecutive days repeat the preceding steps to obtain average density at sensitometric step 9. This value will be the control speed index against which all future sensitometric films will be compared.

Step 9: Plot average speed index on chart/graph paper as obtained over the five days.

Step 10: Draw 2 lines above and below the speed index. One parallel line to be +0,15 of speed index and the other to be at -0, 15 from the speed index. Deviations outside these 2 lines means that there is an unacceptable processor problem. For example replenishment may have been decreased, the temperature may have decreased/increased, and so forth.

NB: Base fog reading of each film, the date the test was done, and temperature of chemistry to be recorded on the chart. Working tip: Always do processor control at the same time.

Some firms supply pre-exposed sensitometric films but it is important to only use the film within a given period because with time film fog increases. If a densitometer is not available then do visual checks by placing the strips on an illuminator but ensure that all extraneous light is masked off and ambient (overhead) light switched off. Visual comparisons are a crude method but preferable to no checks at all. Some film suppliers have facilities to read film for customers. Suggestion: find out from film supplier whether such facilities are available. Arrangements could be made to post batches of film strips to the supplier. Recommendations: density readings to be written next to each sensitometric step on each film then this should allow one to be compared with visual comparisons. However the proper method of processor control should where possible be used for valid objective testing to enhance processor control results which enables speedy problem solving (fig 1.6a, 1.6b).

● **Film-screen contact test**

It is essential that images be obtained with good film-screen contact. Poor film-screen contact causes loss of information which may cause inaccurate pattern recognition. The film-screen contact test tool is readily available but a bit expensive. To perform the test place the contact mesh tool (wire mesh encased in perspex) on the top of the suspect cassette containing an unexposed film. Centre to center of cassette, collimate to cover cassette. Make sure that table on which the cassette is placed and the central ray are at right angles. Expose the test tool using approximately 55–60 kVp and 4 mAs (for 200 speed system) and 100 cms Focal film distance. Process the film and view at a distance of 150–180 cms to evaluate the sharpness of the wire mesh. Poor contact is seen as a “blurred” outline (fig 1.7). Poor film-screen contact usually occurs when a cassette gets dropped when excessive force is used during handling.

● **Collimator-beam alignment test**

This test should be done at least every month to check proper alignment of collimator and primary beam as daily use of the collimator contributes to poor alignment of the light beam and primary beam. This in turn causes suboptimal positioning as it may be difficult to accurately centre as per routine techniques.

Equipment for the test

35 × 43 cassette or smaller 1 loaded with unexposed film. Four coins/steel washers and metal clips/allan keys. Lead markers (L & R).

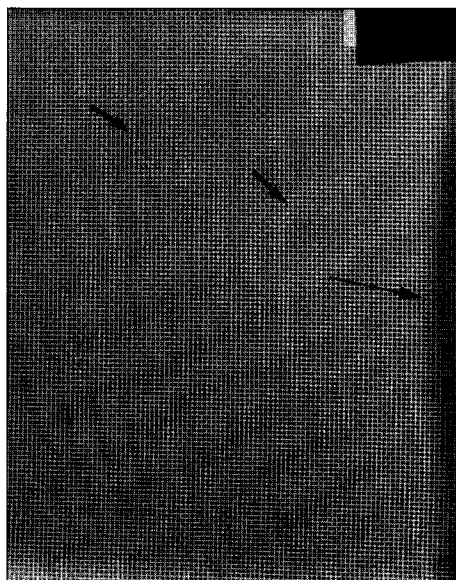


Fig 1.7
Film-screen contact test: arrows show areas of poor contact.

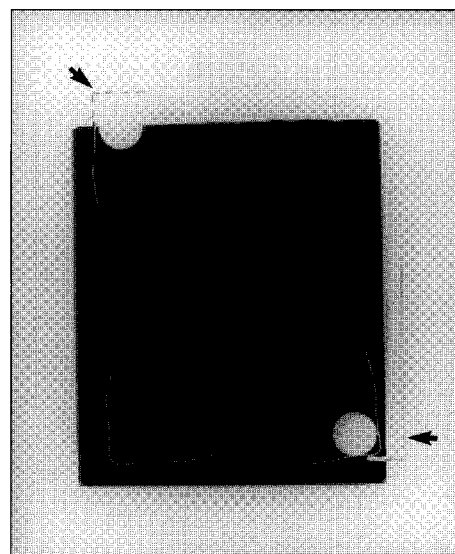
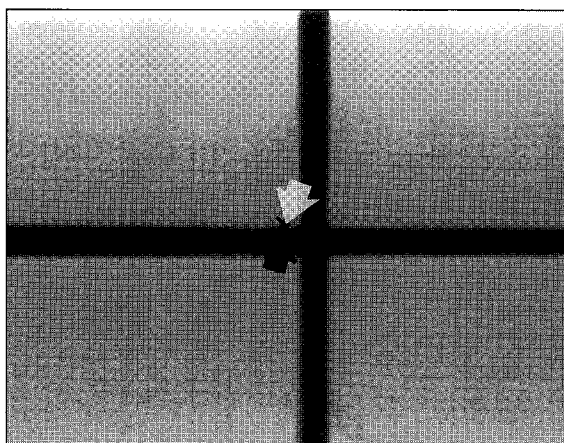


Fig 1.8
Two fields do not match; arrows show actual light-beam edges. Difference within the acceptable range of not more than 2% of FFD.

Fig 1.9
Arrows indicate middle of film; cross and film-centre not aligned.



difference in densities is not very marked; we perceive shades of grey. This means that at times a short scale contrast image may be needed for diagnostic purposes. A typical example is soft tissue thighs to visualise low density calcification for query cysticercosis. Kilovoltage selection of approximately 65–75 is usually recommended for visualisation of renal size, shape, and position. On the other hand >110kVp is required to adequately visualise the gastric-intestinal-tract

when doing contrast studies. Chest radiography should always be performed using moderately high to high kVp (fig 1.10a–1.10g).

Image sharpness refers to the amount of detail that we can see when viewing an image. Good film-screen contact enables high image sharpness. Detail screens are used to visualise fine detail but this results in additional dose to the patient due to mAs adjustments (fig 1.11 and fig 1.12).

- There are several factors that effect contrast and sharpness. Image contrast is broadly divided into three categories: subjective, subject/patient, and objective. Image sharpness is dependent upon geometric factors, movement factors, and systems factors. The most important factor influencing contrast is kilovoltage. Some radiographers make use of a fixed Kv and adjust mAs to suit different types of patients and/or pathology. Most modern units have automatic exposure devices which are programmed for the various anatomical regions. What one has to consider is dose to patients thus it should be borne in mind that high mAs selections result in the patient receiving additional radiation. Selection of the fastest film-screen

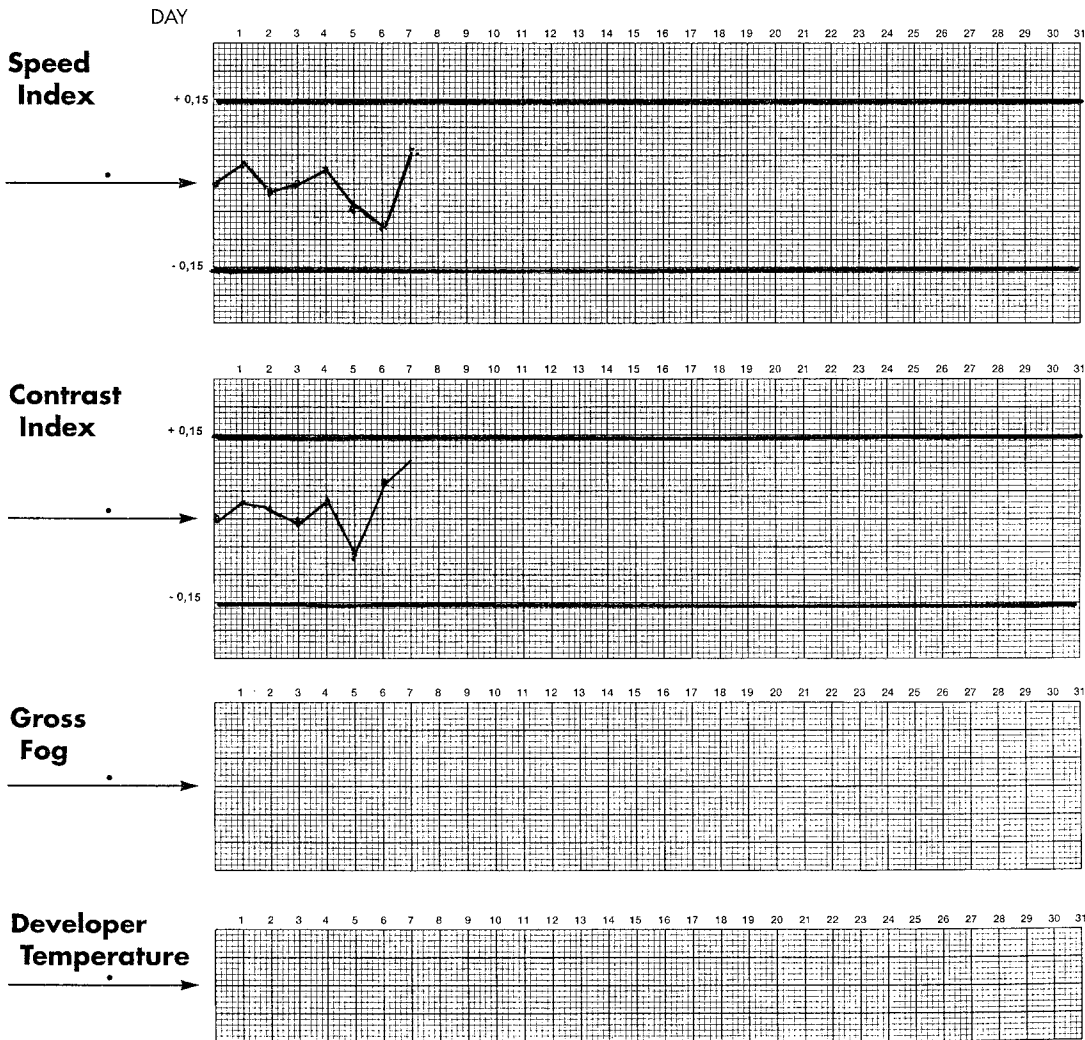


Fig 1.6b
Parallel lines above and below speed and contrast indices.

coins and metal clips and then comparing this measurement with total area of film-blackening to establish performance criteria.

● Test to check alignment of beam

This simple test can be done by placing a cassette loaded with an unexposed film on the table. Reduce lateral diaphragms to a slit. Close the other diaphragms. Centre to cassette and expose using 60 kVp and 4 mAs. Close these diaphragms and open the others to a slit and expose again. Process the film and bend in half to check that exposed “cross” (fig 1.9) is in the middle of the film. If there is not proper alignment check that the tube is straight so that the primary beam is vertical at 90 degrees to the cassette/table top. This test can also be used alignment of central ray to the bucky tray.

Factors relating to contrast and sharpness of the image

Contrast refers to the difference in density (film blackening) of two areas. To put it simply an image that only has two densities/tones will have high contrast as it only has a short scale such as a black/white image. Long scale contrast occurs when the

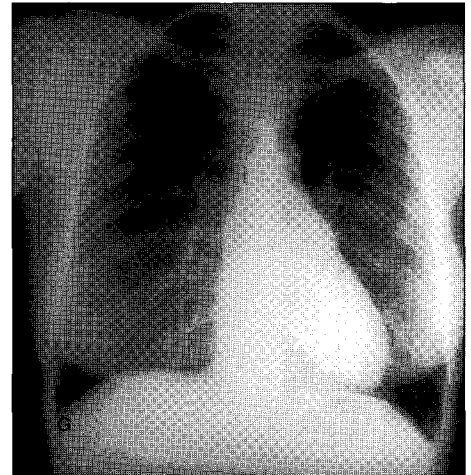
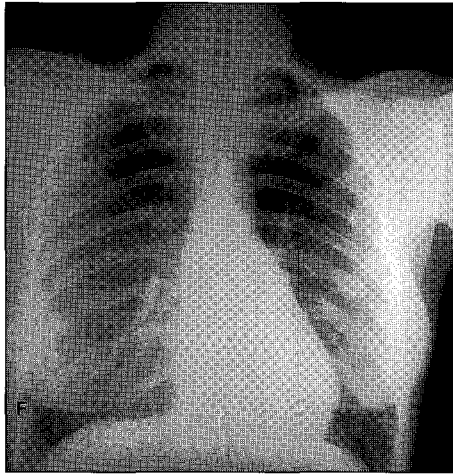
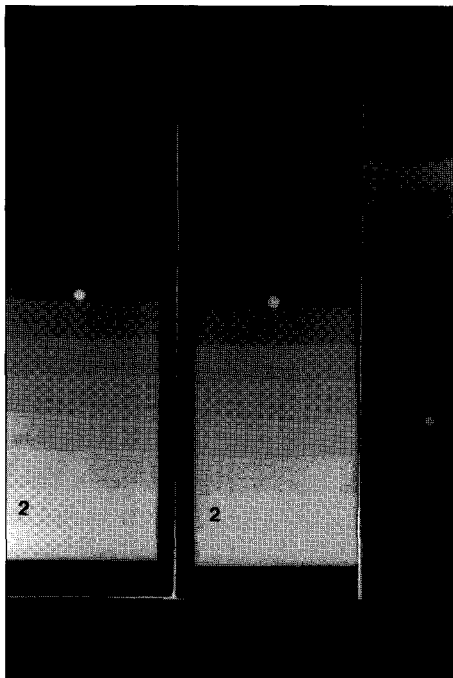


Fig 1.10f, g

PA chest of same patient. Film (f) taken using 75 kV. Film (g) taken using 110 kV and 4 mAs. Note improved visualisation of entire lung-fields and good inspiration.

Fig 1.11
Example of different densities of calibrated step-wedge. Step-wedge of Right not same as the other two. Note ball-bearing taped on step 8 to align similar density steps. On right step 4/5 aligned to match steps of the other two. Right step-wedge of a fast system thus if system on Left is used then mAs has to be adjusted as per scale in Figure 1.13.



combinations will reduce dose but one may not see fine detail. The deciding factor should be the reason for the examination paying attention to ALARA. Careful positioning should be practiced with appropriate exposure factors to produce an image with film blackening within the useful density range. A dark image is unacceptable as is a pale image (fig 1.12).

Factors influencing mAs selection include: FFD as per the inverse square law, speed of imaging system, collimation of the primary which reduces scatter/secondary radiation thus contrast is improved, and use of secondary radiation grids. It is necessary to increase mAs when reducing the area of the primary beam (coning) to compensate for loss of film blackening caused by scatter. Grid exposures require an increase in mAs based on the grid ration. For example a 8:1 grid

ratio has a grid factor of 4 (half of 8) thus the mAs has to multiplied by 4 when moving from non-grid to grid technique. Grids improve contrast but reduce image sharpness as the distance between the patient and film is increased. The output of the generator also influences mAs selection, eg single phase unit requires more mAs than a high output generator. A simple method to establish difference is to perform a stepwedge test as described in this chapter (see page 14). Contrast is high when images are produced using single phase units as the overall kV is less than the selected kV. The benefits of higher output generators far outweigh the loss of contrast as such units enable use of low mAs settings, short exposure times, and a range of kV selections allowing the use of moderately high to high kv techniques to reduce dose to patients in keeping with the ALARA principle.

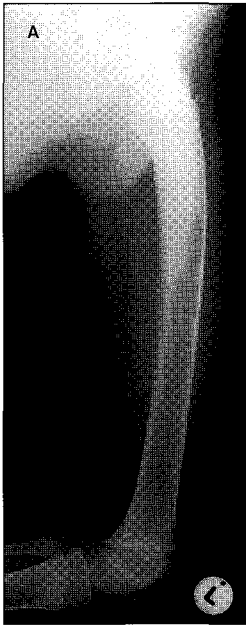


Fig 1.10a
Lateral view of femur a bit over-penetrated for visualisation of soft tissue but image acceptable.

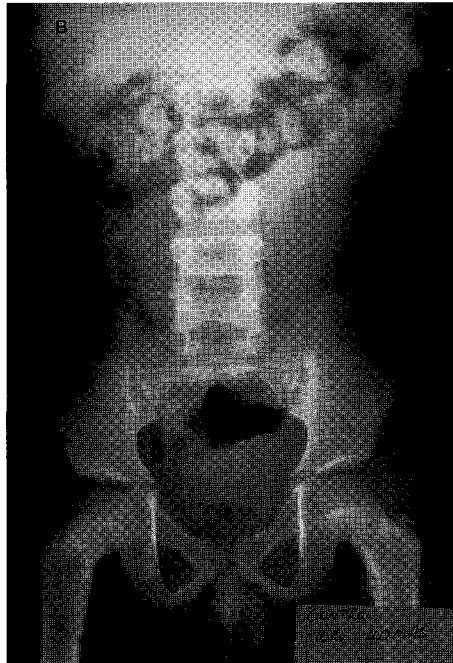


Fig 1.10b
AP supine abdomen (control) of 10 year male patient for barium enema. Note lack of gonad protection. Exposure selection not based on ALARA as low kV and high mAs (70kVp, 40mAs) used.

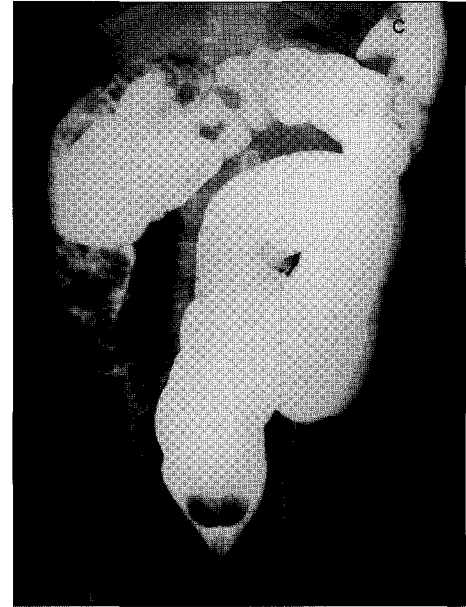


Fig 1.10c
AE film of same patient; again no gonad protection and inappropriate exposure selection.



Fig 1.10d
Delayed AE of same patient. Radiograph taken by different radiographer who applied ALARA principles, gonad protection, 88 kV used and mAs decreased accordingly to 5 mAs. Note improved visualisation of large bowel patterns due to long-scale contrast image.

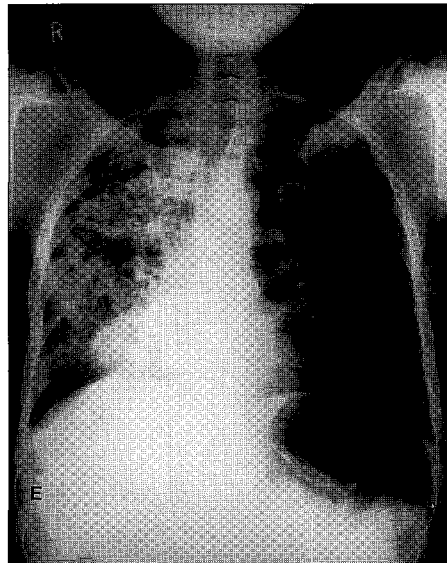


Fig 1.10e
Too much mAs used for the chest hence lung markings not demonstrated.

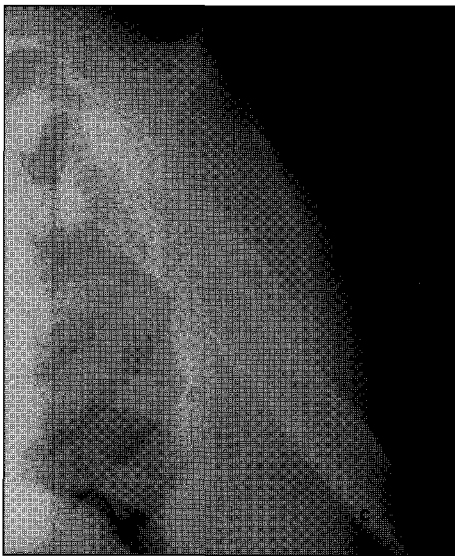
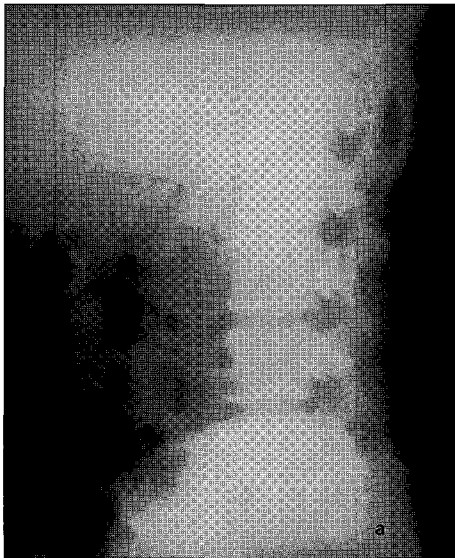
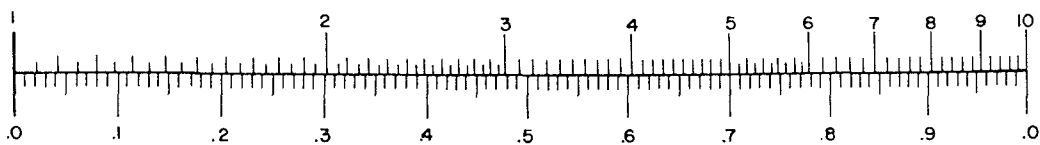


Fig 1.12a, b, c
Range of unacceptable images. Insufficient kV used for lateral spine (a); poor patient positioning for peg view as C1/2 not demonstrated due to overlying occiput (b); not true lateral view for scapula plus insufficient kV used (d).

NUMBER FOR EXPOSURE (mAs) ADJUSTMENT



MANTISSA OF LOGARITHM

Practical use of a stepwedge to determine mAs adjustment when comparing 2 different speed systems. Note if 4 step difference then $\log = 0,304$ then $\text{antilog} = 2$.

Fig 1.13

Scale for determining logarithms to calculate adjustments to mAs for different speed systems.

- Subjective contrast includes how tired one is when viewing an image, the brightness of the illuminator (viewing box), and the brightness of surrounding light. Where possible illuminators should be kept clean and have the same intensity and light colour. Images should be viewed in a room which has subdued lighting.
- Subject/patient contrast includes selection of kVp (exposure factors), the thickness of the part being imaged, use of contrast media, and scatter-secondary radiation. If we require an image with high contrast/short scale then low kVp factors are selected but when a long scale image is important then high kVp should be used.

Determining mAs adjustments: stepwedge tool

A calibrated aluminium stepwedge is a basic useful tool as it can be used to establish mAs adjustments when using different speed systems.

● **Method**

Expose each system with same film type if determining different speed of intensifying screens. The same factors should always be used. For example 70kVp and 5mAs at 120 cms FFD. NB never use less than 0,1 second exposure time to allow the screens to respond to the quanta to emit light (ie to minimise reciprocity failure). Process the films. Place the films edge to edge on a horizontal view box and mask all unwanted light areas. Visually compare the steps and adjust to align with a selected step. It makes it easier to do if a metal ball-bearing is taped to the middle step of the wedge (see fig 1.11). If there are 4 step differences obtained when using a calibrated step-wedge with a calibration factor of 0,076 at 70kVp, 5mAs and at 120 centimetres FFD. then the logarithm value is $4 \times 0,076 = 0,304$ (fig 1.13) The exposure factor for mAs adjustment can be determined by reference to a table of logarithms, by use of a slide rule (D and L scales) or by reference to the scale at the back of the step-wedge (if supplied) or by the above figure. Note that the antilogarithm of 0,3 is 2. The mAs would have to be halved if moving from a slow to faster system or vice versa.

The step wedge method may be used to check output of units. ideally the resultant stepwedges should be the same density for a specific unit. Should there be differences and if the processing factors are optimal then this information could be useful when communicating with the firm/repair technician. Making use of a calibrated stepwedge to regularly check output of units saves money and time. This tool produces crude results but is inexpensive.

Optimal image quality requires careful positioning, regular maintenance and care of equipment, and careful selection of exposure factors. The acid test being that one is confident when engaged in pattern recognition.

References

1. Ballinger PW. 1998. Merrill's atlas of radiographic positions and radiologic procedures. St Louis: Mosby Year Book.
2. Bontrager KL & Anthony BT. *Textbook of radiographic positioning and related pathology*. Second Edition. St Louis: CV Mosby Company.
3. Clifford MA & Drummond AE. *Radiographic techniques related to pathology*. Third Edition. London: Wright PSG.
4. Freeman M. 1988. *Clinical imaging: an introduction to the role of imaging in clinical practice*. New York: Churchill Livingstone.
5. Goldman M & Cope D. *Radiographic index*. Eighth Edition, London: Wright PSG.

6. Swallow RA, Naylor E, Roebuck EJ & Whitley AS. *Clark's positioning in radiography*. Eleventh Edition. London: William Heinemann Medical Books, Ltd.
 7. Barber TC & Thomas JM. 1983. *Radiologic quality control manual*. Reston: Prentice-Hall Company.
 8. Bluth EI, Havrilla M & Blakeman C. 1993. Quality improvement techniques: value to improve the timeliness of the preoperative chest radiographic report. *AJR*, 160: 995-998.
 9. Borras C. Editor. 1997. *Organisation, development, quality assurance and radiation protection in radiology services: imaging and radiation therapy*. Washington DC: PAHO/WHO.
 10. Gould R & Boone JM. 1996. *Syllabus: categorical course in physics: technology update and quality improvement of diagnostic imaging equipment*. Oak Brook: RSNA Learning Center.
 11. Pizzutiello RJ & Cullinan JE. 1993. *Introduction to medical radiographic imaging*. Rochester: Eastman Kodak Company.
 12. Smit KJ. 1996. *Proposed regulations and the role of quality control in diagnostic radiology*. Bellville: Directorate Radiation Control, Department of Health, South Africa.
 13. Thornhill PJ. 1987. Quality assurance in diagnostic radiography: are we using it correctly and what is the future? *Radiography*, Vol 53, No 609: 161-163.
 14. Ball J & Price T. 1990. *Chesneys' radiographic imaging*. Oxford: Blackwell Scientific Publications.
 15. Burns EF. 1992. *Radiographic imaging: a guide for producing quality radiographs*. Philadelphia: WE Saunders Company.
 16. Curry TS 111, Dowdey JE & Murry RC. 1993. *Christensen's introduction to the physics of diagnostic radiology*. Philadelphia: Lea & Fabiger.
 17. Stockley SM. 1988. *A manual of radiographic equipment*. London: Churchill Livingstone.
 18. Wilkes R. 1985. *Principles of radiological physics*. London: Churchill Livingstone.
-

CHAPTER 2

Radiation protection in radiological practice

William Rae

X-ray production

The radiation emitted from X-ray units while taking X-rays is photon radiation, and these photons are known as X-rays. They are generated when high energy electrons, accelerated by a high voltage potential difference, strike a target in the X-ray tube and their energy is converted to photons which radiate out from the target. The energy of the electrons, and hence the resultant photons, is expressed in terms of thousands of electron volts (keV). Photon energies used in diagnostic radiology are in the range 20 keV to 150 keV. These photons have enough energy to cause ionisation, resulting in deposition of energy in the irradiated material. This energy deposition results in a reduction in the number of photons in the beam, and the beam is said to be “attenuated” by the absorbing material. The amount of energy absorbed differs for materials of different density or atomic composition. The differential absorption of X-rays between different structures, allows the creation of the contrast that is seen on X-ray films, and is diagnostically useful.

When a patient is exposed to an X-ray beam a large amount of radiation is also produced in other directions. Much of the radiation entering the patient is scattered and exits the patient in all directions. Some of the photon energy is lost during the scattering process, so the scattered photons are of a lower energy than the primary photons. For most radiographic procedures only about 1 to 10% of the primary beam emitted from the X-ray tube actually interacts with the detector system. (This excludes the photons absorbed by the casing and collimators of the X-ray tube). The rest of the energy is lost due to scatter or absorption in the patient. With newer, and more efficient, detector systems, less radiation is required to produce diagnostic quality images. This reduces exposure to the patient.

Biological effects of X-ray radiation

The damaging (negative) effects of X-rays were noticed soon after their discovery. Early workers were initially unaware of the associated risks and thus took no precautions against being exposed to the X-ray beam whilst imaging patients. Skin damage and induced cancers were soon attributed to the extreme overexposures experienced by early radiation workers. As a result, efforts to understand and limit the negative biological effects have been made since the very early years of diagnostic radiology. Most of the information about the negative effects of radiation comes from nuclear power plant accidents, atomic explosions, radiotherapy patients, and radiation workers.

The biological effects of X-ray radiation are due to the ionisation that occurs when photon energy is deposited in living tissue. Intracellular water is ionised producing free radicals that can damage either the genetic material of the cell in the DNA of the chromosomes, or the intracellular organelles. The resultant effects are related to the amount of radiation absorbed by the tissues.

Negative effects associated with X-ray radiation

The intracellular damage that takes place after exposure results in two main categories of effects. Either the damage to the cells results in immediate effects, which may result in progressively worsening function and eventually cell death, or the damage to the cell's genetic content allows it to live and reproduce, but ultimately result in cancer after some delay period. The risk of seeing both these types of effects increases with increasing radiation exposure to the individual. The direct damage effects are only seen above some relatively high threshold level of exposure and they worsen as the dose increases. The chance of getting cancer though is low, but can be induced by low amounts of radiation. Cancer induction is an all or nothing effect, and there is a statistical chance that it will occur. The chance of occurrence is proportional to the amount of exposure.

Rapidly dividing cells are more sensitive to radiation effects, and the most sensitive tissues are thus gastrointestinal tract, gonads, bone marrow, and skin. The tissues most susceptible to radiation induced malignancy are bone marrow, bowel mucosa, breast tissue, gonads and lymphatic tissues.

The foetus is most susceptible to radiation at about 20 to 40 days post conception, and microcephaly and mental retardation are the most likely effects, followed by an increased incidence of cancer in childhood.

Quantification of radiation dose

The amount of radiation delivered to an object (or person, or tissue) can be quantified as the energy (joules), deposited per unit mass (kilogram), of whatever is being exposed to the radiation. The specific SI unit for radiation dose is the gray (Gy), which is defined as one joule per kilogram. Different biological tissues respond differently to different types of radiation and to account for this a biological weighting factor is used. The SI unit of biologically effective dose is the sievert (Sv). This is also measured in terms of joules per kilogram, but accounts for the biological response of the particular tissue being irradiated.

Radiation protection regulations

Regulations have been developed internationally over many years to control the amount of exposure that is allowed, and thus to minimise the incidence of radiation effects. The latest relevant publications are ICRP Publication 60, printed in 1990, and titled *1990 Recommendations of the International Commission on Radiological Protection*, and the *International Basic Safety Standards for Protection Against Ionizing Radiation and for Safety of Radiation Sources* jointly published in 1996 by the WHO, IAEA and other international Organizations.

The "Alara" principle

The guiding principle used in all these documents is that radiation doses to the public, and to people who work with radiation, must be kept As Low As Reasonably Achievable (ALARA principle). The effect of radiation at very low doses is still debated and the ALARA principle is adopted to avoid radiation exposure as much as possible, knowing that the risk of negative effects from small amounts of radiation approach those seen in the general public for those same negative effects.

Protection regulations

Equivalent dose is the sum of all doses from different types of radiation to an organ in an exposed person. Effective dose is the sum of the weighted equivalent doses, and is the

Table I. Occupational dose limits

Application	Occupation dose limit	Public dose limit
Effective Dose	20 mSv per year, averaged over 5 yrs, and not more than 50 mSv in any year.	1 mSv per year.
Equivalent Dose: Eyes	150 mSv per year	15 mSv per year
Equivalent Dose: Skin	500 mSv per year	50 mSv per year
Equivalent Dose: Hands	500 mSv per year	–
Pregnant Women Workers	2 mSv to the surface of the woman's abdomen for remainder of pregnancy	As for members of the public

dose that gives an indication of the overall effect of the exposure to the person. This is the dose that is limited by the regulations. A radiation worker is defined as a person who works with radiation, and may potentially exceed 30% of the prescribed dose limits.

The regulations impose limits on the radiation doses that may be received by radiation workers and the general public. The dose limits are all set to a level that will reduce the risk of effects to below some arbitrary acceptable level. This level is conservative and the result is that the radiation profession is one of the safest fields of work, if the rules are properly followed.

Dose monitoring of radiation workers

Radiation workers should be monitored at all times when working. The reason for monitoring is to ensure that the practices being followed by the workers in their daily routine are safe and do not result in high doses being received. If monitoring is not done then unsafe practices will not be noticed and excessive exposures to staff may result.

Personnel monitoring is normally the responsibility of national authorities. They should supply pre-packed thermoluminescent dosimeters, which are returned for automatic readout on a monthly cycle. The dosimeter should be worn on the torso and under any protective lead clothing being worn. All radiation workers should wear their own dosimeter at all times during working hours. If the monthly limit exceeded, the responsible radiation protection officer should be informed and a report should be required.

It is good practice to set a local action limit at some lower level than the national level so that the practices in the department are appropriate to the local conditions. Doses above the allowed local limit could be followed up in an attempt to rectify any practices resulting in increased doses to staff. A record should be kept of all radiation doses recorded for all radiation workers.

Recommendations for pregnant radiation workers

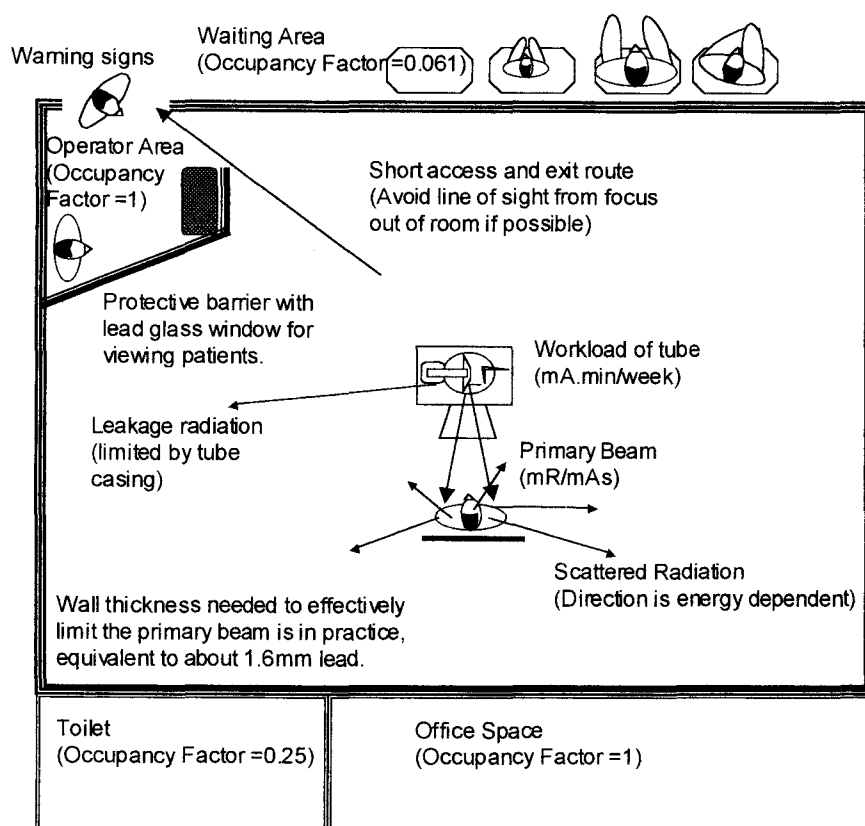
Pregnant radiation workers should not work in areas where there is a risk of getting more than 30% of the allowed whole body limits for radiation workers. They should wear an alarm radiation monitor at all times. They should not be allowed to work with fluoroscopy, theatre radiography, mobile X-ray units, or interventional radiography.

X-ray doses to patients

The skin dose delivered during X-ray investigations has been reduced over the years with the introduction of newer technology equipment using more sensitive detectors and better shielding, but the ability to deliver large doses of radiation very quickly and easily during examinations has also increased. Generally the doses given are lower than

Table 2. Typical effective dose equivalent values for radiological examinations

Procedure	Effective dose equivalent in mSv
PA chest X-ray	0.01-0.05
Skull X-ray	0.1-0.2
Abdominal X-ray	0.6-1.7
Barium enema	3-8
Head CT	2-4
Body CT	5-15
Nuclear Medicine	2-10

**Fig 2.1**

A typical layout of a X-ray suite, showing some of the safety aspects that must be considered when designing a room to be used for taking X-rays. Barrier thicknesses are designed to ensure that exposures are within acceptable limits. Workloads and occupancy factors are used in the calculation of the required thickness of the protective barriers.

the threshold for deterministic effects, but interventional radiology, and similar long procedures, can result in epilation (>3000 mSv), and erythema (>5000 mSv). The doses to patients should be minimised wherever possible, and the following good practices are advised:

1. Only image patients if there are good clinical grounds for doing the procedure.
2. Only image the area required. Proper collimation minimises risk.

3. Gonadal shielding should be used in people of reproductive age.
4. Imaging of pregnant patients should be avoided when medically possible. If the last menstrual period has been missed then the patient should be assumed pregnant.
5. Minimise repeat examinations by using good radiographic practice.
6. Increase the focus skin distance to reduce the entrance dose.

In general the risk of radiation injury from X-ray examinations is far less important than the clinical benefit being derived from doing the examination. The availability of X-ray units has resulted in a marked increase in the medical radiation dose being delivered to the population as a whole. This medical exposure should be limited if possible.

X-ray suite design

The design of a X-ray room takes into account the expected doses in the room and surrounding areas. The dose calculation takes into account occupancy, workload, X-ray energy, beam direction, shielding materials used, and other relevant factors.

Practical ways to minimise radiation doses

Radiation dose increases with decreasing distance from the source ($\propto 1/\text{distance}^2$), time of exposure ($\propto \text{time}$), intensity of the radiation beam ($\propto \text{intensity}$), and the inverse of the thickness of any absorbers between the source and the exposed person ($\propto \exp^{-\mu \cdot \text{thickness}}$).

To reduce the dose to radiation workers the following practices should be adhered to:

1. The distance from the source of the radiation must be increased as much as possible. One way to encourage this is to mark distances from the source on the floor of the X-ray room.
2. The time of exposure should be decreased, and workloads should be shared as much as possible. If it is not required to be present during exposure then leave the room.
3. Protective shields should be used and worn by workers during exposure. Standard lead aprons, lead gloves and thyroid shields substantially reduce the effective dose for most diagnostic examinations. Lead glass shields can also be used to protect the eyes.
4. The primary source of radiation should be collimated as much as possible. For example the smallest fields possible should be viewed when doing fluoroscopy.
5. Controlled access to areas where radiation exposure may be taking place is required. Suitable radiation warning signs should be displayed at entrances to rooms and on any radiation source.

If the above simple principles are applied and all attempts are made to keep the radiation doses to staff and patients “as low as reasonably achievable” (ALARA), then the risks from exposure to radiation in an X-ray department should be minimal.

CHAPTER 3

Contrast media in imaging

Peter Corr

Purpose of contrast media

Contrast media are used in imaging to opacify normal structures including the vascular system, collecting system of the kidneys and the lumen of the gastrointestinal system to obtain further diagnostic information about focal lesions in the body.

How do they work?

Vascular contrast media contain 50% by weight of molecular iodine which absorbs X-rays via the photoelectric effect and appears white on X-ray film. Oral agents consisting mainly of barium works on the same principle.

What are they?

Vascular contrast agents are iodinated organic compounds that are very hydrophilic and have a low lipid solubility and low binding affinity for proteins and membranes. Most agents have a molecular weight of less than 2000 (1). On intravascular injection they are rapidly distributed into the extravascular space but do not enter the intracellular spaces. They are rapidly excreted by normal kidneys some 90% within two hours. They do not cross the blood brain barrier.

What do I need to know to use them safely?

Vascular contrast media are not drugs like antibiotics and are pharmacologically inert. However even though they are very safe when injected intravenously or intraarterially, they can have side effects and complications. Before you use them you must be familiar with their side effects and how to manage them.

Side effects can be classified into allergic idiosyncratic reactions and non idiosyncratic reactions (1). Allergic reactions are the most serious and unpredictable reactions to contrast media. Reactions occur immediately or within 5 minutes of contrast injection. Patients with a history of allergy and atopy, for example hay fever or asthma, are 8 times more likely to have allergic reactions than non-allergic patients. These reactions are not dose dependent and are due to a release of vasoactive molecules such as histamine and kinins.

Non idiosyncratic contrast reactions are due to direct contrast toxicity which is dose dependent. Patients with renal failure or renal impairment from dehydration, diabetes or multiple myeloma are especially susceptible. Newborns and elderly patients are less able to excrete contrast media hence are more likely to have nephrotoxic complications.

Complications of contrast media

Although idiosyncratic reactions are unpredictable, prevention is the best policy. Whenever a contrast injection is performed a resuscitation trolley should be close by in the same room. It must have an "Ambu bag" for ventilation, airways, ECG monitor, oxygen cylinder as well as the following drugs: adrenaline, hydrocortisone, IV fluids,

chlorpheniramine and bronchodilator spray. It is mandatory that the trolley is checked weekly and that all the drugs are in stock. **Do not use intravenous contrast agents without being fully trained in cardiorespiratory resuscitation.**

Complications

Complications are divided into: minor, intermediate, major or life threatening and death.

- **Minor complications** include nausea, facial flushing or a warm sensation and urticaria. These complications usually disappear within 15 minutes and only require reassurance. If the symptoms persist an injection of 10mg of an antihistamine intramuscularly, such as chlorpheniramine, should cure the allergic effects.
- **Intermediate complications** include bronchospasm and hypotension. These complications respond to reassurance and an inhaled bronchodilator such as salbutamol, intravenous hydrocortisone 100mg bolus and **intramuscular** adrenaline 0.3–1.0mls of 1 in 1000 solution.
- **Severe life threatening reactions** include seizures, severe bronchospasm and laryngeal oedema, pulmonary oedema and cardiovascular collapse. These reactions require urgent treatment. The airway must be secure and intravenous access established. Adrenaline 0.3–1.0ml of a 1 in a 1000 solution by intravenous injection is the most effective drug to treat anaphylaxis. Death following contrast injection is extremely rare.

Reference

1. Grainger R. Intravascular Contrast Media. In: *Diagnostic Radiology: A textbook of medical imaging*. 1997. Eds Grainger R, Allison D. Churchill Livingstone, Edinburgh.

CHAPTER 4**Digital imaging and telemedicine***Peter Corr***Digital imaging**

A digital image consists of a matrix of numbers or digits that when processed by a computer will produce an image on a monitor. Digital information is stored as bits, with 8 bits forming a byte that represents a value or character.

Digitization is the process of acquiring or converting analogue images into a digital format. Many imaging modalities acquire the image initially in this format, for example with CT, MR and ultrasound. All images today can be converted into digital format. The advantages of digital imaging are the ease of storing images and the ease of transmitting images and manipulating the images during image interpretation. You no longer have to rely on finding the radiographs! It is important to be aware of the disadvantages. Digital imaging hardware is expensive to purchase and to maintain. Long term storage of digital images is especially expensive. Given these challenges, there is no doubt that as computer processors and storage devices become less expensive, many hospitals in developing countries will use digital imaging in the future. Each medical image is stored as a file on the computer. The file can be compared to the X-ray packet of a conventional radiograph. The files vary greatly in their size or number of bytes they contain. Chest radiographs when in digital format consist of 2 Mbytes (2 million bytes) while an ultrasound or CT scan may be 10 times smaller at 200 Kbytes in size. Generally plain analogue radiographs when in digital format have much larger files than more modern imaging investigations, such as ultrasound or CT imaging.

Teleradiology and telemedicine

Telemedicine is the electronic transmission of medical images from one site to another for interpretation and consultation. The concept of telemedicine is not new and was first used in the 1950s. However with the development of more reliable and cheaper electronic communication and computers, telemedicine is becoming more accessible to many developing countries.

Goals of telemedicine

The goals are threefold:

- i. to provide consultation and interpretation of images in regions of need,
- ii. to provide specialist services in hospitals without specialist support
- iii. to promote educational opportunities for doctors working in rural hospitals.

Advantages and disadvantages

There are many advantages. Specialist advice is available without the patient having to travel to the regional or city hospital. Better utilization of specialist resources is made at the regional hospital. Travel and accommodation costs are reduced for patients who are less likely to be referred to the regional hospital after telemedical consultation.

Telemedicine can be used to provide continual medical education programmes to doctors working in rural areas. Disadvantages of telemedicine include: high initial capital costs of hardware, staff training, requires a good telecommunication network, and patient confidentiality is more difficult to maintain.

Applications in telemedicine

Telemedicine has been successfully used in radiology, ultrasound, surgery, ophthalmology, pathology and dermatology. In imaging it has been used for plain radiographs, CT, MR, ultrasound, angiograms and nuclear medicine.

Image acquisition

Analogue images such as radiographs have to be digitised using a digitiser which currently is the most expensive component of the system. Most radiographs such as a chest radiograph produce large files of up to 2 MB in size which takes a few minutes to digitise. The data are usually compressed using a lossless algorithm to reduce the transmission time.

Image transmission

Conventional telephone lines found in many developing countries have very slow transmission rates however but are inexpensive to transmit data (around 12 kb/sec). This means that a chest radiograph will take 3 minutes to transmit. Integrated services digital network (ISDN) lines which are available in certain countries are twenty times faster than conventional copper telephone lines, in the region of 256 kb/sec. Satellite communication is obviously wireless technology and is very fast but very expensive and not freely available in many countries.

Image display

To read images at the receiving station high resolution monitors are recommended. The American College of Radiology recommends $2000 \times 2000 \times 12$ bit resolution as a standard (1). These monitors are very expensive and not freely available. The monitors must be sufficiently bright to see all levels of grey scale in medical images. Most images can be interpreted using $1000 \times 1000 \times 8$ bit resolution which are much cheaper.

Image files

Each image is kept in its own file. Static ultrasound, CT and MR images are relatively small compared to radiographs: 100 kilobytes versus 2 megabytes. The larger the file the longer transmission time.

Problems with teleradiology

Most teleradiology systems will have limited spatial resolution and subtle lesions in the lungs and fine bone fractures can easily be missed unless the original radiographs are reviewed later (2). As faster computer systems and digital telephone lines become available limited spatial resolution should become less of a problem. The high capital costs of equipment and limited opportunities to train health professionals in some countries are a barrier to the development of telemedicine services in some developing countries (3). WHO is looking into the development of telemedicine services as a way of providing imaging services to rural clinics and hospitals in developing countries.

LEARNING POINTS: DIGITAL IMAGING AND TELEMEDICINE

- Digital imaging is the process of acquiring, storing, transmitting and interpreting medical images in a digital format
- A digital format is when images are stored as a matrix of numbers or digits and can be processed by a computer to produce a medical image on the image
- Files contain an image in digital format
- Files are measured in the amount of digital data they contain in bytes
- Plain radiographs contain the largest amount of data while CT and ultrasound contain the least data
- Transmission of digital images depends on the transmission rate of the communication system used (in bauds)
- Good spatial resolution of the monitors is necessary to interpret images is extremely important

References

1. American College of Radiology: *Telemedicine Standards*, 1994. Reston, Virginia.
2. Corr P. Teleradiology in KwaZulu Natal: a pilot project. *SAMJ*, 1998;88:48-49.
3. Bignault I, Kennedy C. Training in Telemedicine. *J Telemed Telecare*, 1999;5:S112-4.

PART 2



CHEST IMAGING PATTERNS

CHAPTER 5

The normal chest radiograph

Peter Corr

Understanding the anatomy of the chest is critical in interpreting chest radiographs. Only by reading many normal chests will you be able to detect abnormalities. It is important to develop a routine system and to keep to it.

Soft tissues

The soft tissues of the chest consist of the skin, muscle, fat and fascial planes of the chest wall. There are a number of “companion” shadows to bones such as the clavicles. The breast shadows and axillary folds should be symmetrical (figs 5.1a, 5.1b & 5.2).

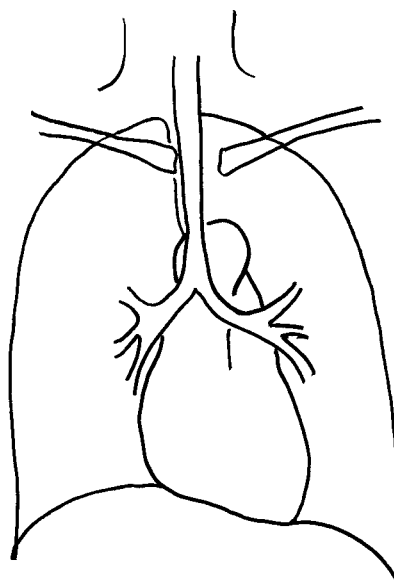
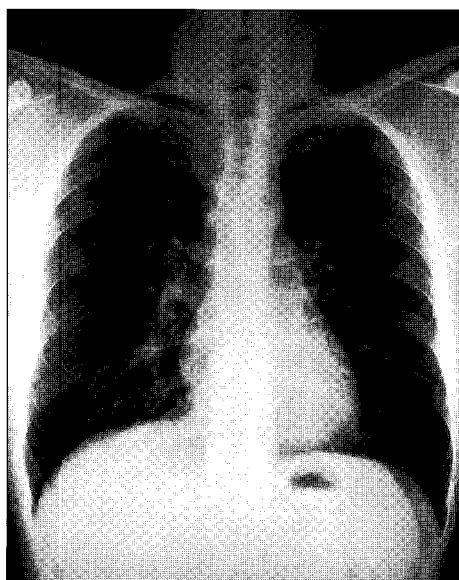


Fig 5.1a
Normal adult male
chest.

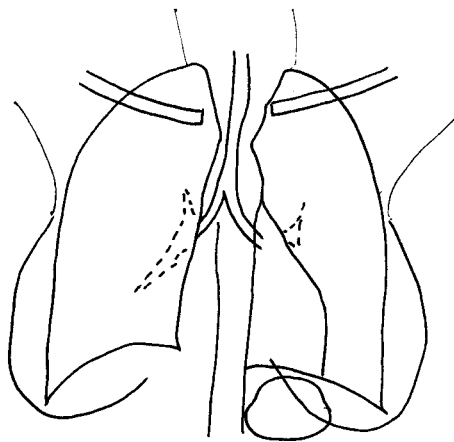
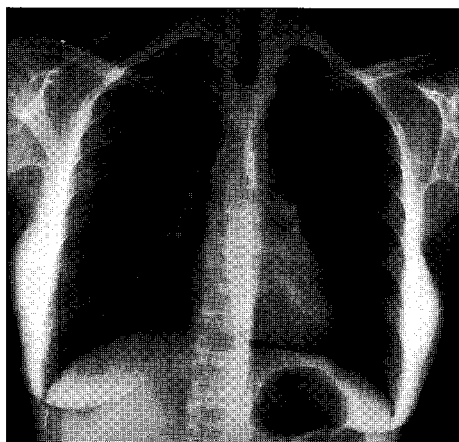
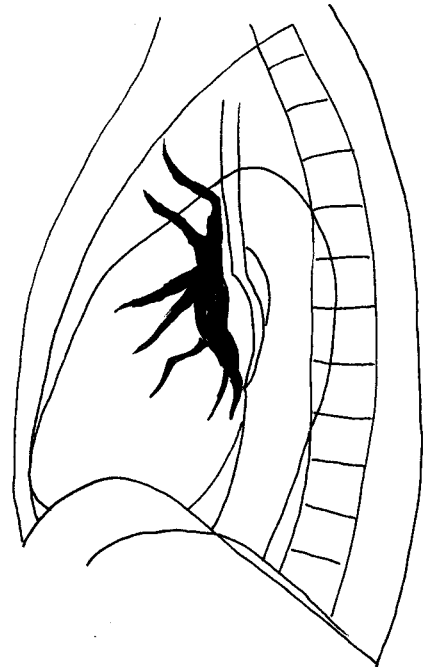
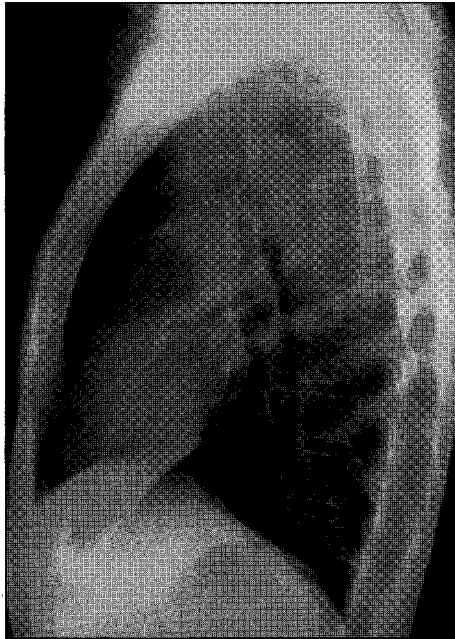


Fig 5.1b
Normal adult
female chest.

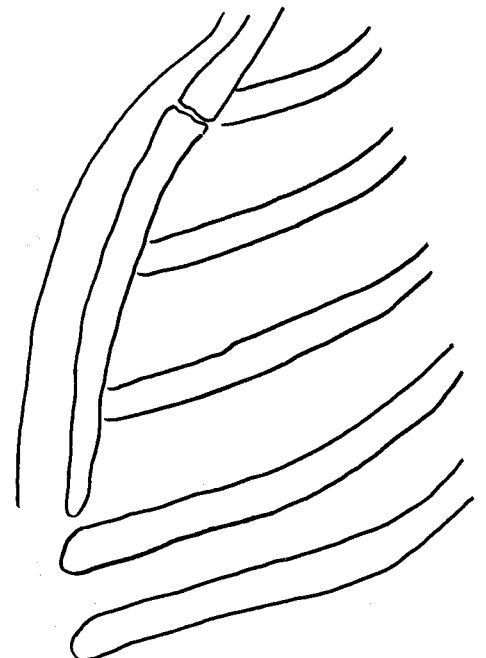
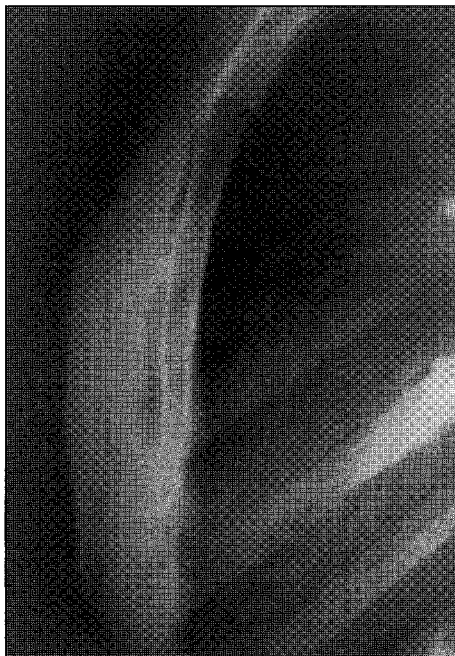
Fig 5.2
Lateral adult chest.



Skeleton

There are 12 ribs which can be traced from their posterior attachment to the spine to their anterior costochondral junctions. The anterior cartilaginous region ossifies especially in women and must not be confused with calcified lung lesions. The 11th and 12th ribs are shorter and do not articulate anteriorly with the sternum. Imaging of ribs requires both PA or AP chest views plus localised oblique views. The clavicles articulate medially at the sternoclavicular junction. This joint is difficult to visualise on PA films. Dislocation or subluxation can therefore be easily missed. Laterally the clavicle articulates with the acromion of the scapula. The sternum consists of two bones; the manubrium superiorly and the body of the sternum which articulate at the manubriosternal junction. The sternum is best imaged obliquely or laterally (fig 5.3).

Fig 5.3
Lateral sternum.



The cervical spine normally has 7 vertebrae, the thoracic 12 vertebrae. Normally the spine has a slight thoracic kyphosis and cervical lordosis. The lower cervical and thoracic spine is visualised best using a high Kvp technique (>120 Kvp).

Mediastinum

To understand the anatomy it is best to think of the mediastinum in the following compartments:

Superior mediastinum

This is the compartment superior to a horizontal plane passing through the aortic arch. It includes the trachea, oesophagus, lymph nodes, superior vena cava and brachiocephalic artery on the right, left subclavian artery, recurrent laryngeal, phrenic and vagal nerves. With age there is widening of the superior mediastinum as the arteries dilate, however the contour is maintained.

Anterior mediastinum

This region is bounded superiorly by the superior mediastinum and posteriorly by the middle mediastinum. It is best visualised on the lateral chest radiograph. It includes the thymus in infants which appears like a sail, lymph nodes and mediastinal fat. The thymus is important to recognise and not to confuse with a pathological lesion.

Middle mediastinum

This region contains the heart, pericardium, lymph nodes, tracheobronchial tree and carina, and the hila regions. The right atrium and right ventricle comprise the anterior half of the heart, with the posterior half composed of the left atrium and ventricle. The carina is where the trachea bifurcates into the left and right main bronchi with the right main bronchus being much steeper than the left. Surrounding the carina and in the hila are numerous lymph nodes which have a maximum diameter of 10mm. The hila are slightly different on each side. The left hilum is located 2 cm superior to the right. The reason for this is the left main pulmonary artery ascends and curves over the superior border of the left main bronchus while on the right, the right main pulmonary artery is located anterior to the right main bronchus. The pulmonary veins enter the hila posteriorly. It is important to understand the hila anatomy so as not to be confused between pulmonary aneurysms and tumours in this region.

Posterior mediastinum

This compartment contains the descending thoracic aorta, the oesophagus, nerves, lymph nodes and paraspinal fascia. The descending aorta is located anterior and to the left of the thoracic spine with the oesophagus situated between them.

Heart (figs 5.1a, 5.1b & 5.2)

The heart is situated within the middle mediastinum with in the pericardium. On PA and AP chest radiograph one third of the heart is to the right of the thoracic spine, two thirds to the left of the spine. On a lateral chest the anterior border of the heart is comprised of the right atrium and right ventricle; the posterior border is comprised of the left atrium and ventricle. It is important to be able to recognize the normal frontal contour of the heart.

Lungs

It is important to remember that the right lung with its three lobes, is different from the left with two lobes. The greater or oblique fissures separate the right upper and middle lobe from the lower lobe and the left upper from the lower lobe. The fissures are best seen on a lateral chest radiograph as thin white lines, the right fissure being steeper than the left. The lesser or horizontal fissure separates the right upper from the right middle lobe and extends from the right hilum to the chest wall. The pulmonary arteries and veins extend out from the hila and are visible to the outer one third of the lungs. The veins tend to be more lateral than the arteries but often cannot be distinguished apart on plain radiographs.

Diaphragm

The diaphragm consists of three parts: the right hemidiaphragm, the central tendon, and the left hemidiaphragm. The right hemidiaphragm is 3 cm superior to the left due to the presence of the liver inferiorly. The hemidiaphragms are muscles under control of the phrenic nerves. The diaphragm inserts peripherally into the costal margin and thoracic wall at the costophrenic angles. The diaphragm may be scalloped as a normal variant.

Pleura

The pleura is a thick fibrous layer consisting of a parietal pleura and visceral pleura. The visceral pleura covers the lungs while the parietal pleura covers the inner surface of the chest wall. Usually the pleural space is a potential space only. The normal pleural surface cannot be visualised using radiographs.

Chest radiography

Good radiographic technique is critical for producing diagnostic chest X-rays. **Important points to remember are:**

- **Exposure factors**—a high kV >120 technique is important to improve visualization of the soft tissue planes of the mediastinum and tracheobronchial tree. The pulmonary vessels are well visualised with this technique.
- **Size and shape of the chest**—exposures will vary depending on the size and shape of the chest.
- **Good inspiration is critical.** You should aim to visualise at least 11 ribs posteriorly above the diaphragm. Poor inspiration will result in difficulties in measuring heart size and assessing the lungs.
- **Patient positioning**—the PA position is best. AP and supine films will result in difficulties in assessing cardiac size and pulmonary vasculature. Check that the patient is not rotated by checking that the medial edges of the clavicles and the spine are equidistant.

Technique

The patient should stand erect with the anterior chest wall flat against the bucky/cassette with the hands on the hips and the elbows rotated forwards. The X-ray tube should be more than 1 m from the cassette and centred at the T3 level.

How to read a chest radiograph

Try to develop a systematic method and keep to it. Start peripherally and read towards the centre of the chest

1. Soft tissues: compare both sides. In females check both breasts shadows are present. Look for focal soft tissue calcification and subcutaneous gas.
2. Skeleton: count all ribs. Check for focal lesions such as metastases (lytic or sclerotic) and fractures. Check clavicles, shoulders, cervical and thoracic spines.
3. Lungs: compare both sides. Divide the lungs into three zones: upper, middle and lower and compare both sides.
4. Diaphragm: the right hemidiaphragm is 2 cm superior to the left. Compare the shape and position. Look for free air beneath the diaphragm.
5. Hilar regions: the left is 2 cm superior to the right. Check position, contour and density
6. Mediastinum: check the position with two thirds of the transverse diameter of the heart to the left of the spine and one third to the right. In the superior mediastinum the trachea should be central anterior to the thoracic spine.
7. Heart: check size (normally <50% CTR), position and contour.
8. Pleura: normally invisible. Check costophrenic angles for pleural fluid and pneumothorax.

Chest patterns**Clinical information**

To improve diagnostic specificity always take a relevant history from the patient. Ask the following questions:

How long have there been symptoms, such as cough?

Is there haemoptysis?

Is there chest pain?

Is there shortness of breath?

Important clinical information includes:

Does the patient have a fever?

Is the patient immunosuppressed or HIV positive?

Is the patient taking any drugs? eg. antibiotics or chemotherapy?

Is the patient exposed to any occupational dusts?

CHAPTER 6

Pulmonary infection

Peter Corr

Most pathological processes involving the lungs will cause increased density of the lung and appear white or appear as focal opacities.

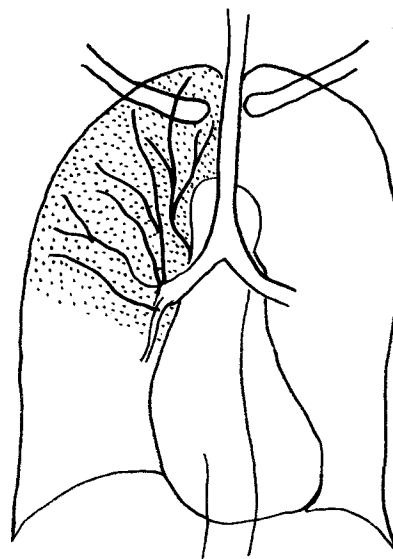
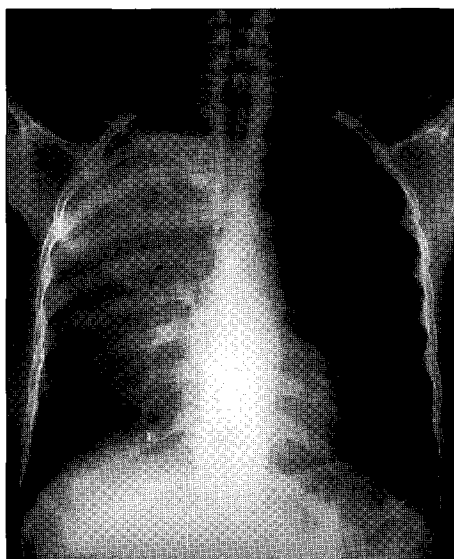
Pneumonia patterns

Pneumonia is air space consolidation in which the alveolar air space is filled with inflammatory exudate from the infection. Pneumonias can be classified both anatomically and by aetiology. Anatomical classification is useful as certain patterns have specific causes, for example lobar pneumonia is often due to streptococcal pneumoniae. Age is also important to consider as childhood pneumonias have a different appearance and cause from adult infections. The presence of immunosuppression from human immunodeficiency virus (HIV) infection has complicated these patterns in many developing countries.

Lobar pneumonia pattern

Pneumonia is airspace opacification of a lung lobe. The alveolar air spaces are filled with inflammatory exudate while the bronchi and bronchioles remain patent. The cause is often strep. pneumoniae. The pattern to identify is opacification of the pulmonary lobe with the presence of air bronchograms which appear like the branches of a leafless tree (fig 6.1). Air bronchograms are the patent air containing bronchial tree, which is surrounded by airspace opacification. Once you see bronchograms these are diagnostic of lobar pneumonia. The important differential diagnosis is lobar atelectasis where there are no air bronchograms as the bronchus is usually obstructed and the air in the distal bronchus is reabsorbed (fig 6.2).

Fig 6.1
Right upper lobe pneumonia from strep. pneumoniae infection with lobar opacification and air bronchograms (arrow).



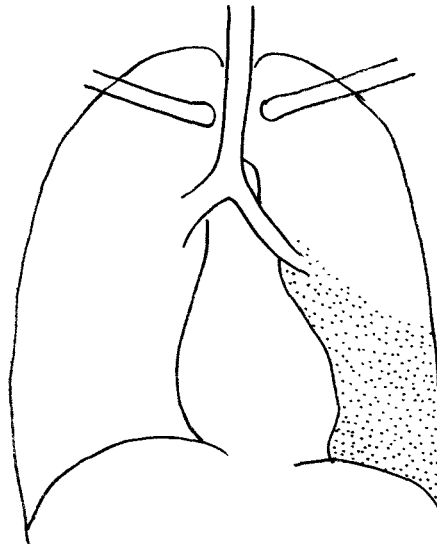
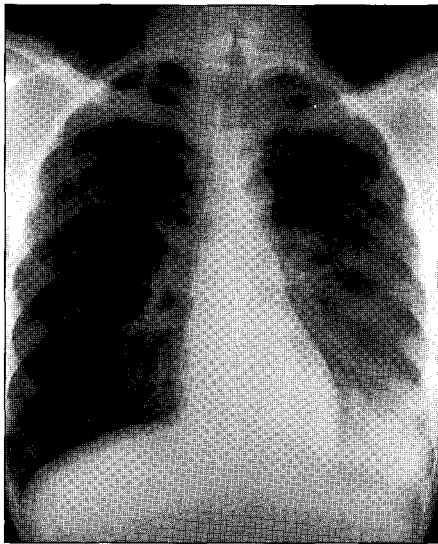


Fig 6.2
 Left lower lobe atelectasis from obstruction of the left lower lobe bronchus. Note absent air bronchograms and slight volume loss.

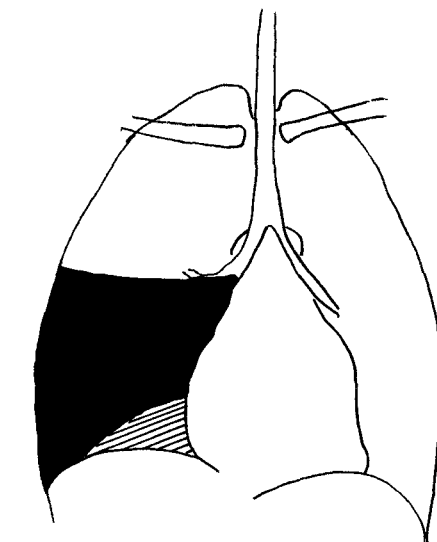
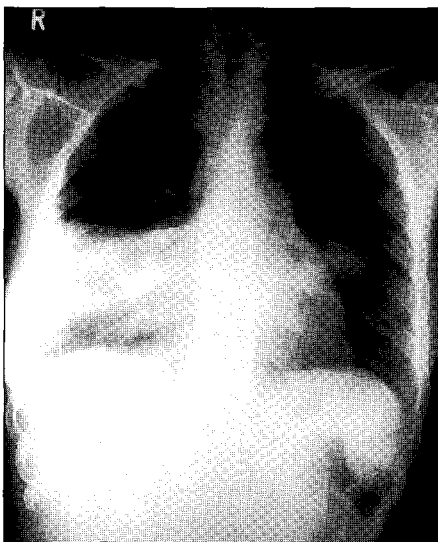


Fig 6.3a
 Right middle lobe pneumonia demonstrates loss of the right heart border (arrow). This is called "loss of the silhouette" sign.

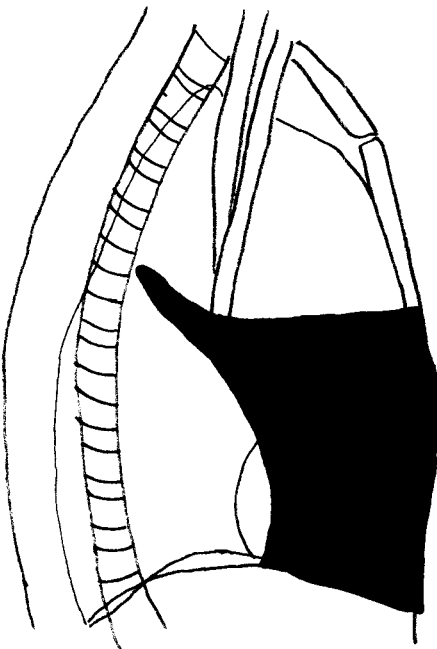


Fig 6.3b
 Lateral chest demonstrates the right middle lobe pneumonia.

To localize a lobar pneumonia anatomically, the loss of the silhouette sign can be used. Right middle lobe pneumonias will cause the right heart border to disappear (figs 6.3a, 6.3b) and lingula left upper lobe pneumonias result in loss of visualisation of the left heart border. In lower lobe pneumonias either hemidiaphragm will not be visualised.

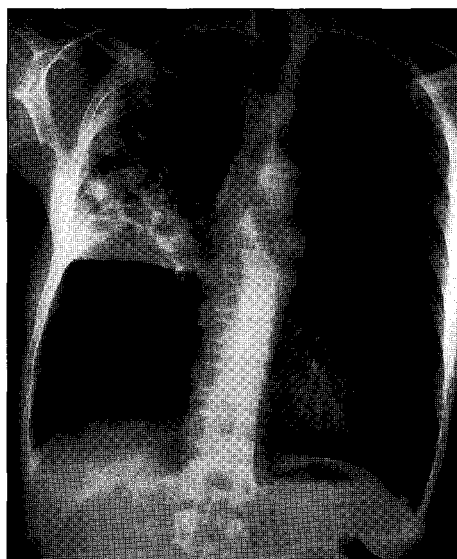
Bronchopneumonia pattern

In this pattern there is multifocal peribronchial opacification bilaterally. This pattern is common in childhood infections. The cause of the infection is often viral or following mycoplasma infection.

Cavitating or necrotising pneumonia (fig 6.4)

Necrotising pneumonia pattern occurs when there is extensive necrosis of lung tissue. Cavities form, which may have multiple fluid levels. Common causes are infections from klebsiella, bacteroides and pseudomonas bacteria. The clue to this pattern is the presence of a cavity within the pneumonia. The differential diagnosis includes cavitating cancer (usually a squamous primary or secondary) and tuberculosis.

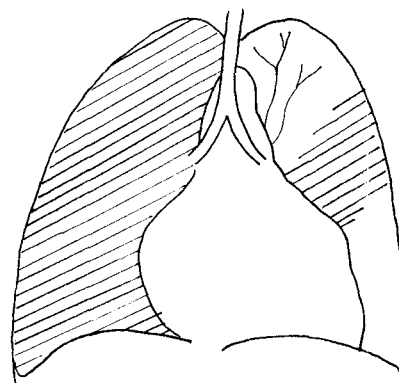
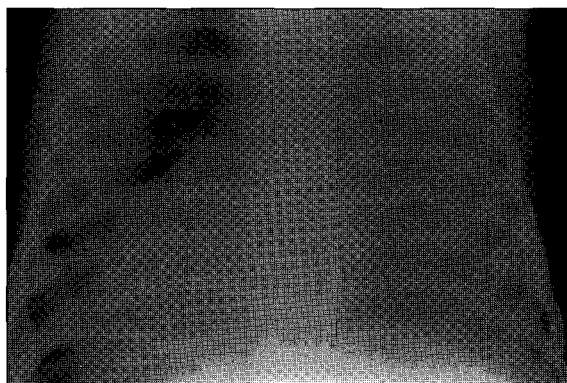
Fig 6.4
Cavitating right upper lobe pneumonia from klebsiella infection.



“Ground glass” pneumonia pattern (fig 6.5)

This pattern is often difficult to recognize initially, however the clue is the pulmonary vessels appear ill defined or “fuzzy” and the lung appears slightly opaque. No air

Fig 6.5
Chest radiograph demonstrates “ground glass” opacification in an HIV positive child with pneumocystis carinii infection.



bronchograms are found. This pattern is found in pneumocystis carinii pneumonia infections in patients who are immunosuppressed especially from AIDS, mycoplasma infection and, viral infections.

Pulmonary tuberculosis patterns

The appearance of pulmonary tuberculosis is changing in many developing countries with the spread of HIV/AIDS. It is therefore very important to establish whether the patient is immunosuppressed.

Primary pulmonary TB pattern (fig 6.6)

This is usually a small focus of opacification in the lung (Ghon focus) with hilar adenopathy and mediastinal adenopathy on the same side. Often the primary pulmonary focus is not detected only the hilar or mediastinal adenopathy which may cause tracheobronchial airway compression in young children.

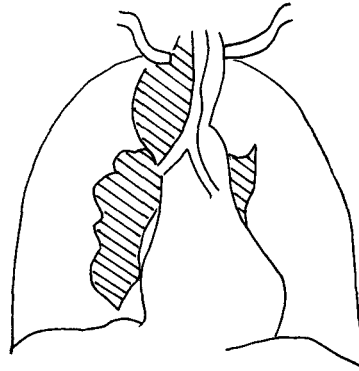
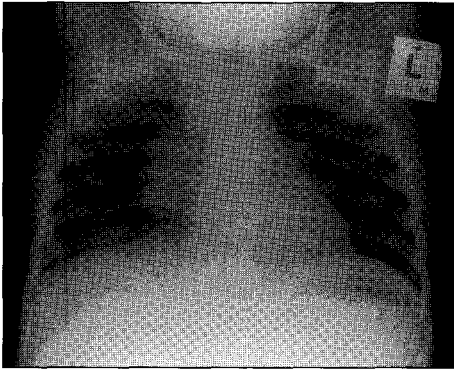


Fig 6.6
Chest radiograph of a child with primary tuberculosis. Note right hilar and paratracheal lymphadenopathy.

Secondary or post primary TB pattern (figs 6.7, 6.8)

In patients with normal immunity this pattern is:

cavitation—usually in the upper lobes or lung apices;

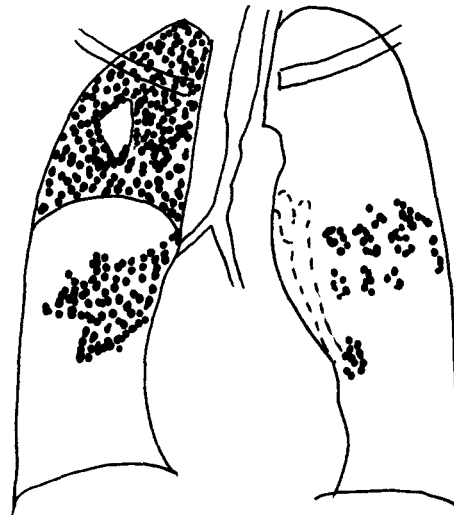
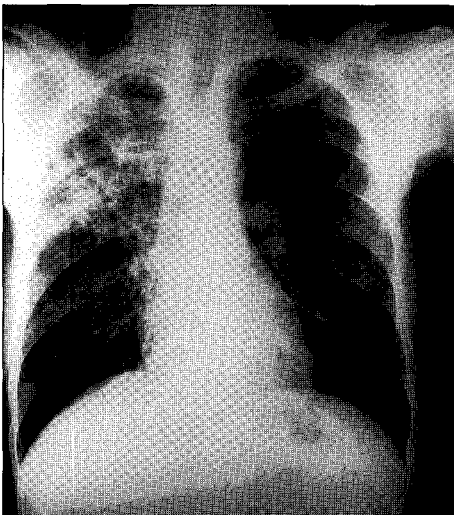
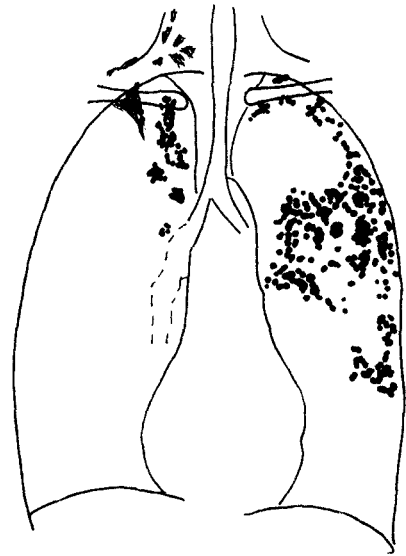
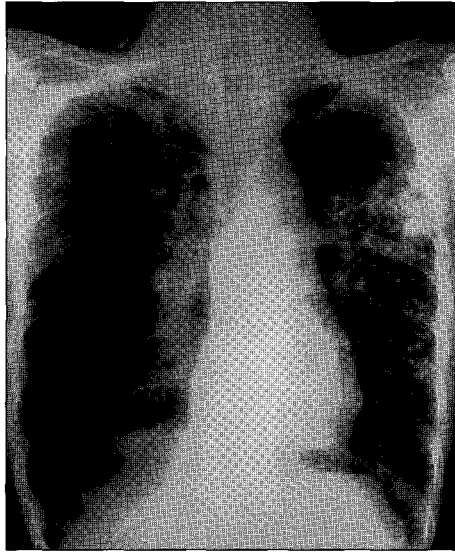


Fig 6.7
Chest radiograph in an adult with post primary or secondary tuberculosis demonstrates right upper lobe infiltrates with cavities which have spread to the right and left lower lobes.

Fig 6.8
Chest radiograph
demonstrates
healed tuberculosis
with focal
calcification in the
left mid zone and
scarring in the right
apex.

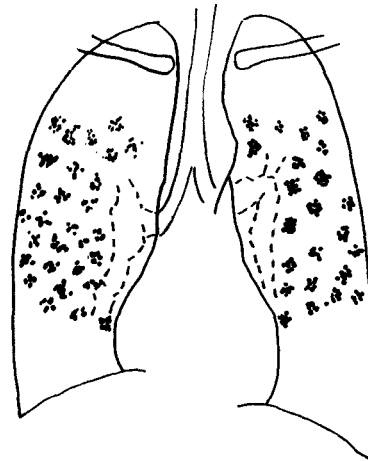
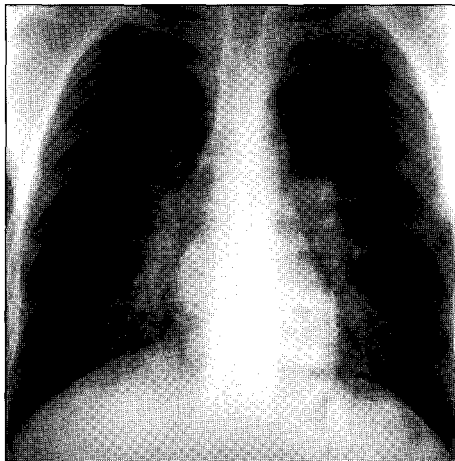


small nodules/infiltrates in the upper lobes. The lesions heal by calcifying with fibrosis of the surrounding lung.

Miliary TB pattern (fig 6.9)

This is a very important pattern to detect as the disease is fatal if untreated. Patients often have non-specific symptoms and signs. Multiple small nodules 2–5 mm in size are detected throughout both lungs from blood borne spread of TB. It is therefore extremely important to exclude miliary tuberculosis in any patient with a miliary infiltrate pattern. The differential diagnosis includes metastases in adults from melanoma, carcinoma of the prostate, pancreas and thyroid, pneumoconioses, sarcoid and lymphoma.

Fig 6.9
Chest radiograph of
a patient with
miliary tuberculosis
demonstrates a
micronodular
infiltrate in both
lungs.



LEARNING POINTS: PULMONARY INFECTIONS

- Lobar pneumonia: air bronchograms in the presence of lobar opacification.
- Broncho pneumonia: diffuse peribronchial opacification.
- Necrotising pneumonia: cavitation in the presence of pneumonia; can progress to a lung abscess.
- Ground glass opacification: in pneumocystis carinii pneumonia, mycoplasma, CMV infection.
- Primary PTB: focal pulmonary opacification and unilateral hilar adenopathy (Ghon focus).
- Secondary TB: upper lobe cavitation, nodular(acinar) infiltrates.

Reference

1. Chapman S, Nakielny R. (eds). In: *Aids to Radiological Differential Diagnosis*. 1995, Saunders, London.

CHAPTER 7

Lung cancer

Peter Corr

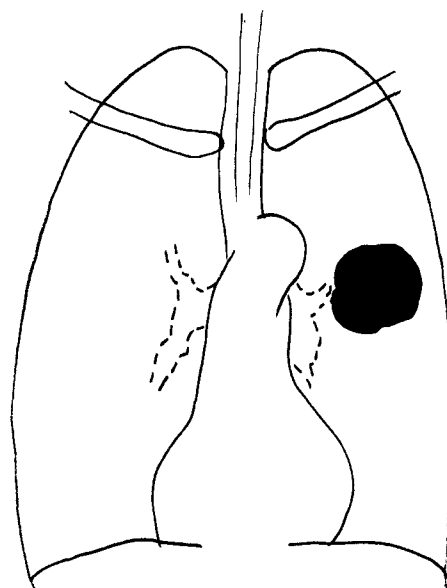
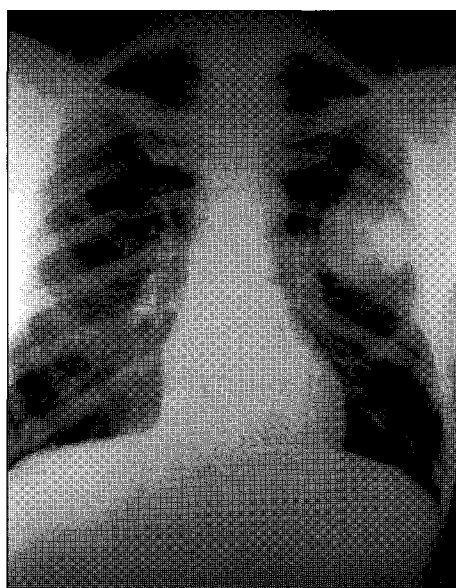
Lung cancer is a serious public health problem in many developing countries due to increasing cigarette smoking especially amongst young women (1). Chest radiographs are important to establish the diagnosis. **The common patterns are:**

- solitary pulmonary nodule
- hilar mass
- lobar atelectasis
- multiple pulmonary nodules.

Solitary pulmonary nodule pattern (fig 7.1)

The commonest cause of a solitary pulmonary mass over 3 cm diameter is a carcinoma. There are usually no specific features to suggest cancer apart from the size of the lesion. The presence of focal “pop corn” type calcification suggests a benign cause such as a hamartoma. The differential diagnosis includes granulomas such as tuberculomas and fungal infections, such as cryptococcoma, benign tumours; and a solitary metastasis. The diagnosis can be confirmed by percutaneous fine needle biopsy using fluoroscopy or bronchoscopic biopsy.

Fig 7.1
Chest radiograph in a patient presenting with haemoptysis demonstrates a left mid zone solitary bronchial carcinoma.



Hilar mass pattern (fig 7.2)

A hilar mass is a common presentation as many cancers involve the proximal bronchi with associated tracheobronchial lymphadenopathy. They present as masses distorting the normal contour of the hilum or causing increased density to the hilum.

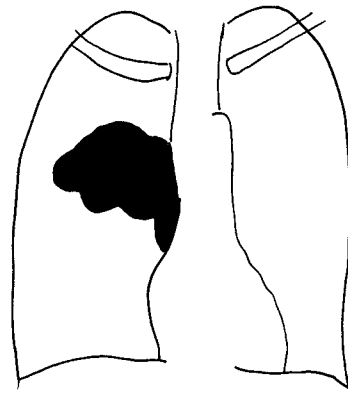
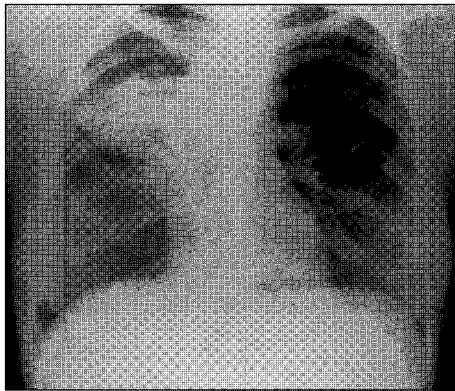


Fig 7.2
Chest radiograph of a patient with haemoptysis demonstrates a large right hilar mass with volume loss of the right lung.

Pancoast's tumour (apical sulcus tumour) (figs 7.3a, 7.3b)

This tumour involving the apex of the lung is often difficult to detect and may often be confused with pleural thickening at the lung apex. Clues to the diagnosis are presence of erosion or destruction of the first three ribs and the presence of a bulging convex inferior to the border to the mass. An apical or lordotic projection is extremely useful to demonstrate this region. The patient may present with pain down the arm from brachial plexus involvement and or involvement of the sympathetic chain with a Horner's syndrome on clinical examination.

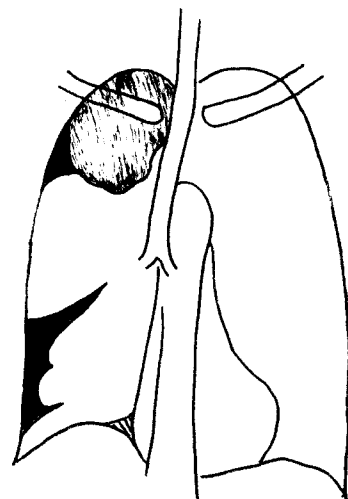
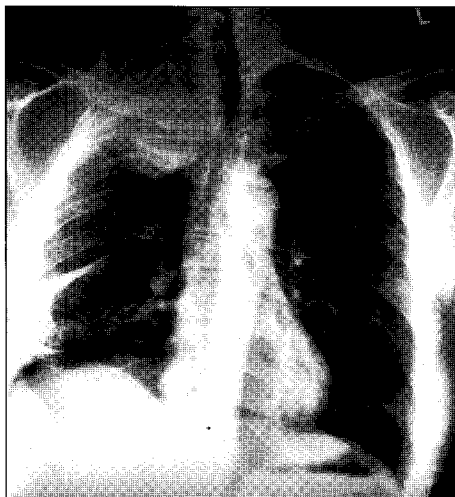
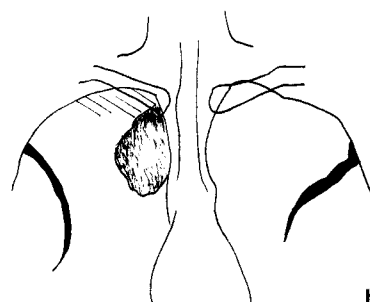


Fig 7.3a, 7.3b
Chest radiograph of a Pancoast tumour in the right apex. Note the elevated right hemidiaphragm from right phrenic nerve palsy from tumour infiltration of the right phrenic nerve. The apical view demonstrates the tumour better (3b).

a

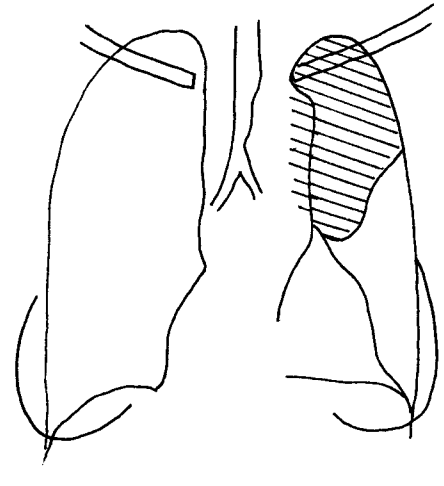
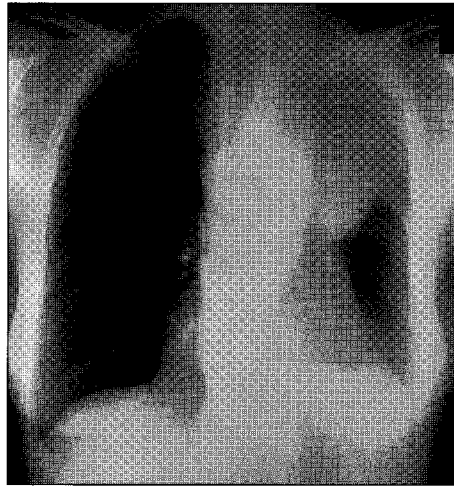


b

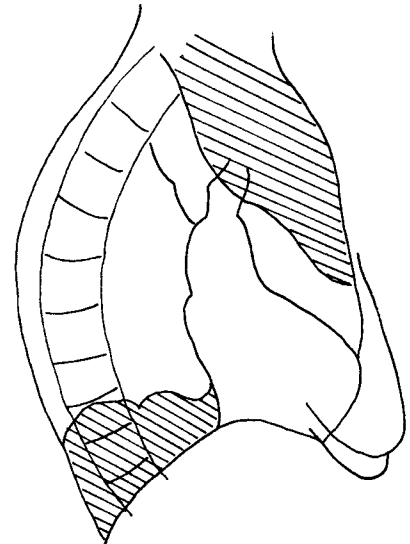
Pulmonary atelectasis pattern (figs 7.4a, 7.4b)

There is a common presentation where there is opacification of a lobe or segment of a lobe with volume loss with no air bronchogram as the airway is obstructed by the tumour with reabsorption of the air distal to the obstruction. This pattern must be differentiated from segmental or lobar pneumonia where there is minimal or no volume loss and air bronchograms are usually present. Where chest infections or pneumonias do not resolve after two weeks of treatment, a follow up chest radiograph is recommended to exclude the possibility of endobronchial obstruction from a tumour or foreign body (in a child).

Fig 7.4a, 7.4b
Chest radiograph demonstrates a left hilar mass and left upper lobe opacification and volume loss caused by a left main bronchus obstruction from a carcinoma.



a



b

Multiple masses pattern (figs 7.5a, 7.5b)

Multiple lung masses or nodules >2 cm diameter are most likely due to metastases or granulomas such as tuberculomas or sarcoid. Metastases commonly originate from the breast, primary lung cancer, colon, kidney, pancreas, thyroid, testis or sarcomas from bone or soft tissue. It is often impossible to differentiate between metastasis and

granulomas, although metastases are of variable sizes and have smooth borders while granulomas are the same size and have irregular borders.

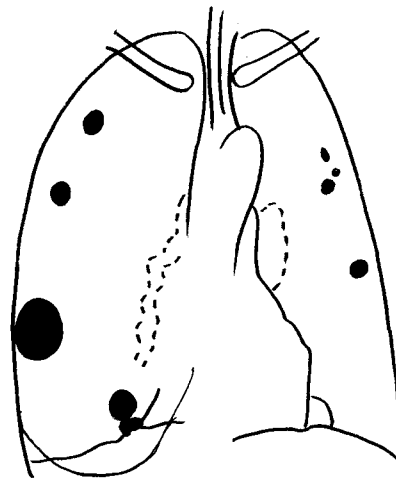
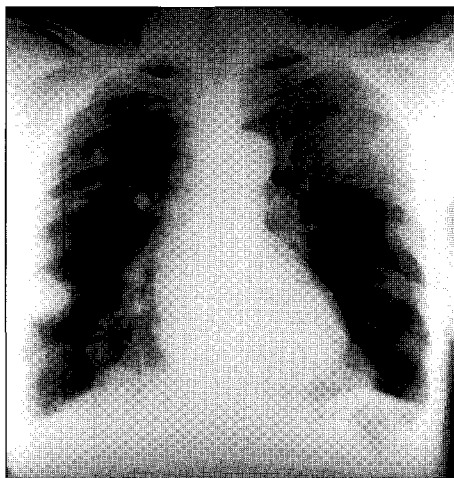
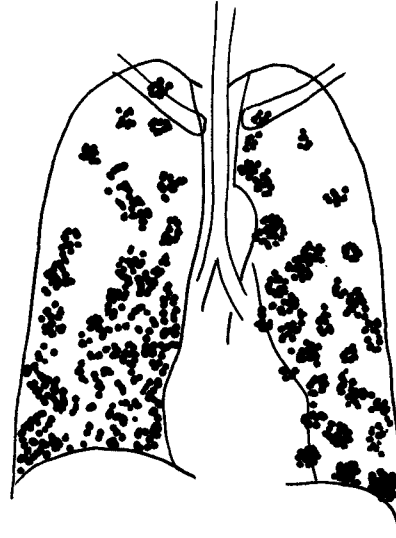
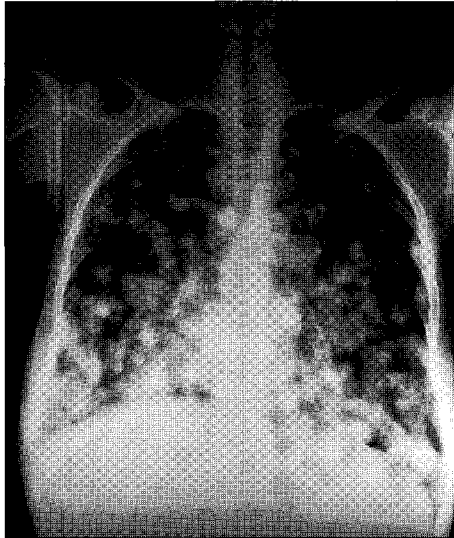


Fig 7.5a, 7.5b
Chest radiographs of two patients with multiple pulmonary metastases. In 5a from choriocarcinoma, in 5b from carcinoma of the breast. Note absent left breast following a mastectomy and destroyed left 5th rib from metastatic disease.

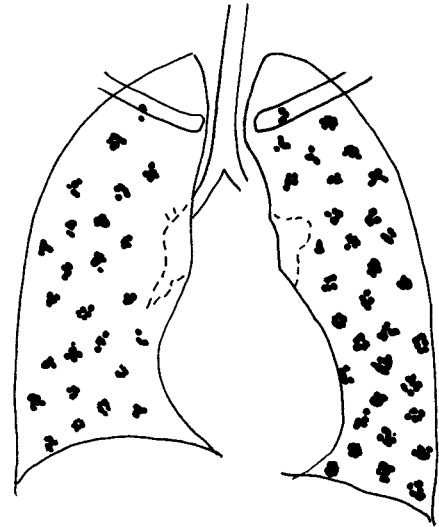
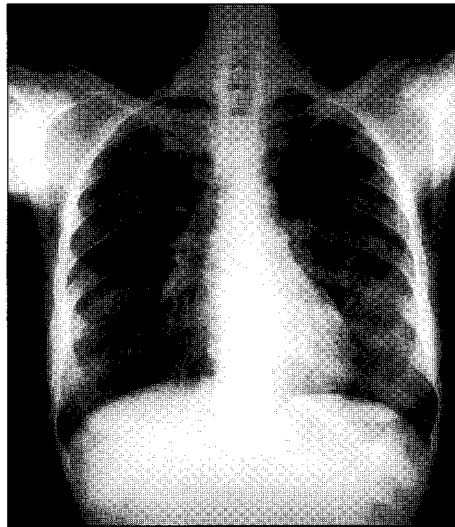
a

b

Multiple micronodular or miliary pattern (fig 7.6)

This is a very important pattern to recognise. These small pulmonary nodules are easy to miss if the radiograph is too dark (over-penetrated film). Patient's symptoms are often non-specific especially with miliary tuberculosis: loss of weight and cough (2). The correct diagnosis is only suspected once the chest radiograph is reviewed. Micronodules are less than 1 cm in diameter. This pattern is also called the "miliary" pattern and is found in metastatic lung disease, lymphoma, miliary tuberculosis, and pulmonary sarcoid. Causes of "miliary" pulmonary metastases include: thyroid, prostate, breast, pancreas, bronchial carcinomas. Miliary tuberculosis micronodules are usually very discrete without associated hilar lymphadenopathy and are distributed diffusely throughout both lungs. On treatment the pattern resolves very slowly compared to the patient's rapid clinical improvement. A common cause in children with AIDS is lymphoproliferative pneumonitis. This is a peribronchial lymphoid reaction to the HIV virus and is common in seropositive children and young adults.

Fig 7.6
Chest radiograph of
a patient with
multiple
micronodular
metastases.



LEARNING POINTS: LUNG CANCER

- Solitary pulmonary nodule >3cm is most likely cancer. Other causes are tuberculomas, benign tumours
- Hilar mass is a common presentation for cancer.
- Pulmonary atelectasis is a common presentation; there is opacification of a segment or lobe with volume loss and absent bronchograms.
- Multiple masses: metastases and granulomas are commonest cause. Cancers are from breast, lung, thyroid, colon, kidney, pancreas, testis and soft tissue sarcoma.
- Micronodular or miliary infiltrates: metastatic disease and TB are common causes. Cancers originate from the thyroid, stomach, prostate, and melanomas.

References

1. Combating the tobacco epidemic. In: *World Health Report 1999*. Geneva WHO.
2. Chapman S, Nakielny R. In: *Aids to Radiological Differential Diagnosis*. 1995. Saunders, London.
3. Hussey G, Chisholm T, Kibel M. Miliary tuberculosis in children: a review of 94 cases, *Pediatr Infect Dis J*, 1991;10:832-6.

CHAPTER 8

Pulmonary hypertranslucency and cystic lungs

Peter Corr

Hyperinflated lung pattern (figs 8.1 & 8.2)

Assessment of lung hyperinflation on chest radiograph is often difficult. Hyperinflation is present if the posterior margins of at least 11 ribs are detected above the diaphragm, which is flattened. An accurate assessment of airways obstruction requires lung

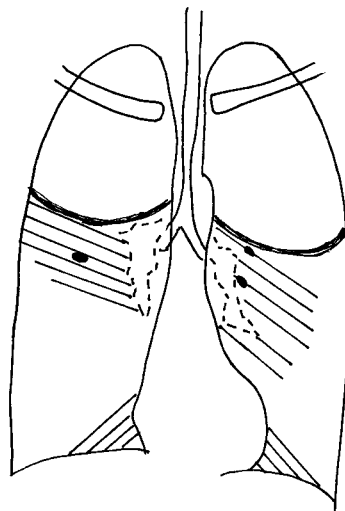
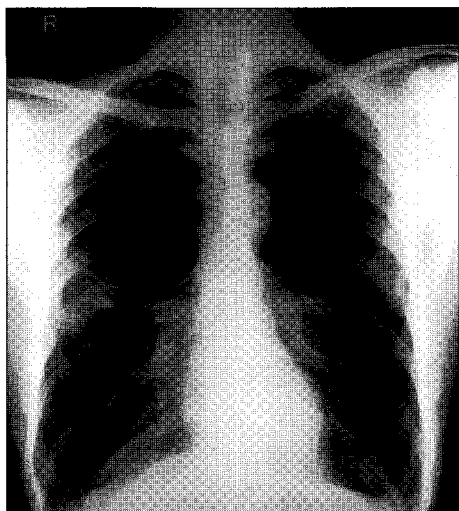


Fig 8.1
Chest radiograph of a patient with hyperinflation and upper lobe bulla from emphysema.

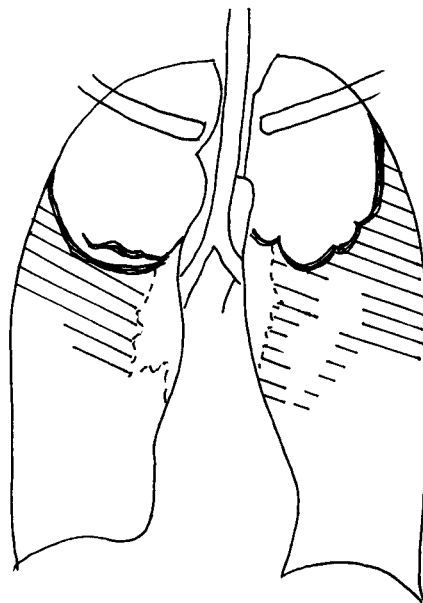
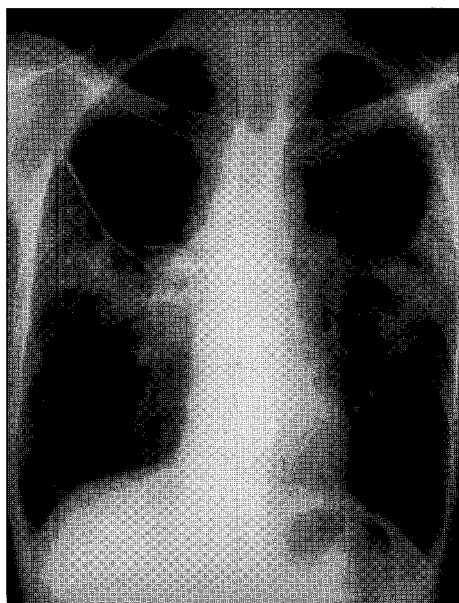


Fig 8.2
Chest radiograph in a patient with emphysema with recurrent chest infection. Note upper lobe bulla with mid zone opacification from pulmonary infection.

function tests, not chest radiographs. Hyperinflation is found in airway obstruction from asthma and chronic obstructive airways disease following cigarette smoking. The presence of focal thin walled cysts in the lung (called bulla) and hyperinflation are seen in emphysema. Patients may have radiographic signs of pulmonary hypertension with prominent central arteries and thin peripheral arteries.

Cystic lung pattern (figs 8.3 & 8.4)

Lung cysts appear as focal translucencies in the lung contained by thin cyst walls which are usually 2 mm or less in thickness. The most common cause is cystic bronchiectasis where there is cystic dilatation of the bronchi usually appearing as multiple basal ring shadows. Often air fluid levels are present if there is superimposed infection. The diagnosis is best made on high resolution CT of the lungs where the bronchial dilatation is better defined. Lung cysts must be differentiated from cavities. Hydatid disease can appear “cystic” if the fluid drains into the bronchi.

Fig 8.3
Chest radiograph of a patient with chronic cystic bronchiectasis demonstrates multiple cysts in the lower lobes many of which containing fluid levels from infected fluid.

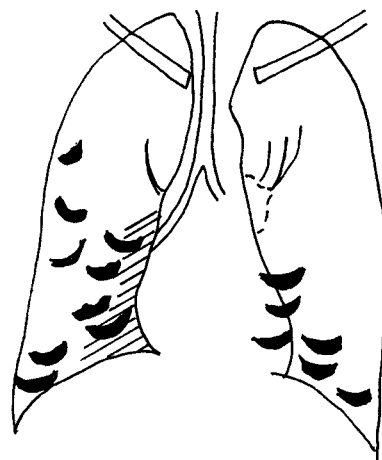
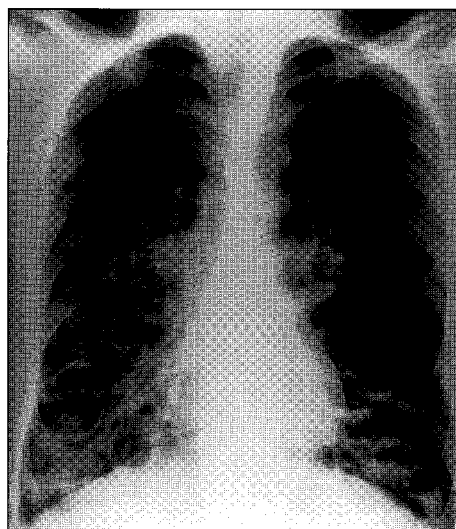
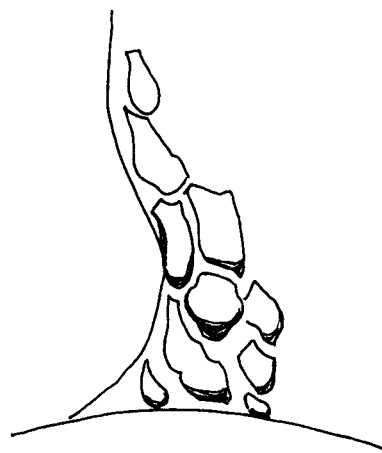
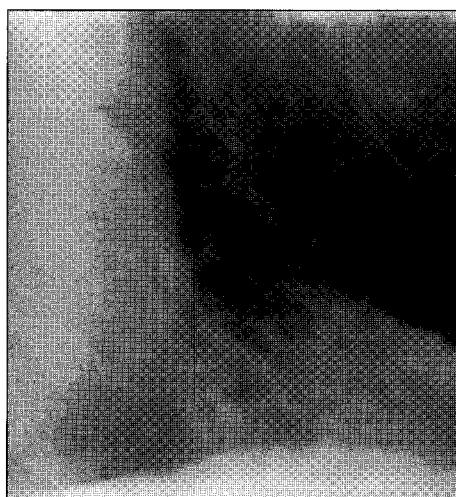


Fig 8.4
Localised view of the left lower lobe of a patient with bronchiectasis demonstrating the multiple dilated bronchi.



Cavities (figs 8.5-8.7)

Cavities occur commonly in pulmonary tuberculosis, necrotising pneumonias or abscesses and cavitating tumours. With cavities the wall of the cavity is irregular and much thicker than 2 mm, usually in the region of 1 cm thick. In necrotising pneumonias or lung abscesses there is often an associated air fluid level within the cavity.

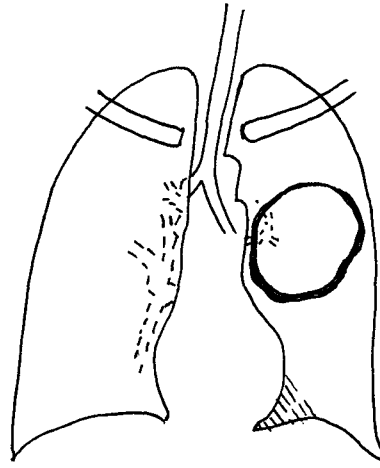
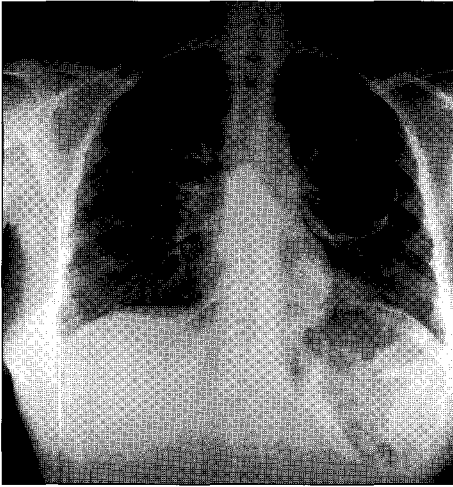


Fig 8.5
Chest radiograph of a patient with active pulmonary TB with a large left mid zone cavity. Note the wall is much thicker than a bulla.

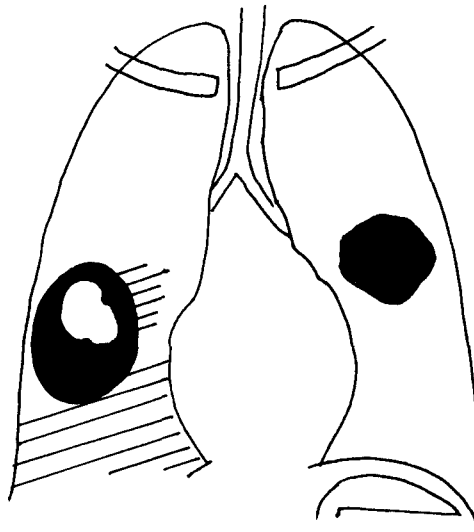


Fig 8.6
Chest radiograph of a patient with pulmonary hydatid disease. The right lower hydatid cyst contents have drained into the bronchial tree leaving a thickened cyst with a nodular border.

Fig 8.7
 Chest radiographs
 of an epileptic
 patient who
 developed two
 abscesses in the
 right lung folowing
 aspiration during a
 seizure.

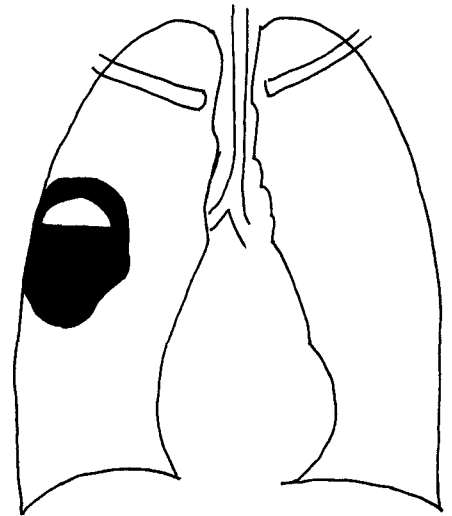
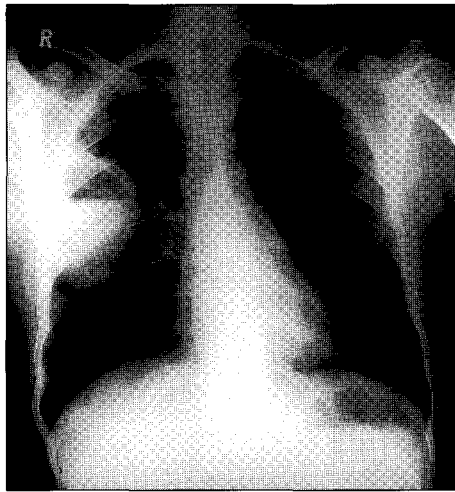
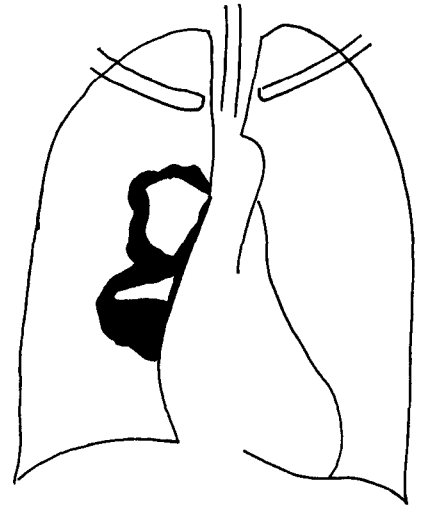
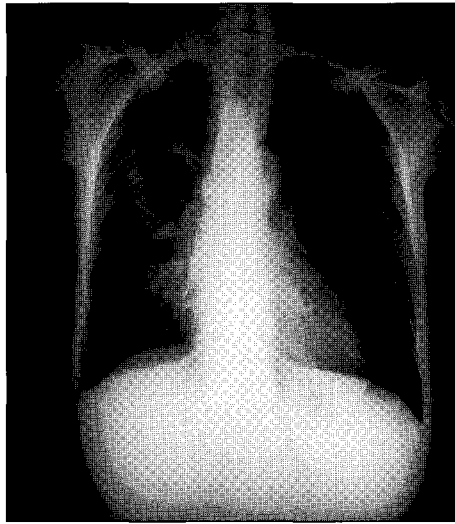
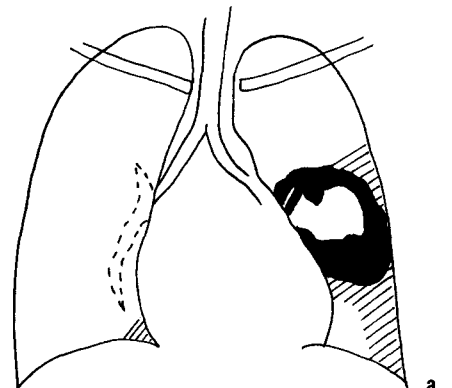
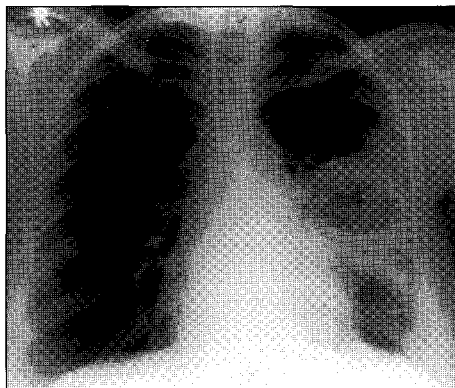


Fig 8.8a & 8.8b
 Chest radiograph of
 a left mid zone
 cavity containing a
 mycetoma which
 moves to the
 dependent region of
 the cavity on
 positioning the
 patient in the left
 decubitus position
 (fig 8.9).



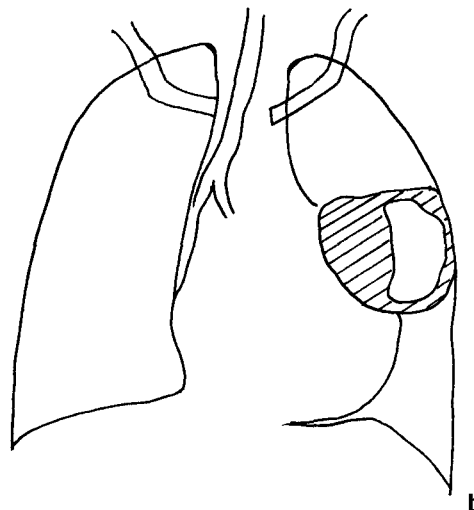


Fig 8.9a & 8.9b
Chest radiograph of the same patient as shown in fig. 8.8, but taken in the left decubitus position.

Mycetomas (figs 8.8 & 8.9)

These are inflammatory masses within prior lung cavities usually from chronic TB. They are due to fungal infections, especially aspergillosis (so called “aspergillomas”). They are not attached to the cavity wall and move on changing the patient’s position to the most dependent position within the cavity. These masses are important to detect as they are an important cause of haemoptysis. Thickening of the lateral wall of the cavity is a good predictor of the presence of a mycetoma. The main differential diagnosis is an intracavitary haematoma. Surgical resection is the treatment of choice.

LEARNING POINTS: HYPERTRANSLUCENCY & LUNG CYST PATTERNS

- Hyperinflated lungs are found in airways obstruction from asthma and chronic obstructive airways disease following cigarette smoking.
- The presence of a bulla and hyperinflation is found in pulmonary emphysema.
- Unilateral hyperlucent lung may be due to technical factors such as chest rotation, a previous mastectomy, or a hyperinflated lung from Swyer James syndrome (bronchiolitis obliterans) or a “ball valve” effect from partial bronchial obstruction by a foreign body especially in young children or rarely an endobronchial tumour.
- Hydatid cysts can mimic bulla.
- A cavity has a thick wall >2mm which is irregular and may contain an air fluid level if there is a communication with the bronchial tree.
- Cavities are found in lung abscess/necrotising pneumonia, tumours especially squamous cancers and pulmonary tuberculosis.
- Mycetomas are intracavitary inflammatory masses of aspergillus. They cause haemoptysis.

References

1. Chapman S, Nakielny R. eds. In: *Aids to Radiological Differential Diagnosis*. 1995, Saunders, London.
2. Sansom HE, Baque-Juston M, Wells AU, Hansell DM. Lateral cavity wall thickening as an early radiographic sign of mycetoma formation. *Eur Radiol* 2000;10:387–90.

CHAPTER 9

Pleural and extra pleural disease

Peter Corr

Pleural effusions (figs 9.1-9.3)

Pleural fluid is first detected in the costophrenic angles and subpulmonic pleural spaces (fig 9.1a). There may be actually 250mls of fluid present before it is detected radiologically. Subpulmonic fluid collections are common particularly in trauma where

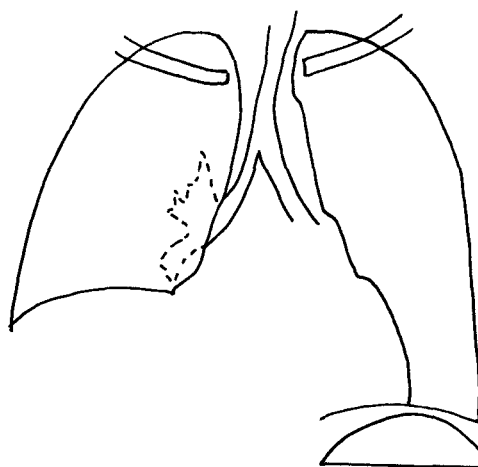
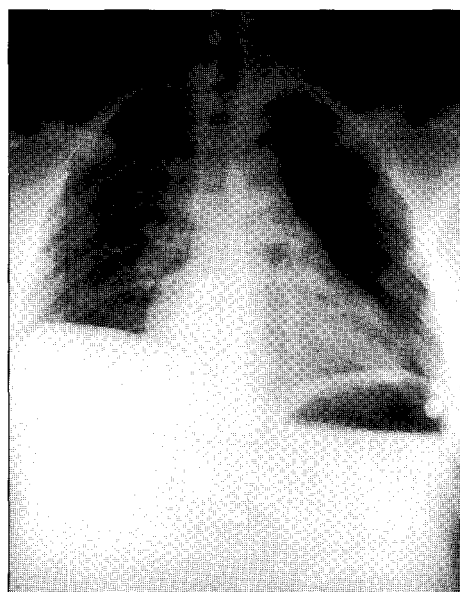
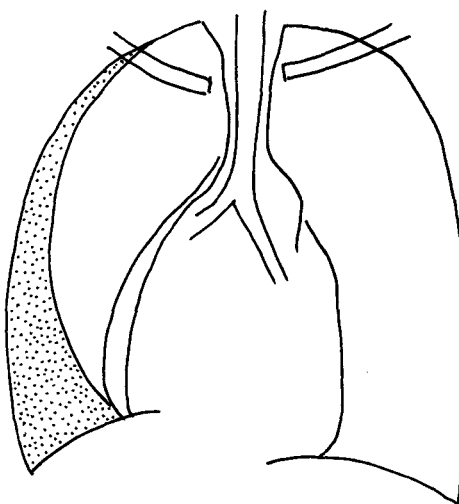
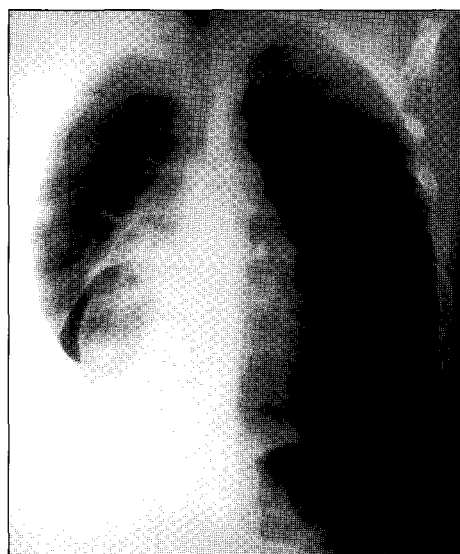


Fig 9.1a, 9.1b
Chest radiograph of a patient with a right subpulmonic pleural collection. Note the pseudo elevated hemidiaphragm with a more lateral apex than normal. On the right side down decubitus film the pleural fluid is now demonstrated laterally. Note the presence of a small medial pneumothorax.

a



b

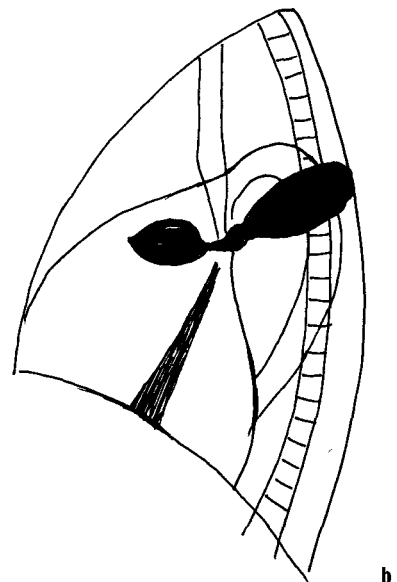
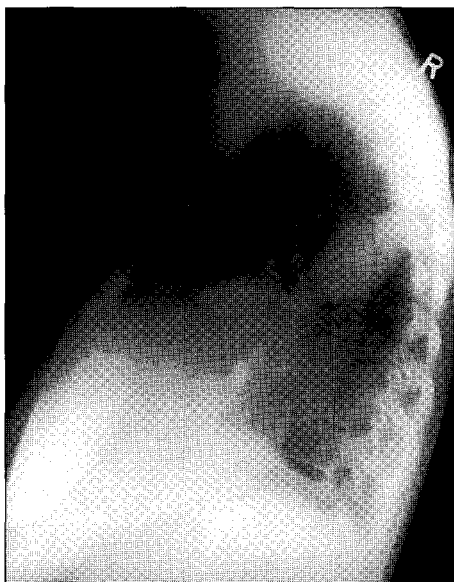
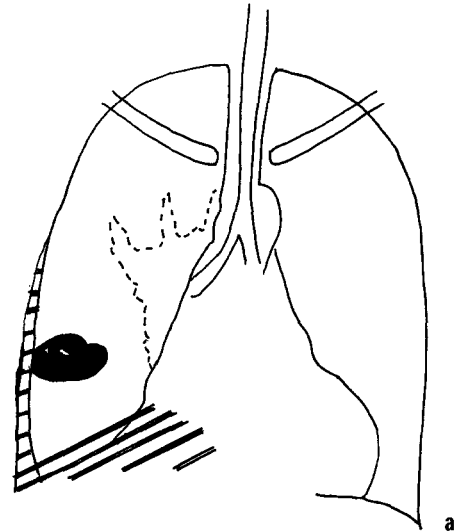
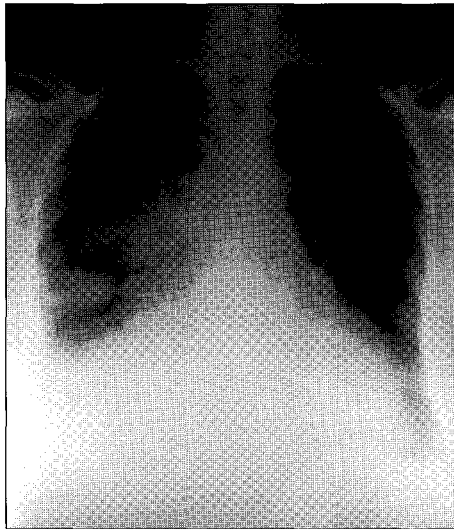
the apparent hemidiaphragm appears elevated and the apex is displaced laterally. To confirm the diagnosis a decubitus chest radiograph will detect the subpulmonic collection (fig 9.1b). Encysted collections are common due to pleural adhesions and can appear like masses on radiograph. Fluid encysts in the fissures and can also appear as a pseudo mass (fig 9.2). The diagnosis becomes more evident on the lateral chest film where the fluid loculates in a “aeroplane propeller” configuration. **Common causes of pleural effusions are:**

tuberculosis

malignancy (either primary or secondary cancer).

Ultrasound using a high frequency transducer (>5 MHz) will confirm the presence of fluid as opposed to a mass. Ultrasound is very useful to direct aspiration of encysted effusions.

Fig 9.2a, 9.2b
Chest radiograph of a patient in cardiac failure demonstrating a “pseudomass” in greater and lesser right fissures from encysted pleural fluid.



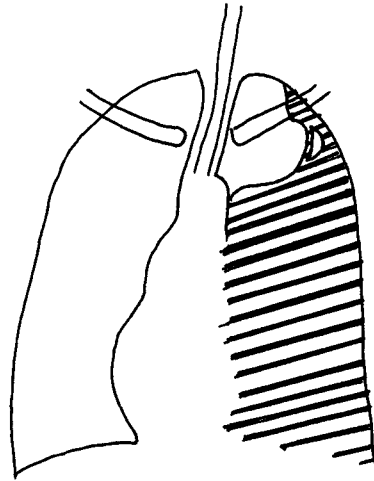
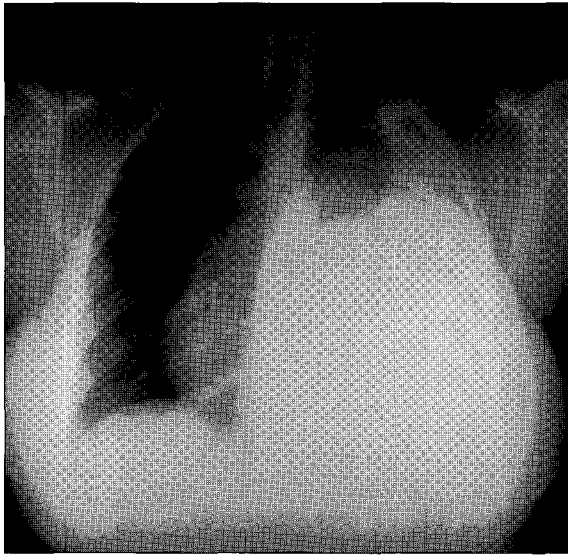


Fig 9.3
Chest radiograph demonstrates a large left pleural effusion with mediastinal shift to the right.

Empyema (figs 9.4a & 9.4b)

Empyema is a collection of pus in the pleural space. The pleura is thickened and bulges outwards. It may not be possible to differentiate between a pleural effusion and empyema on the chest radiograph alone. Empyemas appear echogenic on ultrasound. Ultrasound is excellent in guiding a needle into the the collection for aspiration.

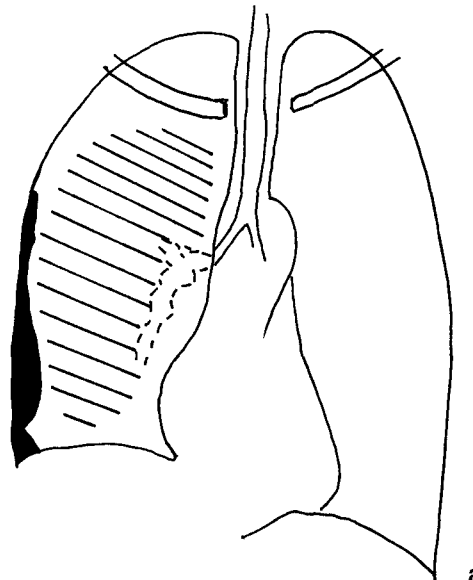
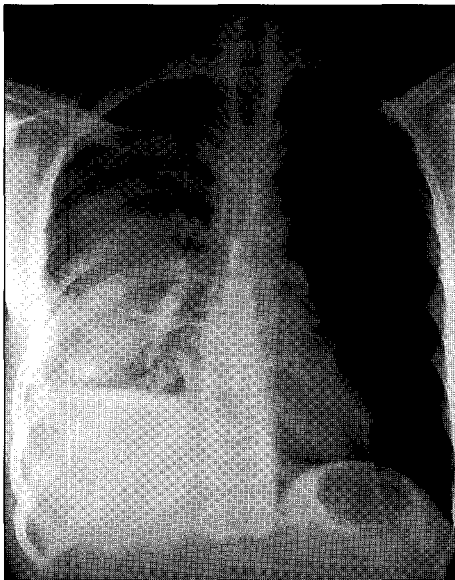
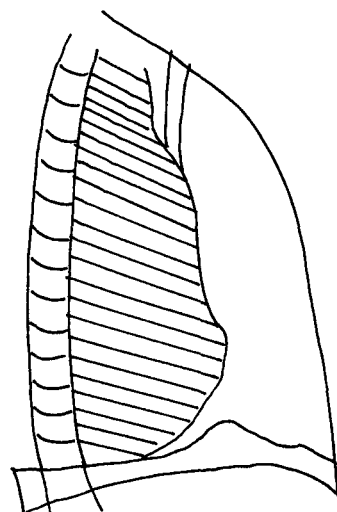


Fig 9.4a, 9.4b
Chest radiograph of a patient with a right empyema. Note the anterior convex margin of the pleural collection suggesting the pus in the pleural space is under pressure.



b

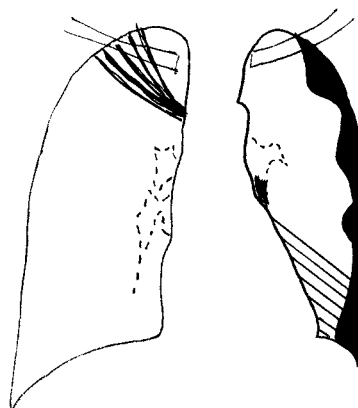
Pleural mass (figs 9.5-9.7)

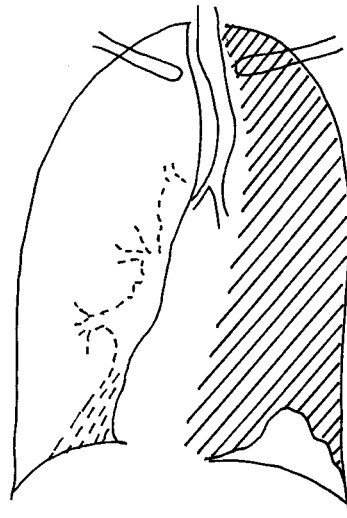
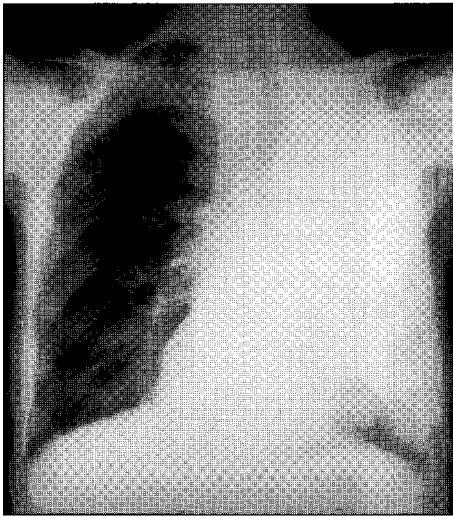
Pleural masses are either benign or malignant. **Malignant pleural masses** include metastases from adenocarcinoma often from breast cancer, lung primary, bowel, ovary or a primary cancer such as a mesothelioma from asbestosis exposure. **Benign masses** include inflammatory masses, fibrosis, benign fibromas and pleural plaques from asbestos exposure. Inflammatory lesions include tuberculosis. It is not possible to differentiate benign from malignant masses. Rib destruction is more common with malignant tumours but is also detected with granulomatous infections such as tuberculosis.

Extra pleural masses

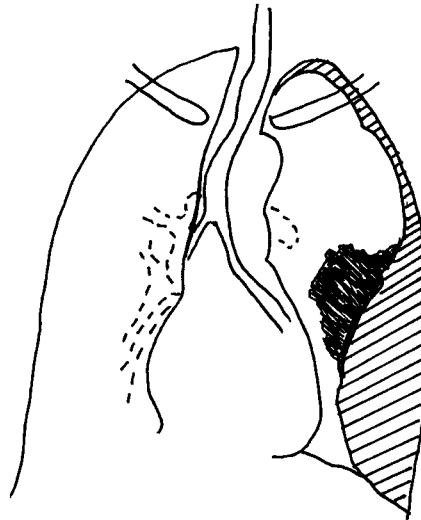
Extrapleural masses which may be associated with rib destruction. Metastatic involvement of the ribs often has an associated soft tissue mass. Similarly chronic infections of the rib such as TB, actinomycosis can be associated with an abscess or granulomatous mass. Plasmacytomas causes localised rib expansion and a soft tissue mass. To differentiate an extrapleural mass from a pleural mass, look at the medial border of the mass. If it is convex medially it is probably extrapleural while if it is concave medially it is probably pleural in origin.

Fig 9.5
Chest radiograph of a patient with breast cancer and pleural metastases. Note right mastectomy from the absent breast shadow and the left peripheral pleural metastases.



**Fig 9.6**

Chest radiograph of a patient with a left pleural mesothelioma. Note mediastinal shift to the left and opacification of the left pleural space.

**Fig 9.7**

Chest radiograph of a patient with left lower zone pleural fibrosis following a haemothorax. Note the crowding of the left lower ribs and the pleural calcification.

LEARNING POINTS: PLEURAL DISEASE

- Subpulmonic effusions result in an apparent elevation of the hemidiaphragm, the diagnosis can be confirmed on an ipsilateral decubitus chest radiograph.
- Common causes of unilateral pleural effusions are malignancy (primary and secondary) and tuberculosis.
- Encysted pleural collections resemble pleural masses; ultrasound can differentiate between a mass and fluid.
- Pleural masses are most commonly adenocarcinoma metastases, mesothelioma, inflammatory masses or benign fibromas.
- Extrapleural masses often have associated rib destruction.

Reference

1. Chapman S, Nakielny R. *Aids to Radiological Differential Diagnosis*. 1995 Saunders, London

CHAPTER 10

Rib lesions

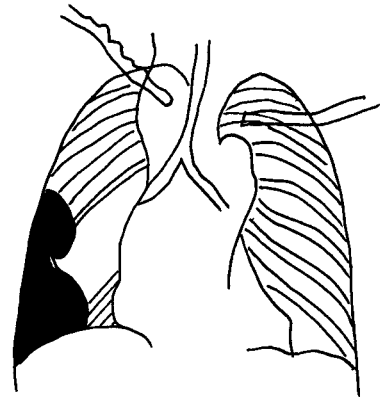
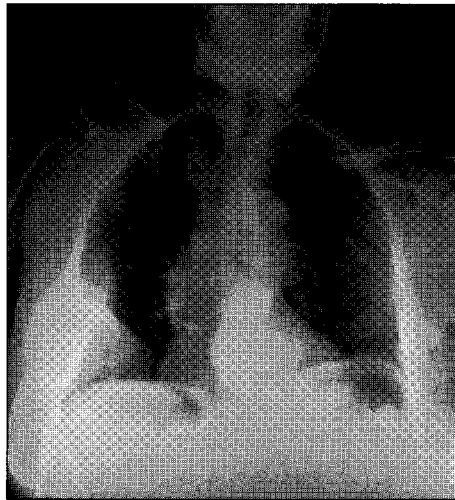
Peter Corr

It is always important to scan the bones of the chest for both focal and diffuse abnormalities. Often the presence of bone lesions will suggest the correct diagnosis of the pulmonary abnormality.

Focal rib lesions

Lytic lesions are usually due to tumours especially metastases or myeloma. They can be difficult to detect initially if the individual rib contours are not carefully traced out from posterior to anterior. The patterns of these lesions appear as if the ribs have been “erased” with a rubber eraser with an associated extrapleural soft tissue mass (fig 10.1). Bronchial carcinoma, especially Pancoast’s tumour at the apical sulcus of the lung, invades the pleura and overlying brachial plexus to cause early lytic destruction of the first and second ribs. Occasionally pleural tuberculosis involves the overlying ribs. With myeloma it is particularly useful to assess other flat bones such as the clavicles and scapulae for similar lesions as the presence of such lesions will suggest the diagnosis.

Fig 10.1
Chest radiograph of a patient with multiple myeloma. There is a soft tissue mass in the right lower zone with destruction of the lower right ribs. A lytic lesion in the right clavicle is noted.



Sclerotic rib lesions in which bone density is increased are especially common with prostate and breast metastases. Occasionally all the ribs become diffusely sclerotic (fig 10.2).

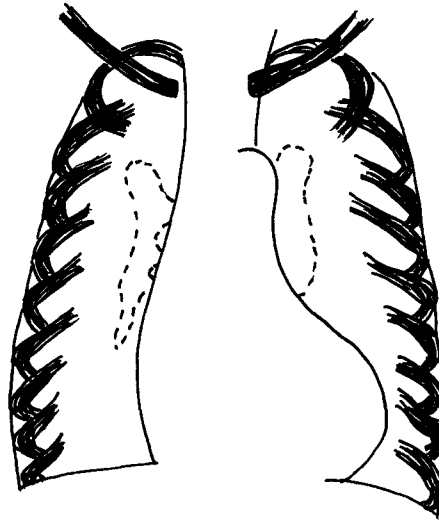
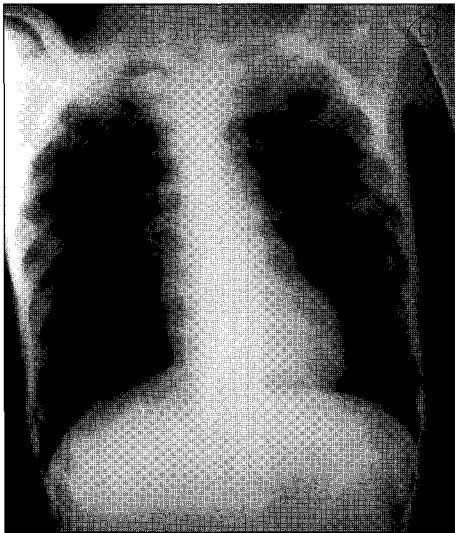


Fig 10.2
Chest radiograph of a patient with diffuse sclerotic metastases in the ribs from carcinoma of the prostate.

Rib erosions usually destroy the superior or inferior rib cortex. Inferior rib notching or erosions are often due to erosion from neurofibromas or collateral vessels in aortic coarctation (fig 10.3). In neurofibromatosis the ribs may appear thin and gracile because of the associated mesodermal dysplasia. Superior cortical erosions are detected in collagen vascular disorders such as rheumatoid arthritis, systemic lupus erythematosus and scleroderma. Erosions of the lateral margins of the clavicles are common in advanced rheumatoid arthritis.

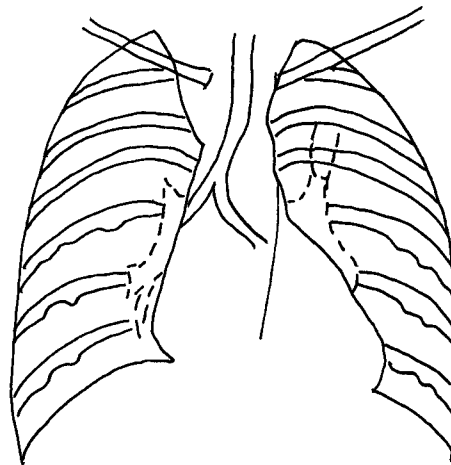
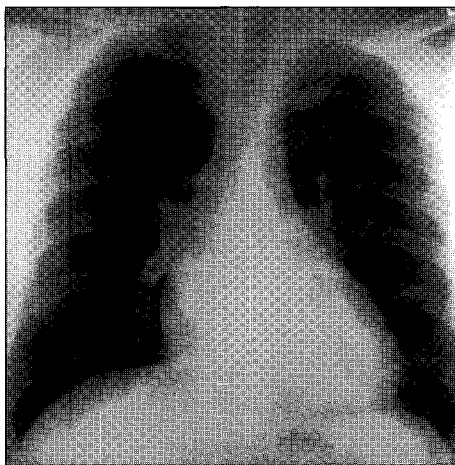


Fig 10.3
Chest radiograph of a patient with coarctation of the aorta. Note left ventricular hypertrophy, small aortic arch and bilateral inferior rib notching of the ribs.

Diffuse rib lesions

Metabolic bone disease, such as osteomalacia, hyperparathyroidism, Paget's disease and rickets in children, may demonstrate bone softening and rib deformity. Microfractures with exuberant callus may be detected in osteomalacia, Cushing's syndrome and Paget's disease.

Diffuse osteopenia or decreased bone density occurs in osteoporosis, osteomalacia, and Cushing's syndrome. Diffuse bony sclerosis occurs in Paget's disease, sclerotic metastases from breast and prostate cancer.

LEARNING POINTS: RIB LESIONS

- Common cause of focal lytic rib lesions are lytic metastases for breast and lung carcinoma, and multiple myeloma
- Common cause of focal and diffuse sclerotic rib lesions are sclerotic metastases from prostate and breast carcinoma, and Paget's disease
- Common causes of rib notching and erosion include coarctation of the aorta, collagen vascular disorders, and neurofibromatosis
- Common causes of decreased bone density are osteoporosis, hyperparathyroidism, osteomalacia, and rickets in children

Reference

1. Chest wall, pleura and diaphragm. Wilson AG, Flower CDR, Verschakelen JA. In: *Diagnostic Radiology: a textbook of medical imaging*. 1997. Eds Grainger RG, Allison DJ. Churchill Livingstone, Edinburgh

CHAPTER 11

Chest trauma

Peter Corr

Good quality radiographs are critical for evaluation of chest trauma patients. An erect chest radiograph is important to detect pneumothorax and haemothorax. If the patient is unable to sit or stand a decubitus chest is useful to detect a pneumothorax and or subpulmonic haemothorax.

Blunt trauma

Bony injury (fig 11.1)

Ribs usually fracture laterally after blunt trauma; the lower six are commonly involved. Fractures in two places may lead to a flail chest. Fractures of the upper four ribs are usually associated with severe blunt injury and vascular injury must be excluded if there is widening of the superior mediastinum. Sternal injuries are detected on lateral coned views of the sternum. It is important to check the thoracic spine carefully for associated fractures in these patients.

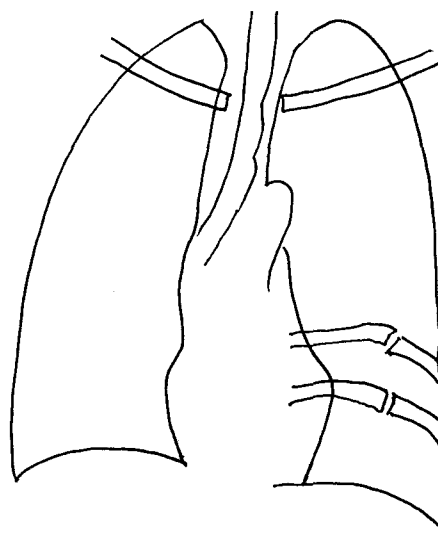
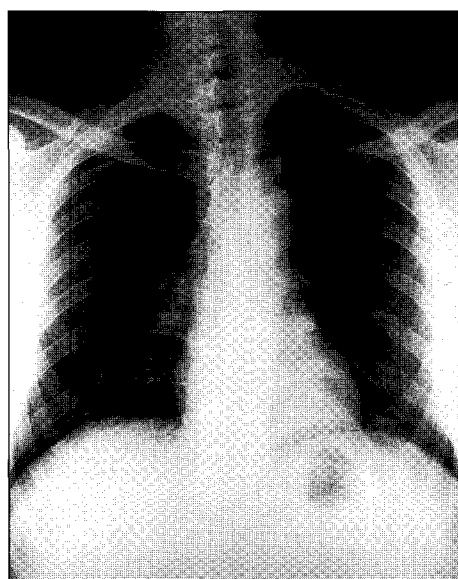


Fig 11.1
Chest radiograph of a patient following chest trauma. Note fractures of the left 8th and 9th ribs.

Pneumothorax (figs 11.2a, 11.2b)

This is an important diagnosis and can be detected as a fine white line of the visceral pleura with absent peripheral lung markings. Pneumothoraces can also be medial or subpulmonic in position. A decubitus chest radiograph will identify a shallow pneumothorax. If the pneumothorax is large and there is mediastinal shift away from

the side of the injury, the pneumothorax is considered to be under tension. This is extremely important to recognise because if left undetected this can be rapidly fatal. A clue to the presence of a pneumothorax is gas in the soft tissues, which appears as low density streaks (surgical emphysema).

Fig 11.2a
Chest radiograph of a patient who sustained a penetrating chest wound. Note the shallow left pneumothorax.

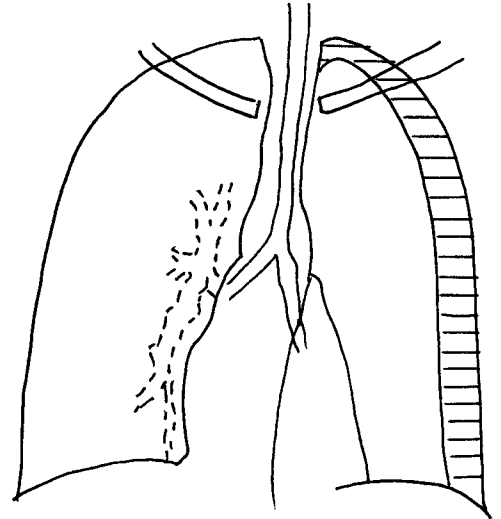
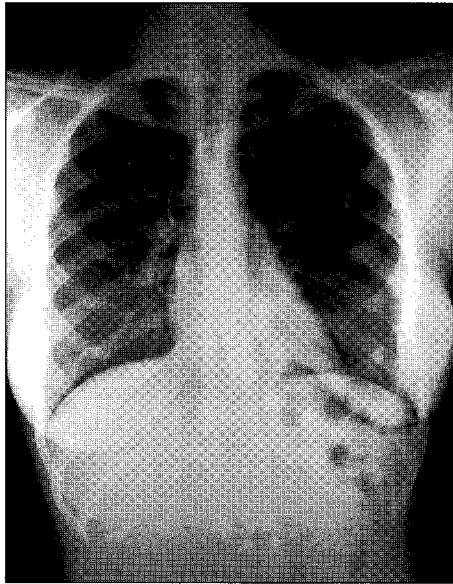
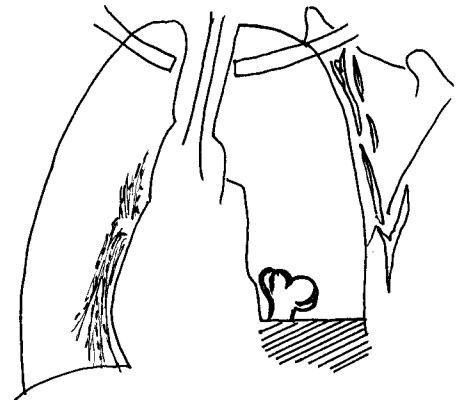


Fig 11.2b
Chest radiograph of a patient with a large left haemopneumothorax, with mediastinal shift to the right and surgical emphysema in the chest wall.



Haemothorax (fig 11.3)

Blood collects inferiorly in the pleural spaces beneath the lung to form a subpulmonic haemothorax. The hemidiaphragm appears elevated with the apex of the dome displaced more laterally than normal. A decubitus chest radiograph with the affected side dependent will confirm the presence of blood in the pleural space.

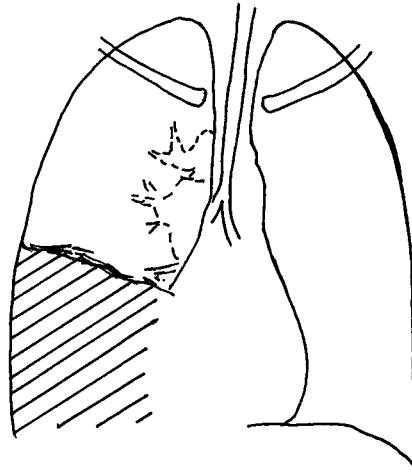
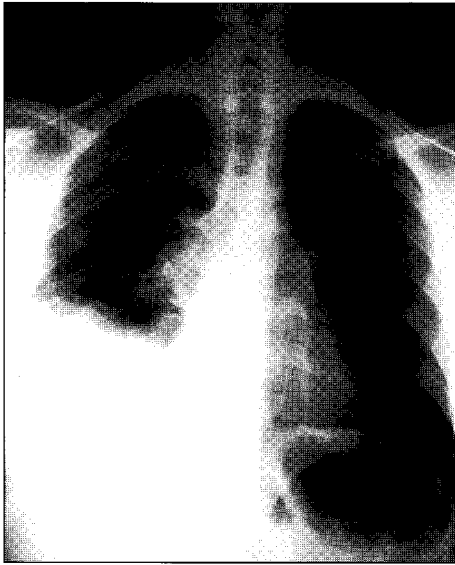


Fig 11.3
Chest radiograph of a patient with a right subpulmonic haemothorax. Note the "pseudo elevated" right hemidiaphragm.

Pulmonary lesions (fig 11.4)

Haematomas within the lungs appear as pulmonary masses that resolve over days. They can be differentiated from other masses by reviewing serial radiographs. Contusion appears as opacification of the lungs.

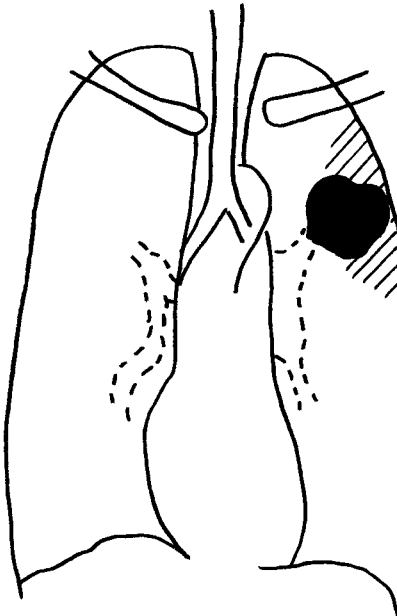
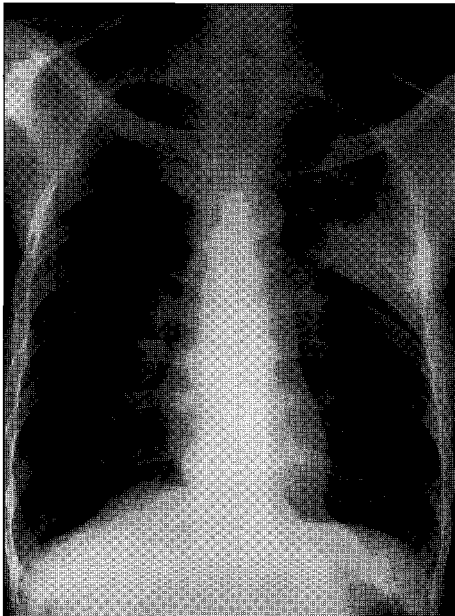


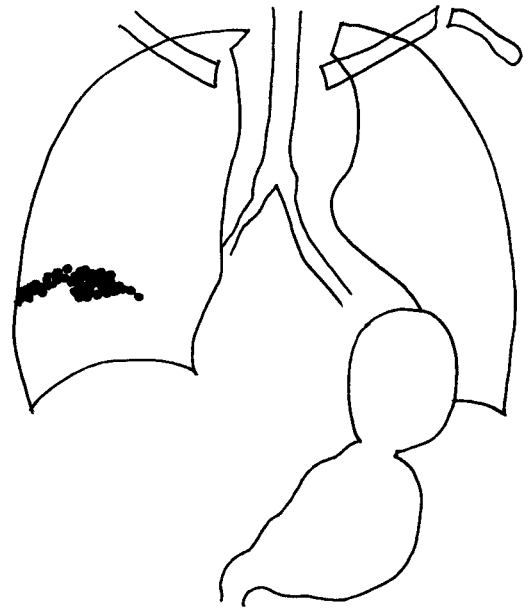
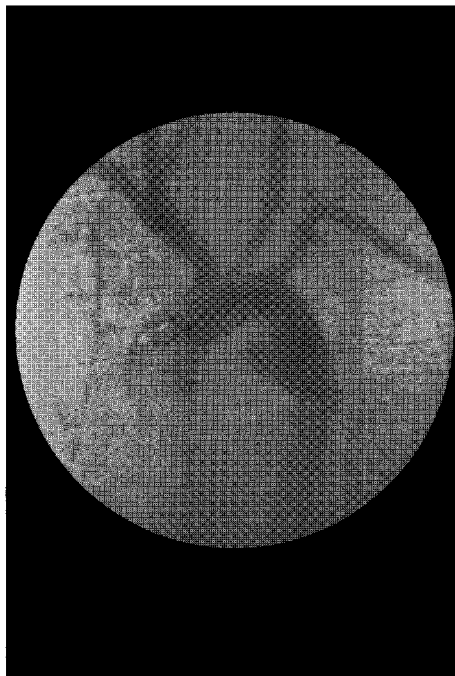
Fig 11.4
Chest radiograph of a patient with a left upper lobe pulmonary haematoma following blunt trauma.

Vascular injuries (figs 11.5a, 11.5b)

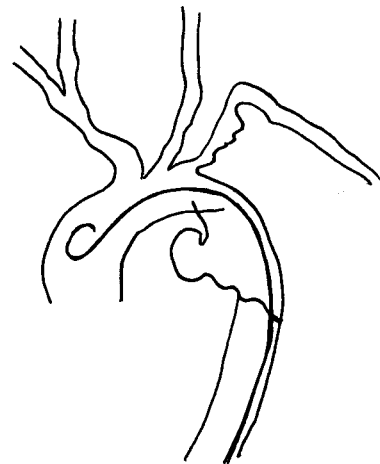
Aortic arch injuries are important to detect especially after deceleration injuries to the chest and mediastinum. The aorta tears transversely at the level of the ductus arteriosus. The important signs on the chest radiograph are:

- A widened mediastinum >8 cm wide on an erect film
- Loss of the normal mediastinal outline

Fig 11.5
Chest radiograph of a patient following blunt trauma to the sternum, demonstrates a markedly widened superior mediastinum with loss of the normal aortic arch outline from a false aneurysm of the aortic arch and a rupture of the left hemidiaphragm and herniation of the stomach in the chest. Fig 11.5b demonstrates the false aneurysm of the proximal descending aorta.



a



b

- Fracture of the upper ribs
- Apical cap from haematoma

If these signs are present the patient should be transferred for aortography to confirm the diagnosis. It is important to measure the superior mediastinum on an erect chest radiograph if possible. Note a supine radiograph may falsely suggest a wide mediastinum.

Trauma to the tracheobronchial tree

Injury to the trachea or bronchi leads to a pneumomediastinum and pneumothorax and often a collapsed lung.

Diaphragmatic injury (fig 11.6)

Rupture of the diaphragm usually involves the left hemidiaphragm. Diaphragmatic tears can often be asymptomatic until bowel herniation and incarceration occur. The diagnosis is easily missed and this can be fatal. Contrast studies of the stomach and left colon demonstrate the position of these structures in relation to the diaphragm and, to detect herniation.

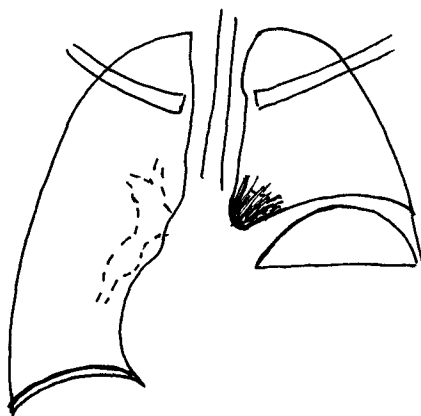
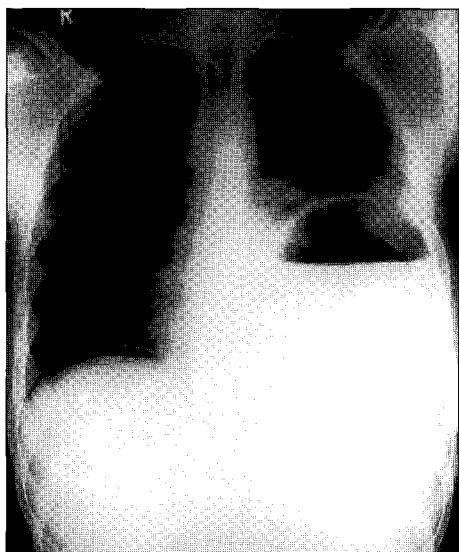


Fig 11.6
Chest radiograph of a patient following blunt trauma demonstrates a large left traumatic diaphragmatic hernia and free intraperitoneal air below the right hemidiaphragm.

Penetrating trauma

Penetrating trauma often causes haemopneumothorax and pneumomediastinum. Vascular injury will be detected by a widened mediastinum; the patient will require arteriography to confirm the diagnosis. Injuries may involve the oesophagus with perforation (fig 11.7) A swallow using water-soluble contrast will detect the leak.



Fig 11.7
Barium swallow of a patient who sustained a knife wound to the superior mediastinum demonstrates an oesophageal perforation and leak of contrast into the mediastinum.
Important: Use water-soluble contrast medium when perforation is suspected!

Injuries of the lower chest may cause a defect in the diaphragm with the possibility of bowel herniation and incarceration. This is very dangerous and needs to be detected early when asymptomatic by checking the diaphragm carefully in a patient with a history of penetrating injury.

LEARNING POINTS

- Pneumothorax is best detected on erect chest or decubitus chest radiograph.
- Mediastinal shift away from the injured side indicates a tension pneumothorax
- Subpulmonic haemothorax causes apparent elevation of the hemidiaphragm with a laterally displaced dome. Diagnosis confirmed on a decubitus chest radiograph.
- Aortic injury suggested by a wide mediastinum >8 cm diameter, loss of normal mediastinal outline, apical cap. Requires aortography to confirm the diagnosis.
- Diaphragmatic injury is often missed, it commonly involves the left hemidiaphragm. Requires contrast study of stomach and left colon to confirm the diagnosis.
- Always attempt to assess mediastinal widening on an **erect chest radiograph** if possible.

Reference

1. Chest trauma Flower CDR. In: *Diagnostic Radiology—a textbook of medical imaging*. Eds Grainger RG, Allison DJ, 1997, Churchill Livingstone, Edinburgh.

CHAPTER 12

Pulmonary AIDS

Peter Corr

There has been a rapid increase in AIDS in many countries in Africa and Asia over the last ten years. An understanding of common presentations of pulmonary opportunistic infections and AIDS related neoplasms is important as 80% of AIDS patients will have respiratory disease (1).

Tuberculosis patterns in AIDS (fig 12.1)

The human immunodeficiency virus is synergistic with tuberculosis (2). Tuberculosis infection is progressive, often extrapulmonary and multifocal in patients with AIDS (2). Adults present with a pattern similar to primary TB in children with unilateral hilar or mediastinal adenopathy and lower lobe opacification. Cavities are uncommon. Progressive disease follows spread along the bronchial tree in addition to blood borne spread. Patients often have skeletal or abdominal tuberculosis as well (2).

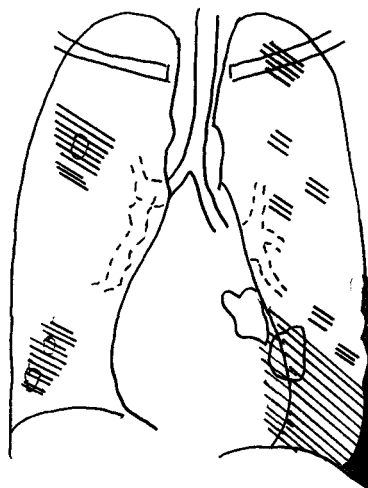
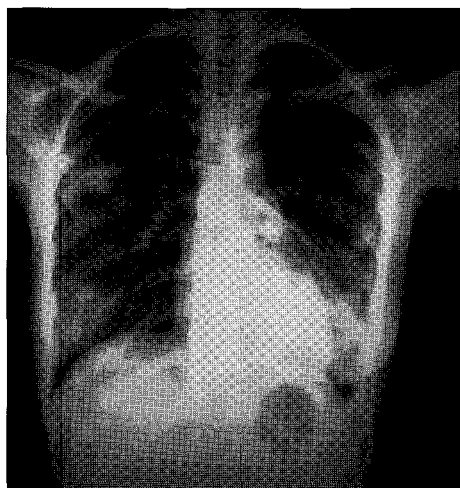


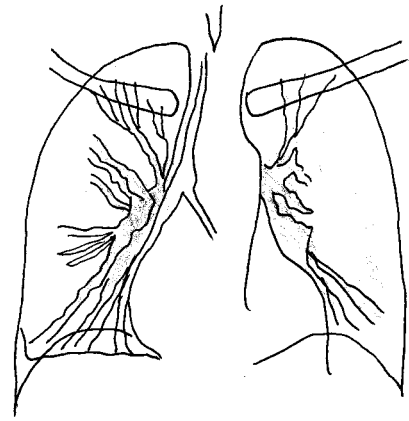
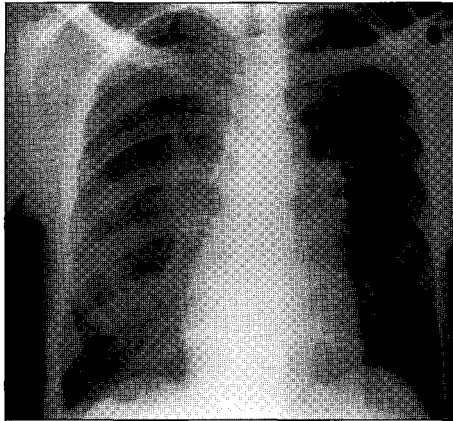
Fig 12.1

Chest radiograph of an AIDS patient with pulmonary TB. Note the predominantly lower lobe distribution of the opacification with perihilar cavities.

Ground glass pattern (fig 12.2)

The cause is pneumocystis carinii and or cytomegalovirus infection. Patients have a “ground glass” opacification of the lungs that obscures the pulmonary vessels. It starts around the hila and spreads outwards. It is easy to miss in early cases but the clue is the lung vessels appear blurred and ill defined. Lymphadenopathy is rare in pneumocystis infection. However not all patients have the typical “ground glass” pattern, a large number also have consolidation, nodules, cavitating masses, subpleural cysts and spontaneous pneumothorax (3).

Fig 12.2
Chest radiograph of
a patient with
pneumocystis
carinii infection.
Note the perihilar
“ground glass”
opacification.



Bacterial infection patterns

Bacterial pneumonias are very common in AIDS patients especially streptococcus pneumoniae, haemophilus influenza, pseudomonas infection because the HIV infected lymphocytes cannot destroy bacteria with capsules. A destructive pneumonia or bronchiectasis often results from inadequate treatment especially in children.

Viral infection patterns

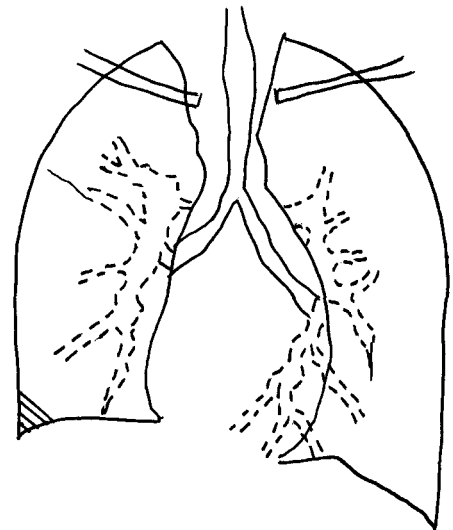
Cytomegalovirus infection and herpes simplex cause a bronchiolitis and pneumonitis with a “ground glass” pattern identical to pneumocystis carinii infection.

Neoplasm patterns (fig 12.3)

Kaposi's sarcoma is a vascular tumour that occurs in up to 25% of all patients with AIDS. It is caused by the herpes type 8 virus and causes masses in the skin, bowel and lungs (4). In the chest, nodules are noted spreading from the hila peripherally along the pulmonary vessels and bronchi in “tongue” like projections.

Non Hodgkin's lymphoma presents in the lungs of these patients with pulmonary nodules or cavitating masses, however lymph node involvement in the hila and mediastinum is uncommon.

Fig 12.3
Chest radiograph of
an AIDS patient
with pulmonary
Kaposi's sarcoma.
Note the hilar
lymphadenopathy
and the thickened
bronchovascular
markings in the
perihilar regions.



Lymphoproliferative interstitial pneumonia (LIP) pattern (fig 12.4)

Benign lymphocyte proliferation is a common cause of the miliary or small nodular pattern in AIDS patients (5). It is a benign response by lymphocytes to the HIV virus and is found in children and young adults. It is important to consider this pattern in the differential diagnosis of miliary tuberculosis.

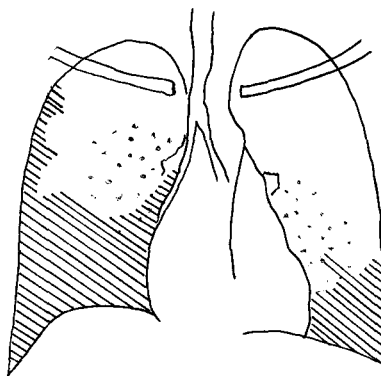


Fig 12.4
Chest radiograph of an AIDS patient with lymphocytic interstitial pneumonitis. Note the miliary nodules in the lungs.

LEARNING POINTS: PULMONARY AIDS

- Tuberculosis is progressive, multifocal and often extrapulmonary in AIDS patients. Cavities are uncommon in severe immunosuppression. Lower lobe infiltrates and hilar adenopathy are common in adults.
- Pneumocystis pneumonia is common in severe immunosuppression. Ground glass opacification is common in both pneumocystis and cytomegalovirus infections.
- Bacterial infection is very common, and leads to destructive pneumonia and bronchiectasis.
- Viral infections especially cytomegalovirus and herpes simplex infections are common.
- Kaposi's sarcoma is the commonest neoplasm. Multiple nodules along the bronchovascular bundles are noted on chest radiographs and CT.
- Lymphocytic interstitial pneumonia (LIP) is a benign lymphocytic response to HIV. It causes multiple small pulmonary nodules. Main differential is miliary TB.

References

1. Fauci A. The AIDS epidemic-considerations for the 21st century. *NEJM* 1999;341:1046–1050.
2. Havlir D, Barnes P. Current concepts: Tuberculosis in patients with the human immunodeficiency virus infection. *NEJM* 1999;340:367–373.
3. Boisselle PM, Crans CA, Kaplan MA. The changing face of pneumocystis carinii pneumonia in AIDS patients. *AJR* 1999;172:1301–1309.
4. Antman K, Chang Y. Kaposi's sarcoma-review article. *NEJM* 2000;342:1027–1033.
5. Berdon WE, Mellins RB, Abramson SJ, Ruzal-Shapiro C. pediatric HIV infection in its second decade-the changing pattern of lung involvement. Clinical, plain film, and CT findings. *Rad Clin N America* 1993;31:453–463.

CHAPTER 13

Paediatric chest

Peter Corr

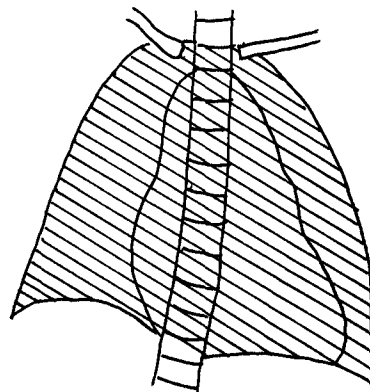
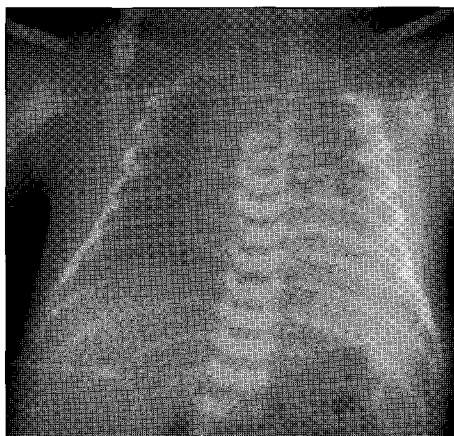
Children present challenges for the radiographer. The child will often not keep still for the radiograph so immobilization is important. This requires an assistant wearing a lead rubber apron and gloves to hold the child by the outstretched arms. Chests are taken in the AP position. You must be aware of the radiation exposure to the gonads of the child, and a lead strip must be placed over the gonadal area.

NEONATAL CHEST PATTERNS

Ground glass pattern in premature babies (fig 13.1)

A bilateral “ground glass” appearance to the lungs is found in premature babies with hyaline membrane disease and viral infections. Hyaline membrane disease is due to insufficient surfactant. Lung volumes are small and air bronchograms are commonly detected.

Fig 13.1
Chest radiograph of a premature infant with hyaline membrane disease. Note the pulmonary opacification and small volume lungs.



“Bubbly” or cystic lungs

Cystic lesions in the lungs of a neonate may be due to congenital diaphragmatic herniation of bowel that requires urgent surgery. This is due to a congenital defect in the left hemidiaphragm (fig 13.2). There is usually mediastinal shift to the opposite side. Usually both the compressed lung and contralateral lung are hypoplastic. Cystic adenomatoid malformation of the lung is a congenital malformation of the lung that usually presents as a cystic mass. There is usually no mediastinal shift away from the lesion.

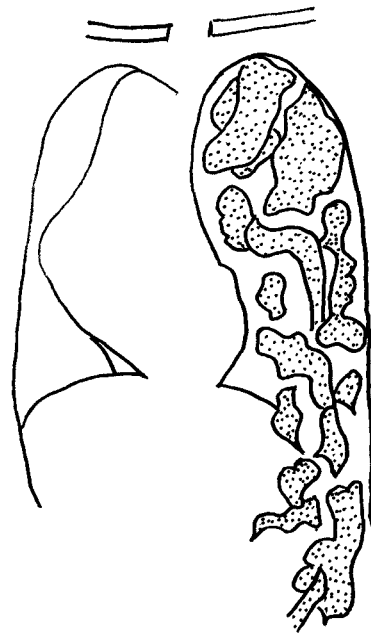
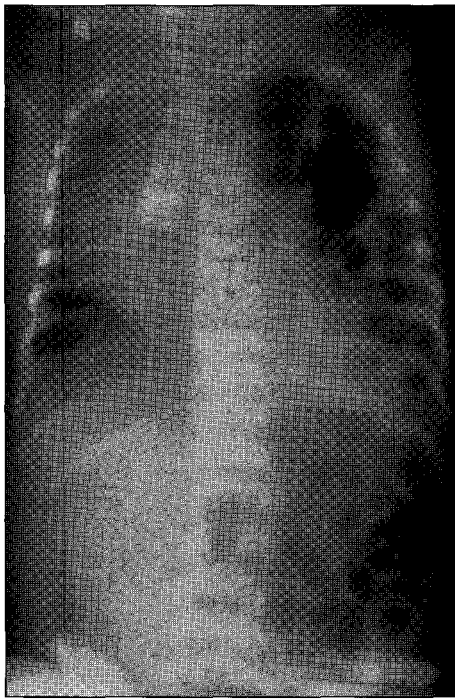


Fig 13.2
Chest radiograph of an infant with respiratory distress from a congenital diaphragmatic hernia in the left hemithorax.

Meconium aspiration pattern (fig 13.3)

The lungs are hyperinflated with perihilar opacities in these full term babies who have aspirated meconium into their lungs during labour. There are streaky linear opacities in both lungs.

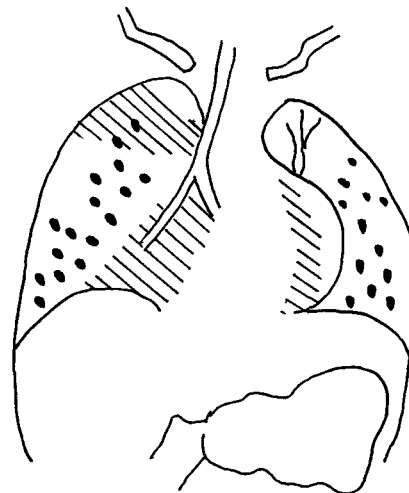
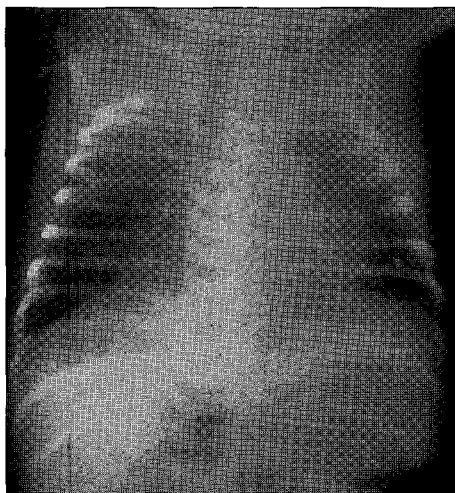


Fig 13.3
Chest radiograph of a neonate with respiratory distress following meconium aspiration. Lungs are hyperinflated with perihilar infiltrates.

INFANT CHEST PATTERNS

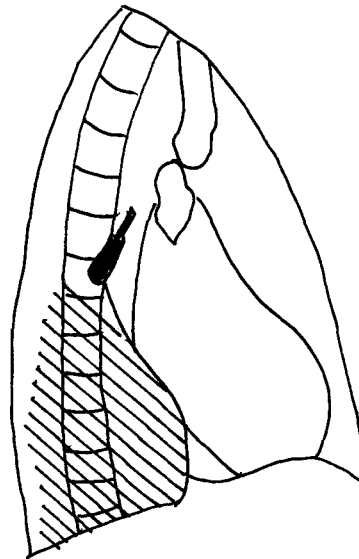
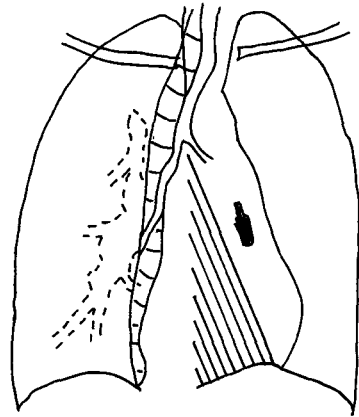
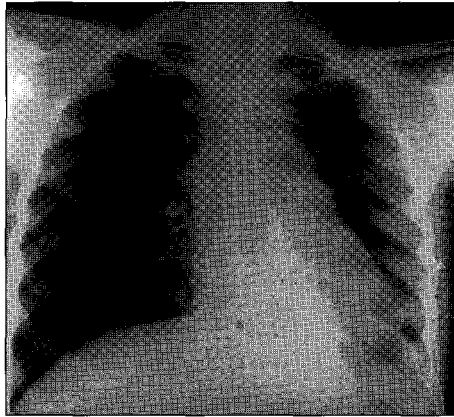
Bilateral air trapping pattern

Hyperinflated lungs with peribronchial infiltrates are found in bronchiolitis from viral infections especially the respiratory syncytial virus and adenovirus infections. It is important to exclude pneumonia, which may require antibiotic treatment.

Unilateral lung hyperinflation pattern

Unilateral lobar or segmental hyperinflation should suggest a foreign body in the bronchus causing a “ball valve” effect with air trapping in the lobe. By taking chest radiographs in inspiration and expiration the hyperinflation can be accentuated. Similarly lobar atelectasis in a child is due to an impacted foreign body until proven otherwise (fig 13.4).

Fig 13.4
Chest radiograph of a child who aspirated a ball point pen tip (foreign body) into his left lower lobe bronchus causing lower lobe atelectasis.

**Bronchopneumonia pattern**

This is a very common pattern of peribronchial opacification of both lungs from viral and or bacterial infection. It is important not to confuse this pattern with cardiac failure where the heart is enlarged and there are often pleural effusions.

Pulmonary atelectasis pattern (figs 13.4a & 13.4b)

Unilateral volume loss and opacification of a lobe or segment of the lung may be due to bronchial obstruction from a foreign body, mucus plug as seen in pertussis, asthma, or enlarged hilar nodes in tuberculosis.

CHILDHOOD PNEUMONIA PATTERNS

Round pneumonia (fig 13.5)

This pattern is common in childhood infection and can mimic a mass in the lung. The key to this pattern is the presence of air bronchograms within the opacification. Round pneumonias occur because infection spreads easily through the interalveolar foramina.

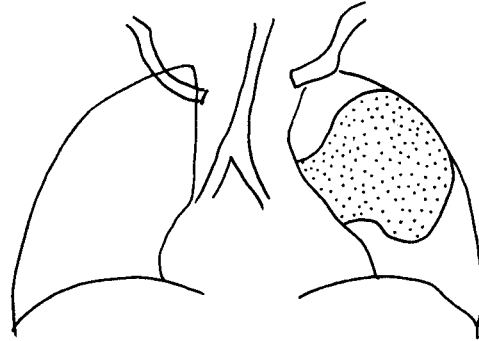
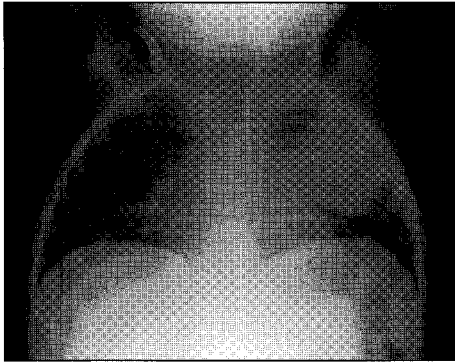


Fig 13.5
Round pneumonia.

Staphylococcal pneumonia pattern (figs 13.6a & 13.6b)

This is a serious pneumonia in children. There are features of a bronchopneumonia with multiple cavities or cysts. It is important to recognise this pattern because untreated or treated with the incorrect antibiotic will lead to very serious complications such as pneumothorax and empyema.

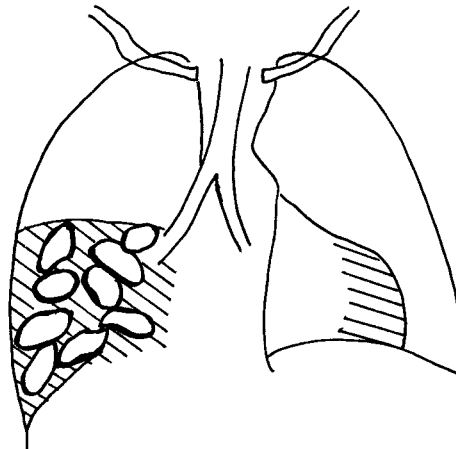
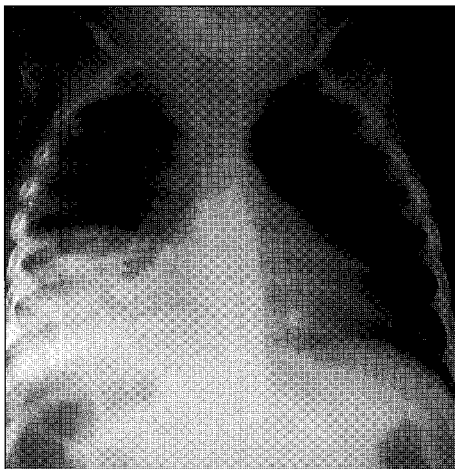
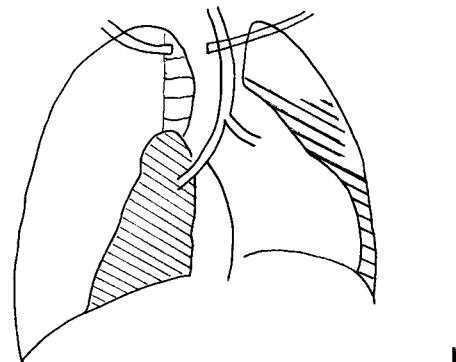


Fig 13.6a, 13.6b
Chest radiograph of an infant with staphylococcal pneumonia in the right lower zone with cavitation. A tension pneumothorax with collapse of the right lung is a recognised complication 6b.



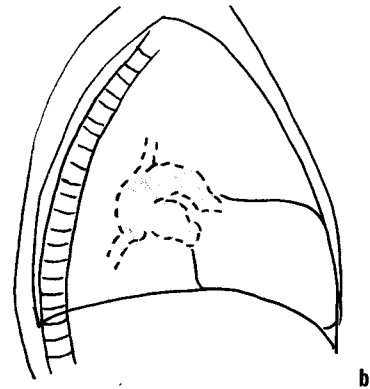
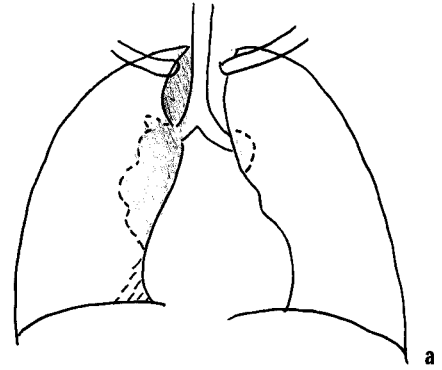
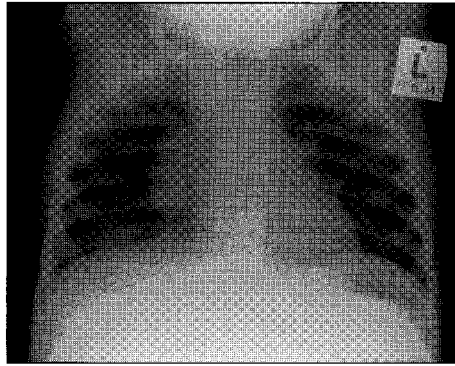
a

b

Primary TB pattern (figs 13.7a & 13.7b)

This pattern is detected in primary tuberculosis where there are large unilateral hilar and mediastinal lymph nodes which may cause bronchial obstruction and lobar atelectasis. The primary lung lesion is often not detected as an area of focal pulmonary opacification (Ghon focus).

Fig 13.7
Chest radiograph of an infant with primary TB demonstrates right hilar and paratracheal lymphadenopathy.



LEARNING POINTS: PAEDIATRIC LUNG PATTERNS

- Hyaline membrane disease presents in premature babies with small volume lungs and ground glass opacification.
- Bubbly lungs in a neonate must suggest congenital diaphragmatic herniation if there is mediastinal shift to the opposite side.
- Meconium aspiration syndrome results in hyperinflated lungs with a streaky appearance in full term infants following meconium aspiration.
- Bilateral air trapping in infants should suggest bronchiolitis.
- Unilateral hyperinflation or lobar atelectasis of a lung or lobe should suggest an impacted foreign body in the bronchial tree.
- Round pneumonias in children can mimic lung masses but they often have bronchograms.
- Staphylococcal pneumonia presents with cavitating bronchopneumonia or cyst formation. Serious complications of pneumothorax and empyema can occur if not recognized early and treated.

CHAPTER 14

Cardiac disease

Peter Corr

Cardiac size (fig 14.1)

The heart size is normally 50% or less of the thoracic diameter in adults as measured from the inner borders of the lower ribs. It is important to use an erect chest film, preferably a PA film, with a good inspiration. A film focal distance of 180cm is important for cardiac assessment. A poor inspiration and or a supine film is suboptimal as it results in the heart having an apparently increased transverse diameter and apparent cardiomegaly. In children up to 12 years of age the maximum heart size is 60% or less of the internal thoracic diameter.

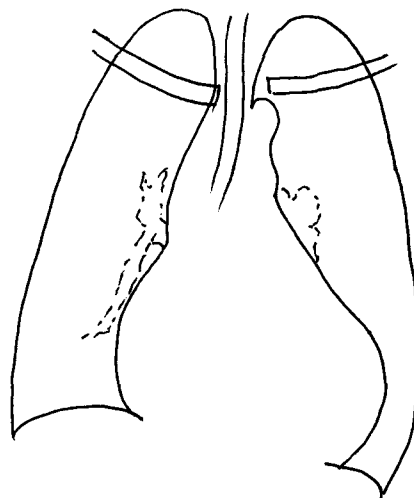
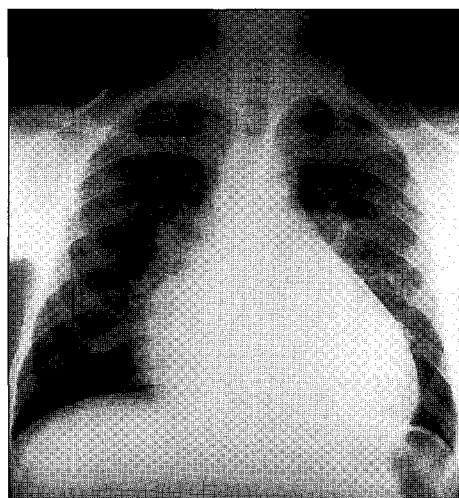


Fig 14.1
Chest radiograph of
a patient with
cardiomegaly.

Cardiac silhouette enlargement (fig 14.2)

Enlargement of the cardiac silhouette may be due to cardiomegaly or pericardial effusion. Pericardial effusion gives the heart a globular appearance with loss of the normal cardiac contour (fig 14.3). The diagnosis of pericardial effusion can be made by ultrasound examination using a 2MHz transducer. There is a hypoechoic fluid collection in the pericardium surrounding the heart. **Common causes of pericardial effusions are:**

- **infection**—viral, pyogenic and tuberculous
- **neoplastic**—metastatic disease and direct invasion from breast and lung cancer
- **trauma**—haemopericardium or sympathetic effusion

Tuberculous pericarditis can be identified by detecting strands of fibrin in the pericardial effusion. As the effusion resolves pericardial constriction may occur. This can be identified as faint calcification of the pericardial lining on the PA chest radiograph.

Fig 14.2
Chest radiograph of
a patient with a
pericardial effusion.
Note the globular
contour of the
cardiac shadow.

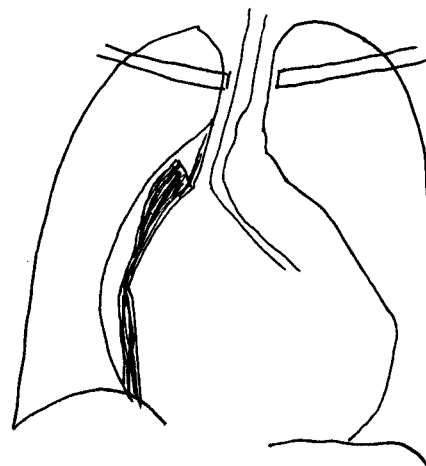
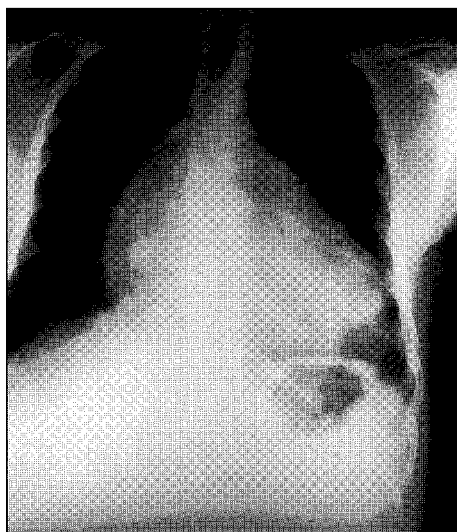
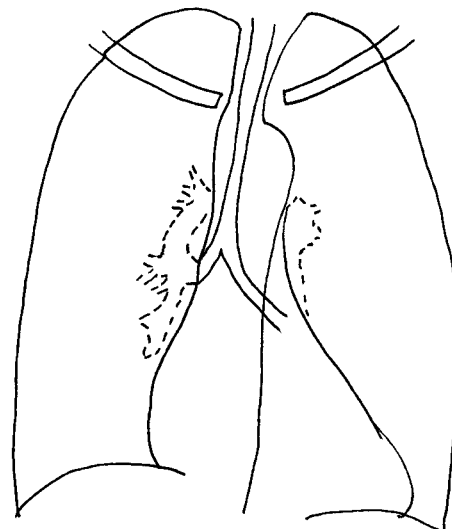
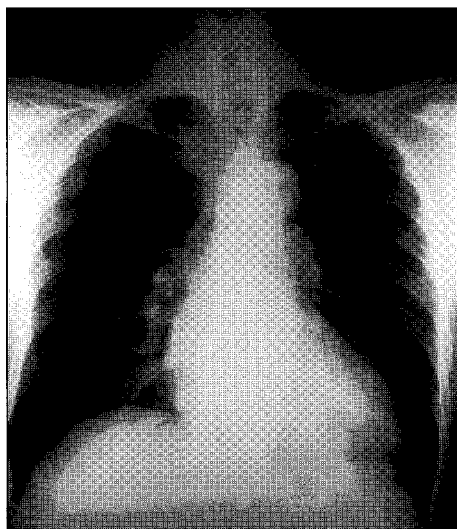


Fig 14.3
Chest radiograph of
a patient with
hypertension with
left ventricular
cardiomegaly. Note
how the left cardiac
border slopes
towards the left
costophrenic angle.



Mitral valve disease

Mitral valve disease causes enlargement of the left atrium and right ventricle following either mitral valve stenosis or incompetence as the end result of rheumatic heart disease. Enlargement of the left atrium is detected as a double shadow behind the right atrium on the PA chest radiograph with splaying of the carina of the trachea and posterior displacement of the oesophagus on barium swallow.

Aortic valve disease

Aortic valve stenosis causes left ventricular hypertrophy that is recognized as left displacement of the cardiac apex on the PA chest radiograph. Aortic valve incompetence, usually following rheumatic fever or infective endocarditis leads to left ventricular dilatation.

Cardiac failure pattern (figs 14.4 & 14.5)

Left ventricular failure initially causes pulmonary venous distension in the upper lobes and constriction of the pulmonary veins in the lower lobes. As the venous pressure

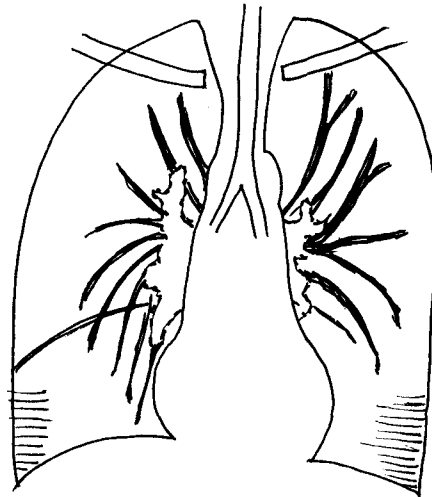
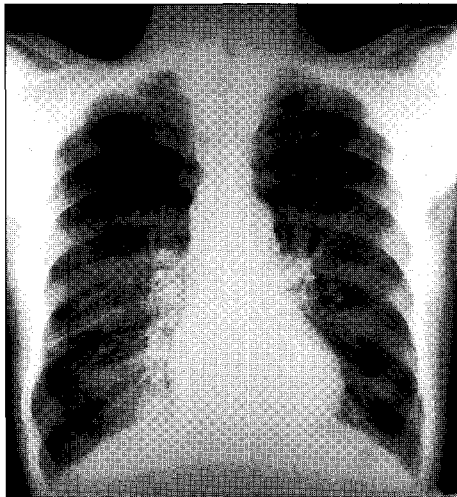


Fig 14.4
Chest radiograph of a patient with interstitial pulmonary oedema. Note the septal lines and prominent upper lobe pulmonary veins.

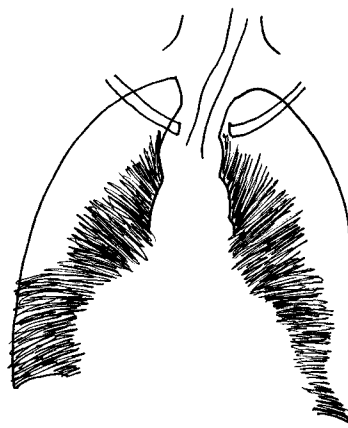
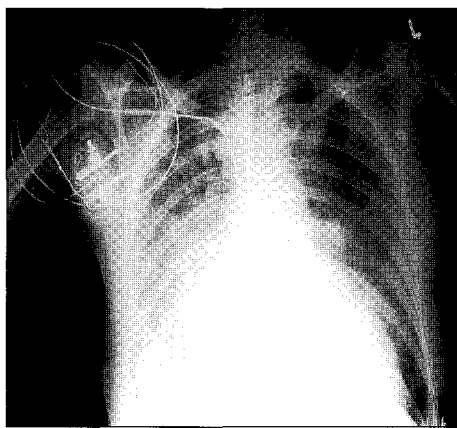


Fig 14.5
Patient in acute pulmonary oedema demonstrates pulmonary opacification and dilated upper lobe veins.

rises, there is perihilar oedema, detected as blurring of the hilar vessels and perihilar opacification. Pleural effusions develop at the costophrenic angles, then septal lines form at the CP angles.

Septal lines are 1–2 cm long and 1 mm thick in the region of the costophrenic angles. They represent distended lymphatics and are an early sign of **interstitial pulmonary oedema**. As the cardiac failure progresses there is perihilar opacification (“bat wing” distribution) which represents **alveolar pulmonary oedema**. Pulmonary oedema usually resolves rapidly over hours with diuretic and anti failure treatment. This pattern can be used to differentiate alveolar oedema from other air space opacification from pneumonia or pulmonary haemorrhage.

Pulmonary plethora pattern

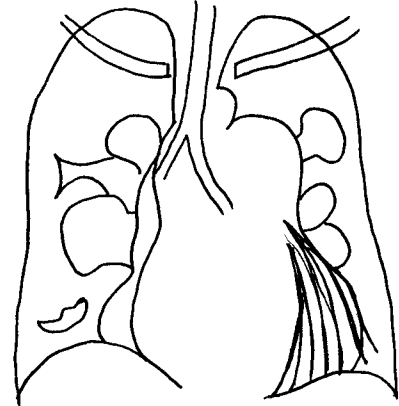
Plethora means increased blood flow and is usually due to left to right intracardiac shunts such as an atrial septal defect, ventricular septal defect and patent ductus arteriosus. Pulmonary arteries are dilated from the hila out to the periphery of the lungs. This pattern should not be confused with pulmonary venous dilatation that involves only the upper lobes.

Pulmonary oligoemia pattern

This pattern is often difficult to recognise unless you have a history of cyanotic heart disease to suggest the correct diagnosis. The lungs have diminished pulmonary blood

flow however the bronchial arteries often enlarge to compensate for the pulmonary oligoemia and the lungs may appear plethoric. Pulmonary oligoemia is detected in the “3 T’s”: Tetralogy of Fallot, truncus arteriosus, and transposition of the great vessels. It is also seen in reversed left to right intracardiac shunts (ASD with pulmonary hypertension: Eisenmenger’s syndrome fig 14.6).

Fig 14.6
Patient with pulmonary hypertension from an atrial septal defect (Eisenmenger syndrome). Note cardiomegaly, with dilated pulmonary arteries centrally and peripheral pruning.



LEARNING POINTS: CARDIAC DISEASE

- Cardiomegaly >50% cardio thoracic ratio in adults, >60% in children less than 12 years.
- Remember cardiac silhouette enlargement may be due to cardiac dilatation, hypertrophy and pericardial effusion (globular contour). Pericardial effusion can easily be diagnosed by ultrasound.
- Signs of cardiac failure are upper lobe pulmonary vein distention, blurring of the perihilar vessels and pleural effusions and septal lines.
- Signs of pulmonary oedema are septal lines and perihilar opacities that often resolve within hours on anti-failure treatment.

CHAPTER 15

Mediastinal masses

Peter Corr

The mediastinum can be divided into superior, anterior, middle, and posterior compartments.

Superior mediastinum

The superior mediastinum is superior to the level of the aortic arch. Masses in this region include retrosternal thyroid masses and aneurysms of the ascending aorta and great vessels. Retrosternal goitres cause displacement of the trachea, extend inferiorly from the neck, and may have focal calcification within them. The diagnosis can be confirmed by ultrasound of the neck or by using A common cause of a superior mediastinal mass on the right is a dilated brachiocephalic artery in an elderly patient. Here the diagnosis can be easily confirmed by ultrasound. The important point to remember is that this is a normal aging phenomenon and not to do any further investigations on these patients.

Anterior mediastinum

This region is between the heart and ascending aorta and the sternum and inferior to the aortic arch. It is best visualized on a well penetrated lateral chest radiograph. The region contains lymph nodes, the thymus in children and the thymic remnant in adults, and the pericardium. Masses include: enlarged lymph nodes, thymic masses, teratomas or dermoids, and aneurysms of the ascending aorta. Often it is not possible to differentiate between these masses on radiographs however if the mass has a lobulated contour it suggests enlarged lymph nodes. Focal calcification is detected in dermoids and teratomas. Linear calcification may be detected in aortic aneurysms from syphilis or Takayasu's disease.

Middle mediastinum

This region is between the anterior and posterior mediastinum and contains the heart, great vessels, pulmonary vessels and lymph nodes. Masses in this region include: enlarged hilar and tracheobronchial lymph nodes, bronchogenic cysts, aortic arch aneurysms, and bronchial carcinomas.

Posterior mediastinum

The posterior mediastinum extends from the middle mediastinum to the spine and paraspinous gutters. It includes the descending thoracic aorta, lymph nodes, nerves and the oesophagus. Masses in this region: neurogenic tumours, paravertebral masses, tuberculous abscesses, oesophageal tumours, hiatus hernia, and dilated oesophagus. It is very important when a posterior mediastinal mass is detected to clearly visualise the spine, so as to detect early bony destruction or erosion from tuberculosis or bony metastases.

LEARNING POINTS: MEDIASTINAL MASSES

- Common superior mediastinum masses: retrosternal thyroid goitre, aneurysms of great vessels
- Common anterior mediastinum masses: 3T's teratomas or dermoids, retrosternal thyroid, thymoma and ascending aortic aneurysm
- Common middle mediastinum masses: lymphadenopathy, bronchogenic cysts, bronchial carcinoma
- Common posterior mediastinum masses: lymphadenopathy, neurogenic tumours, paraspinal abscess especially TB, oesophageal tumours

References

1. Chapman S, Nakielny R. *Aids to Radiological Differential Diagnosis*. 1995, Saunders, London.
2. Armstrong P. The Mediastinum. In: *Diagnostic Radiology—Textbook of Medical Imaging*. Grainger RG, Allison DJ. 3rd edition 1997 Churchill Livingstone, Edinburgh.

CHAPTER 16

Diaphragm lesions

Peter Corr

Diaphragmatic elevation

Eventration is a congenital deficiency of the muscle in the hemidiaphragm usually the left, resulting in non-function and resultant elevation. The diagnosis is confirmed on fluoroscopy/screening when there is limited or no movement on deep inspiration and expiration. If fluoroscopy is unavailable perform one chest film using a double exposure in inspiration and an expiration at 50% normal mas, this will show movement of the diaphragm. Eventration must be distinguished from phrenic nerve palsy.

Phrenic nerve palsy results in paralysis of diaphragmatic movement on one side resulting in elevation of the hemidiaphragm and limited or paradoxical movement on deep inspiration and expiration. There are many causes, however the commonest causes is carcinoma of the bronchus.

Subphrenic masses, liver enlargement and abscesses will elevate the hemidiaphragm. On the chest radiograph with a liver or right subphrenic abscess, the right hemidiaphragm is elevated and its outline becomes “fuzzy” or ill-defined with associated linear atelectasis in the right lower lobe. This is a very important pattern to recognise as you need to perform an ultrasound examination of the right subphrenic space and liver to detect an abscess. Pseudo elevation is seen with **subpulmonic pleural effusions** and haemothoraces. The apex of the “elevated hemidiaphragm” is usually displaced more laterally than what is normally seen. A decubitus chest film with the affected side dependent will confirm the diagnosis.

Diaphragmatic injury is commonly missed especially following penetrating trauma. Injury is nine times more common on the left. The diagnosis can be difficult to make. On the left, detection of bowel loops above the hemidiaphragm or a soft tissue mass contiguous to the diaphragm is suspicious. A contrast study of the stomach and colon will confirm the diagnosis. If there is incarcerated bowel present it will be opacified by contrast above the diaphragm.

CHAPTER 17

Pneumoconiosis

Peter Corr

Occupational dust exposure is a common cause of lung disease in many developing countries. You must always ask whether the patient has been exposed to dust at work.

Small nodules

This is the commonest occupational dust exposure pattern and results from inorganic dust exposure such as silica. The nodules are around 1–2mm size and dense compared to the granulomas of tuberculosis (fig 17.1). Hilar nodes may be enlarged and have peripheral calcification (“egg shell” calcification). A complication of silicosis is conglomeration of the nodules into large masses of fibrosis called progressive massive fibrosis (fig 17.2).

Fig 17.1
Patient with silicosis. Note dense bilateral pulmonary nodules in mid zones of the lungs.

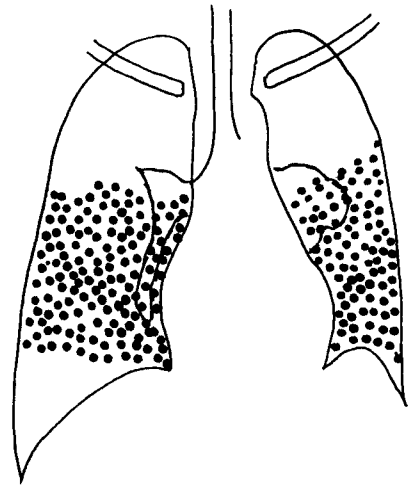
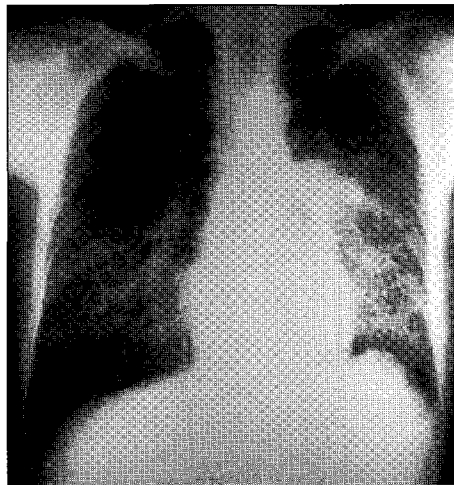
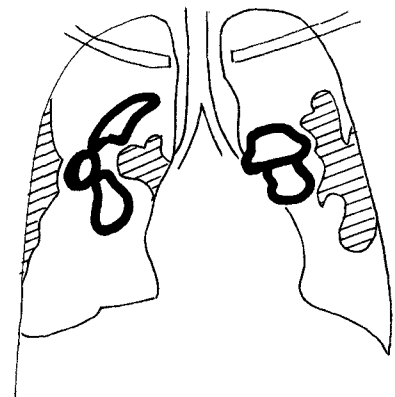
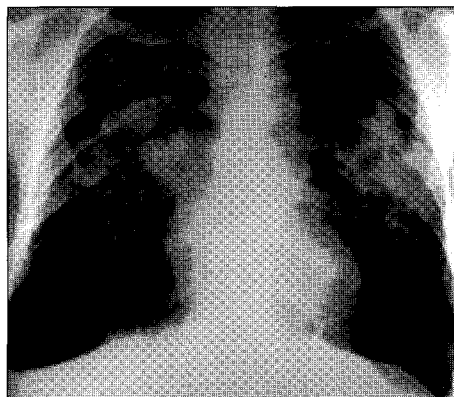


Fig 17.2
Patient with progressive massive fibrosis with bilateral perihilar masses centrally.



Asbestos exposure

The most common appearance are pleural plaques which become easier to see once they calcify giving a “holly leaf” appearance. Diaphragmatic calcification is also common. These findings indicate asbestos exposure (fig 17.3). Pulmonary asbestosis presents with a linear or reticular fibrosis of the lower lobes and represents pulmonary fibrosis from asbestos exposure. Mesothelioma is a pleural malignancy that spreads circumferentially along the pleura. The diagnosis is usually made by biopsy. The differential diagnosis is encysted pleural fluid that can be detected by using a 5 MHz ultrasound transducer on the chest wall.

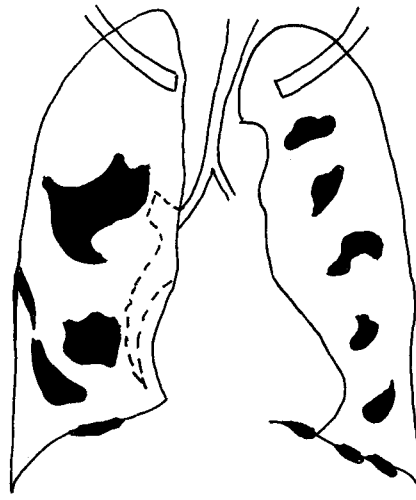
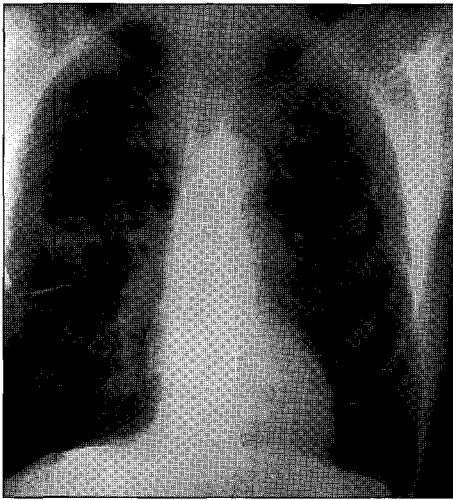


Fig 17.3
Patient with asbestos dust exposure demonstrates multiple calcified plaques on the parietal pleural surface.

LEARNING POINTS: PNEUMOCONIOSIS

- Always ask the patient about dust exposure
- Consider silicosis in the small nodular lung pattern especially when the nodules appear very white or dense
- Consider asbestosis exposure when there are calcified pleural plaques and or calcification of the diaphragm

PART 3



MUSCULOSKELETAL PATTERNS

CHAPTER 18

Approach to focal bone lesions

Fei-Ling Thoo & Wilfred C.G. Peh

Focal bone lesions can generally be divided into benign and malignant bone lesions. The malignant group can be further subclassified into primary and secondary tumours. The secondary tumours can arise from transformation of benign conditions or from metastatic lesions.

Clinical information

The patient's age and determination of whether a lesion is solitary or multiple are important approaches in the diagnosis of bone tumours. Aneurysmal bone cysts rarely occur beyond 20 years of age. Giant cell tumour usually occurs after the closure of the growth plate. Metastases tend to be multi-focal and are more common in the older age group. The rate of tumour growth may be an additional factor in differentiating malignant tumours (usually rapid growing) from benign lesions (slower growing). It is also important to know if a lesion is an incidental finding or is symptomatic. If painful, the lesion requires attention regardless of its imaging appearance. Some benign osseous tumours may undergo sarcomatous transformation and this should also be considered in a patient who presents with pain and a lesion that appears benign.

Imaging modalities

In the evaluation of bone tumours, plain radiographs are the standard imaging study. The choice of the imaging technique is dictated by the type of the suspected tumour and also by equipment available. Imaging modalities for bone tumours include bone scintigraphy, CT scan, MRI and angiography. CT is superior to MR for the detection of calcification in the tumour matrix, cortical erosions and periosteal reaction. If the radiographs suggest cortical destruction and soft tissue mass, MRI would be the preferred as it provides excellent soft tissue contrast and can determine the extraosseous extent of tumour much better than CT.

Site of the lesion

The bone tumour can be epiphyseal, metaphyseal or diaphyseal in location. There is predilection of some bone tumours for specific sites in the bone.

Skeletal predilection of benign osseous neoplasms include

Enchondroma—short tubular bones (fig. 18.1)

chondroblastoma—epiphyses

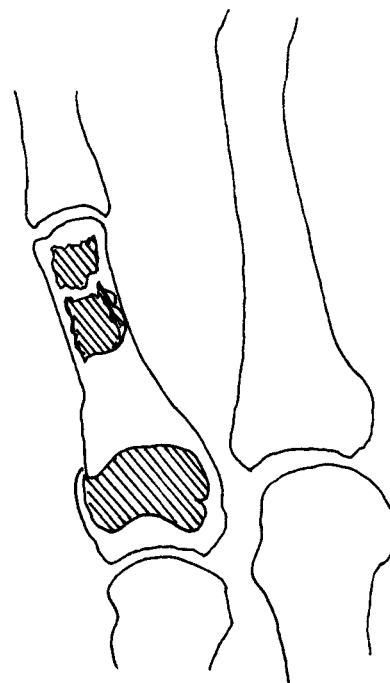
giant cell tumour—articular ends of the femur, tibia and radius chondromyxoid

fibroma—tibial metaphyses

simple bone cyst—proximal humerus and femur

osteoid osteoma—femur and tibia

Fig 18.1
Shows fracture through an enchondroma located in the proximal phalanx of the little finger. The tubular bones of the fingers are typical sites for enchondroma.



Skeletal predilections for malignant osseous tumours include

- chordoma—sacrum, clivus, C2
- multiple myeloma—pelvis, spine and skull
- parosteal osteosarcoma—posterior cortex of posterior femur
- chondrosarcoma—epiphyseal lesion of femur and humerus
- adamantinoma—tibia, fibula

Lesions that have a predilection for flat bones such as the scapula body and the iliac wing or the diaphyses of long bones include Ewing sarcoma, lymphoma and Langerhans cell histiocytosis (eosinophilic granuloma). Ewing sarcoma would be more likely in a younger age group. Lymphoma can be seen in any age but peaks later in life. Langerhans cell histiocytosis can be seen at any age.

Borders of the lesion

Slow growing lesions are usually benign and have sharply outlined sclerotic borders (narrow zone of transition). An example of a benign lesion (non ossifying fibroma) is shown in fig 18.2. Aggressive or malignant lesions typically have indistinct borders (a wide zone of transition) with either minimal or no reactive sclerosis (fig 18.3). This is seen in fig 18.4 of a child with osteogenic sarcoma. Treatment can alter the appearance of malignant bone tumours; they may exhibit sclerosis as well as a narrow zone of transition.

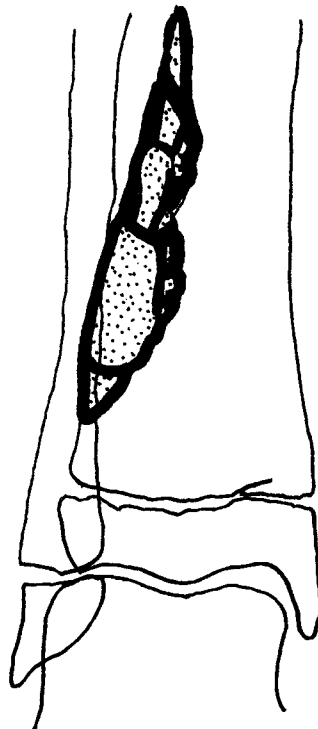
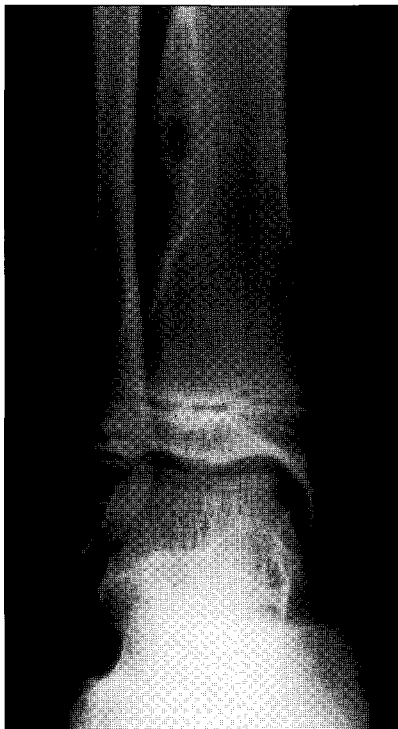


Fig 18.2
Well defined osteolytic lesion with sharply outlined sclerotic border and a narrow zone of transition in the distal right tibia due to a non-ossifying fibroma.

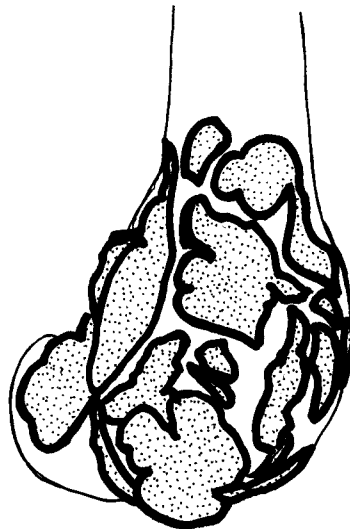
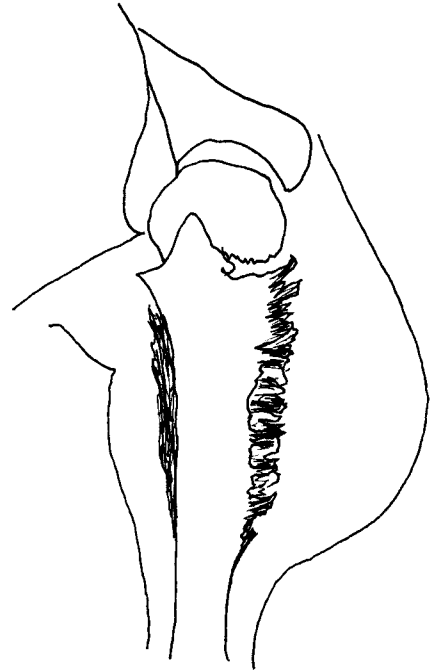
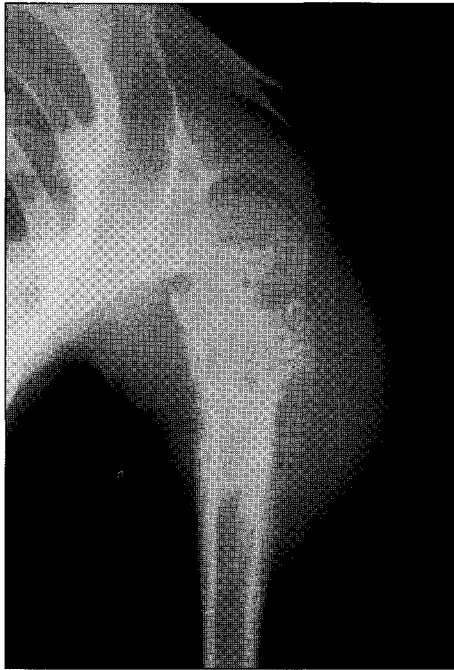


Fig 18.3
Expansive osteolytic lesion in the subarticular region of the distal femur in keeping with a giant cell tumour.

Fig 18.4
Plain radiograph of
an osteogenic
sarcoma in the
proximal left
humerus of a child.

There is an
osteolytic lesion in
the diaphyseal
region which shows
a poor zone of
transition. Adjacent
sunburst periosteal
reaction and soft
tissue mass are
present.



Type of matrix

Osteoblastic and cartilaginous matrix can be recognized radiographically. Osteogenic sarcomas can form cloud-like dense osteogenic matrix. Cartilaginous tumours can be identified by popcorn-like, punctate, annular or comma-shaped calcifications. Cartilage tumours tend to grow in lobules and can be identified by their lobulated growth (fig 18.5).

Fig 18.5
Plain radiograph
shows calcification
within the medullary
cavity from a
chondroid tumour.



Type of bone destruction

The type of bone destruction can be described as geographic, moth-eaten or permeative. A benign process tends to show a geographic—uniformly destroyed area with sharply

defined border. A likely malignant process shows moth-eaten areas of destruction with ragged borders. It should be kept in mind that non-neoplastic lesions like osteomyelitis may also appear as an aggressive destructive bone lesion with moth eaten areas. The clinical presentation, radiographic findings of cloaca and sequestrum and uninterrupted periosteal reaction would be helpful in the diagnosis of osteomyelitis. The permeative bone destruction is indicative of a more aggressive (malignant) process with ill-defined area spreading through the bone marrow. This is seen in Ewing's sarcoma and bone lymphoma.

Periosteal reaction

The type of periosteal reaction is one of the most important features in determining the aggressiveness of the bone lesion. Periosteal reactions are discussed in the next chapter.

Soft tissue extension

Benign tumours do not exhibit soft tissue extension. Few exceptions are giant cell tumours, aneurysmal bone cysts, osteoblastomas and desmoplastic fibromas. It should be kept in mind that non-neoplastic conditions such as osteomyelitis also show a soft tissue component, the involvement of the soft tissue is usually poorly defined, with obliteration of the soft tissue layers. In a malignant process, the soft tissue component is sharply defined, extending through the destroyed cortex.

If a bone lesion is associated with a large soft tissue mass, round cell tumours should be a consideration. These include metastatic neuroblastoma (seen in infancy), Ewing's sarcoma, primitive neuroectodermal tumour (paediatric patients), lymphoma (most common in adults) and plasmacytoma (seen in the middle-aged to elderly population).

Multiplicity of lesions

- i) Multiple malignant appearing lesions usually indicate metastatic disease, multiple myeloma or lymphoma.
- ii) Benign lesions with multifocal presentations include polyostotic fibrous dysplasia, multiple enchondromas, enchondromatosis, histiocytosis, haemangiomas, and Paget's disease.

Management: biopsy versus "do not touch lesions"

There are certain features of a bone lesion on a radiograph, which help distinguish between benign and malignant lesions. Benign lesions usually have well defined sclerotic borders, a geographic type of bone destruction, an uninterrupted solid periosteal reaction and no soft tissue mass. Malignant lesions have poorly defined borders with a wide zone of transition, a "moth eaten" or permeative pattern of bone destruction, an interrupted periosteal reaction of a "sun burst" or "onion skin" type and an adjacent soft tissue mass. The analysis of a lesion involves clinical and radiological information. A decision must be made whether the lesion is definitely benign and not to be biopsied ("a do not touch" lesion) but rather monitored or whether a biopsy is required.

The following is a list of "do not touch" lesions

- Tumour and tumour-like lesions
 - Fibrous cortical defect
 - Non ossifying fibroma
 - Cortical desmoid

Solitary fibrous dysplasia
 Pseudotumour of haemophilia
 Intraosseous ganglion
 Enchondroma of a short tubular bone

Non neoplastic processes
 Stress fracture
 Avulsion fracture
 Bone infarct
 Bone island
 Myositis ossificans
 Degenerative or post traumatic cysts
 Brown tumour of hyperparathyroidism
 Discogenic vertebral sclerosis

LEARNING POINTS: FOCAL BONE LESIONS

- Helpful clinical data are:
 - (a) age of the patient
 - (b) duration of symptoms and
 - (c) growth rate of the tumour
- Key radiographic features:
 - (a) site of tumour
 - (b) border of the lesion
 - (c) type of matrix
 - (d) type of bone destruction
 - (e) type of periosteal reaction
 - (f) the presence of absence of soft tissue extension
- A lesion is slow growing (likely to be benign) when it shows:
 - (a) geographic bone destruction
 - (b) sclerotic margin
 - (c) solid, uninterrupted periosteal reaction, or no periosteal response
 - (d) no soft tissue mass
- A lesion is aggressive (likely to be malignant) when it shows:
 - (a) poorly defined margins
 - (b) moth-eaten or permeative type of bone destruction
 - (c) interrupted periosteal reaction
 - (d) soft tissue mass
- A lesion is likely to represent a cartilage tumour when it shows:
 - (a) lobulation (endosteal scalloping)
 - (b) calcifications in the matrix

CHAPTER 19

Periosteal reactions

Lai-Ping Chan & Wilfred C.G. Peh

The periosteum is a thick layer of fibrous tissue that covers the surface of the bone. The periosteum has abundant neurovascular supply and the cells in the deeper layers are able to form bone. The periosteum is not normally seen on imaging but when it responds to various bony insults, the resultant periosteal reaction is seen as projections of bone arising from the bony cortex. There are several patterns of periosteal reaction, and they can be due to benign or malignant conditions. Careful perusal of the underlying bone will give important clues about the etiology of the periosteal reaction.

Patterns of periosteal reactions

Periosteal reactions can be solid or interrupted. Four types are described:

SOLID PERIOSTEAL REACTIONS

Thin undulating periosteal reaction (diagram 19A)

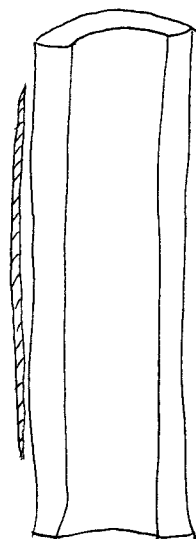


Diagram 19A

This appears as an undulating bony margin around the shafts of the bone, sparing the epiphysis. This type of periosteal reaction tends to be bilateral and symmetrical and is commonly due to systemic disease rather than a localized process. This pattern, when due to vascular insufficiency (either arterial, venous or lymphatic) is usually found in the legs with soft tissue swelling. Another cause of an undulating periosteal reaction is hypertrophic pulmonary osteoarthropathy (HPOA). In these patients, the underlying bone may appear osteoporotic. Patients with HPOA have painful swelling of the joints, especially the wrists and ankles. They may also have clubbing of the fingers. HPOA is often secondary to chronic pulmonary disease, heart disease, inflammatory bowel disease, liver disease and malignancy. It is important to do a chest X-ray to exclude thoracic causes of the disease.

Thick solid periosteal reaction (diagram 19B)

This periosteal reaction tends to merge with the cortex of the bone. The cortex of the bone can appear sclerotic and thickened. This can be due to an osteoid osteoma, a benign neoplasm of the bone. This occurs in young patients who usually present with pain. The lesion tends to occur in the long bones such as the femoral neck, the proximal tibia, fibula, and humerus. The lesion appears as a radiolucent area within the

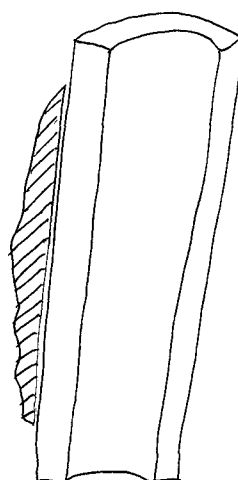


Diagram 19B

thickened bony cortex with a central sclerotic nidus (fig 19.1). A Brodie's abscess can have a similar appearance (fig 19.2). This is a subacute osteomyelitis that is most commonly due to staphylococcus aureus. The tibial metaphysis is the most common site and the lesion appears as a lucent area surrounded by dense sclerosis. The bony cortex may be thickened. The lesion can be cortical or intra-medullary in location. A Brodie's abscess can be differentiated from an osteoid osteoma if a sinus track or channel can be detected.

Fig 19.1
Osteoid osteoma of the shaft of the tibia with a thick solid periosteal reaction and thickened cortex. Note the small radiolucent nidus.

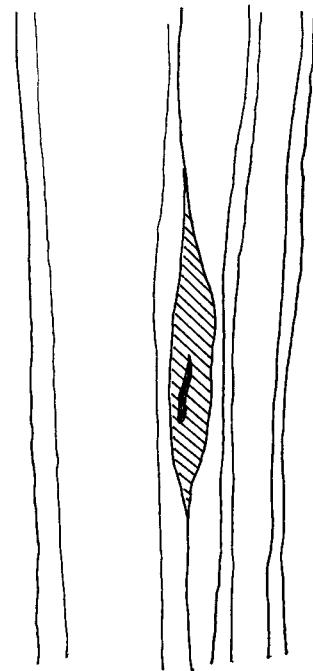
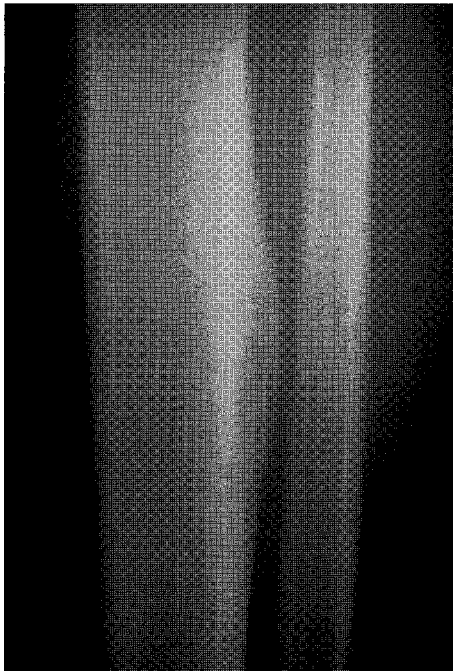
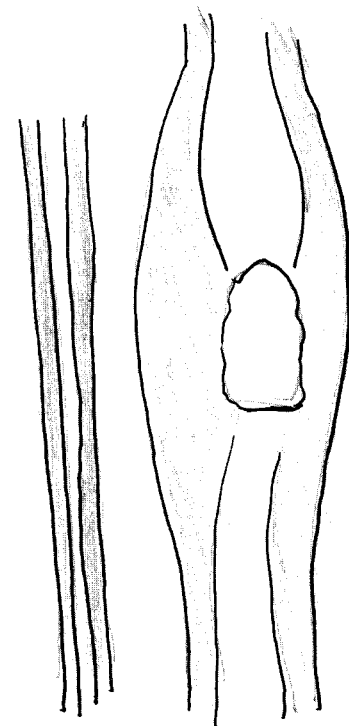
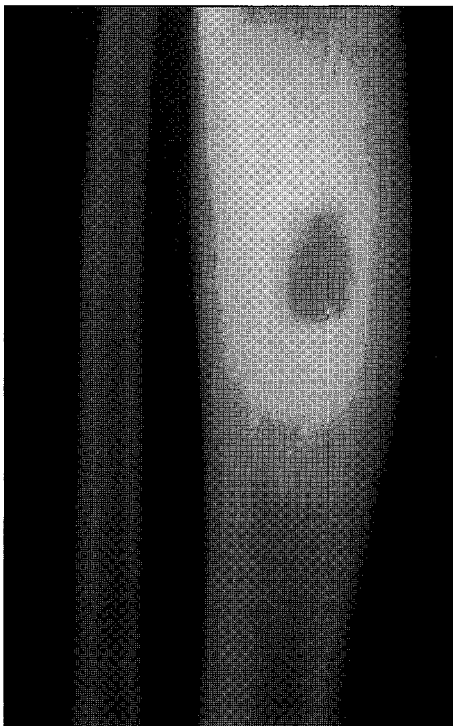


Fig 19.2
Brodie's abscess of the proximal tibia demonstrates a thick periosteal reaction with surrounding sclerosis.



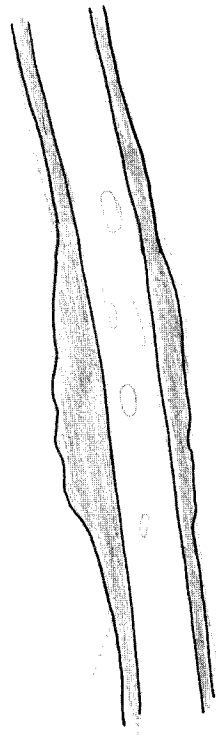
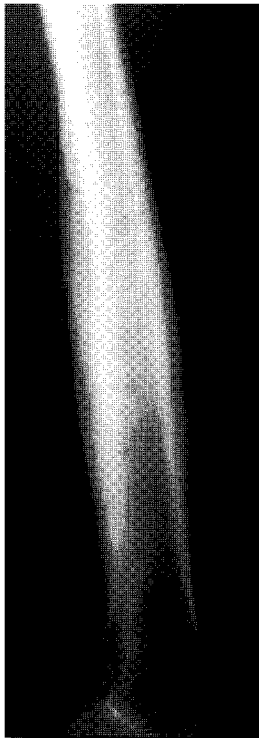


Fig 19.3
Chronic osteomyelitis of the humerus demonstrates marked cortical thickening with a thick periosteal reaction.

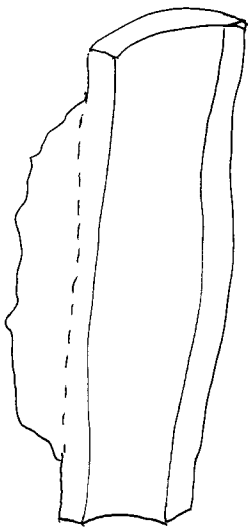


Diagram 19C

Cloaking periosteal reaction (diagram 19C)

This type of periosteal reaction is very abundant and covers almost the entire bone. If it occurs in a single bone, this is usually due to chronic osteomyelitis. There is usually associated thickening and sclerosis of the underlying bone (fig 19.3). There may be underlying radiolucent areas present due to involuted bone and also dead detached cortical bone, which appears very dense (sequestrum). There is often underlying bone destruction and new bone formation. There may be soft tissue swelling present. A sinus track leading to the skin may be present within the soft tissue. If this type of periosteal reaction occurs in multiple bones in young infants, the diagnosis can be congenital syphilis whose hallmark is a bilateral symmetrical osteomyelitis involving multiple bones (fig 19.4). The underlying bone

will show evidence of bony destruction in the metaphysis, which appears as lucent bands adjacent to a widened epiphyseal plate. The metaphysis may also appear frayed. Bilateral and symmetrical focal bone destruction in the medial aspects of the proximal tibial metaphyses is known as Wimberger’s sign and is almost pathognomonic of congenital syphilis.

Lamellated periosteal reaction (diagram 19D)

In this pattern, the periosteum has an appearance like an “onion skin” with many layers around the shaft of the bone. This can

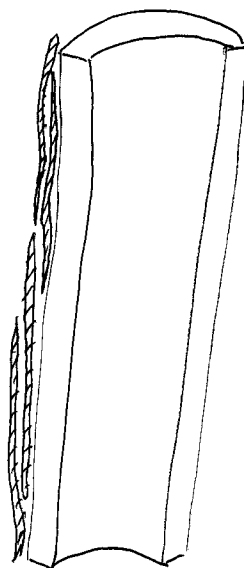


Diagram 19D

Fig 19.4
Cloaking periosteal reaction along the shaft of the tibia in keeping with congenital syphilis.

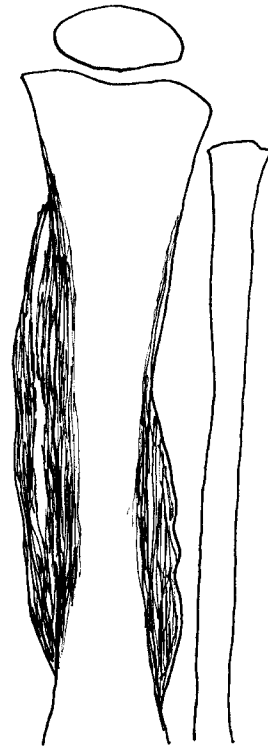
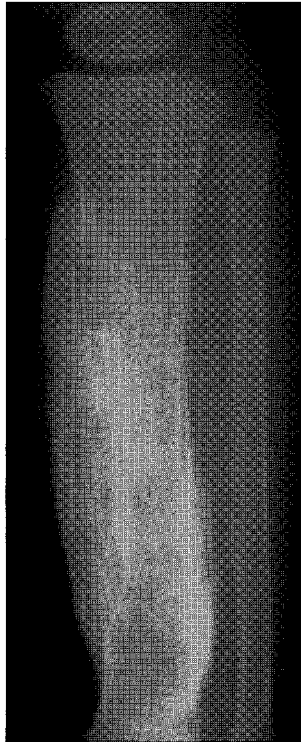
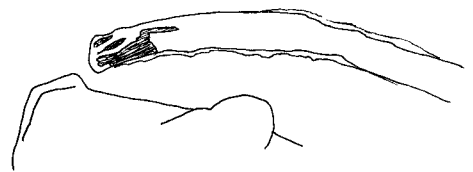


Fig 19.5
"Onion skin" periosteal reaction in Ewing's sarcoma of the clavicle.



be due to tumours such as osteosarcoma and Ewing's sarcoma (fig 19.5), or chronic osteomyelitis.

In children, rickets can also give this appearance as uncalcified subperiosteal osteoid separates the periosteum and the ossified cortex of the bone. The underlying bone appears poorly mineralised and there may be deformities such as bowing. The epiphyseal appears widened due to an abundance of unossified osteoid and there may be cupping and fraying of the metaphysis. In scurvy, subperiosteal haemorrhages can occur and during healing, the periosteum can calcify, giving the appearance of lamellae around the bone (fig 19.6).

INTERRUPTED PERIOSTEAL REACTIONS

Four types are discussed:

"Hair-on-end" periosteal reaction (diagram 19E)

These appear as straight projections of bone that are parallel to the bony cortex, like hairs standing on-end.

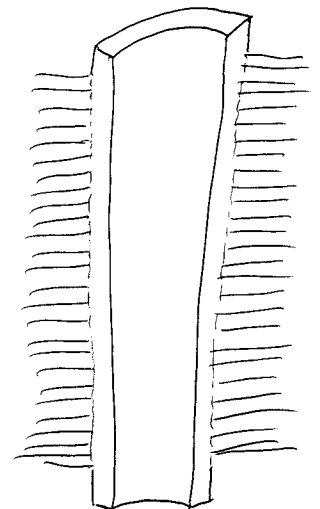


Diagram 19E

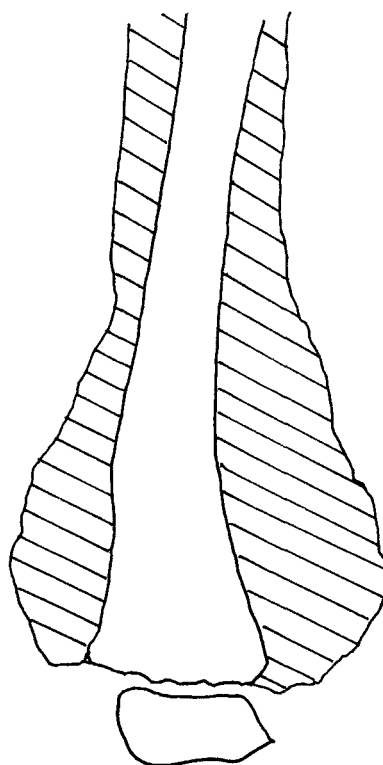


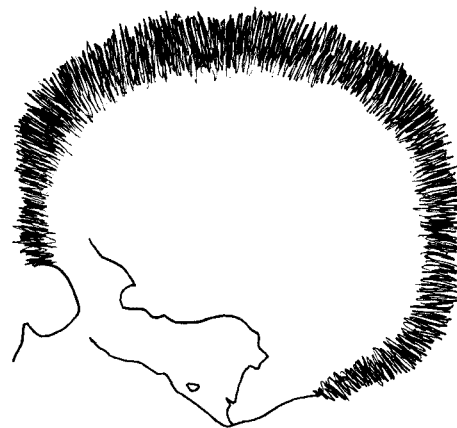
Fig 19.6
Large calcified
subperiosteal
haematoma around
the distal femur in
a patient with
scurvy.

This is usually due to an aggressive process such as a bone tumour or acute osteomyelitis. Ewing's sarcoma is a tumour that typically causes this appearance. There is usually associated destruction of the bony cortex. Ewing's sarcoma occurs in the young, with most cases occurring in patients less than 20 years of age. The long bones are affected in 60% of patients and the flat bones in the other 40%. This tumour tends to involve the diaphysis and there are mottled "moth-eaten" destructive changes in the underlying bone. There may also be soft tissue swelling but unlike osteomyelitis, the soft tissue planes are usually preserved. The radiographic changes of acute osteomyelitis begin usually after a few days (initial radiographs tend to be normal). There is soft tissue swelling adjacent to the bone and the fat planes are obliterated. There may be elevation of the periosteum associated with the periosteal reaction (especially in children). The underlying bone will show destructive changes. In children, the common site to be affected is the bony metaphysis. As the disease progresses, involucrum and sequestrum can develop. Growth disturbances to the bone may occur, either shortening of the bone due to epiphyseal destruction or premature maturation of the epiphysis due to hyperemia. A "hair-on end" appearance can also be seen in the skull vault (sparing the occipital bone) and this is usually due to chronic haemolytic anaemias such as sickle cell anaemia and thalassaemia (fig 19.7). In these patients, the bone marrow expansion within the skull causes this appearance.

"Sunray" periosteal reaction (diagram 19F)

In this pattern, spicules of bone radiate from the bone in a divergent manner, just like the rays of the sun (fig 19.8). This type of periosteal reaction typically occurs in osteosarcoma. This common malignant primary bone tumour has a peak age of involvement from 10 to 25 years of age, and another peak after 60 years. The tumour tends to involve the metadiaphyseal region of long bones and is especially common around the knee. The tumour can be seen usually expanding and destroying the

Fig 19.7
 "Hair on end"
 periosteal reaction
 of the skull in a
 child with
 thalassemia major.



underlying bone. At the margins of the lesion, periosteum is lifted up by the tumour and this elevation is termed a "Codman's triangle". There is usually a soft tissue mass and abnormal tumourous new bone formation is a prominent feature. A pathological fracture may also be present. Codman's triangle is not pathognomonic of osteosarcoma, and can occur in any condition that elevates the periosteum. At the periphery of the lesion, the elevated periosteum calcifies, forming a triangle with the cortex of the bone. Though not specific, Codman's triangle does tend to occur in more aggressive lesions such as tumour or infection. Bony metastases, especially those from colonic tumours, can also cause a sunray periosteal reaction.

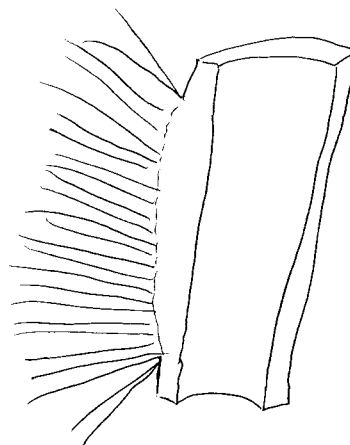


Diagram 19F

Interrupted amorphous periosteal reaction (diagram 19G)

This type of periosteal reaction is discontinuous and appears irregular. It is usually a result of reaction to a localised process. A healing fracture is a common cause of this pattern and careful study of the underlying bone will show a fracture line. There may also be thickening of the cortex of the bone. In some instances, the periosteal reaction is due to stress fracture and common sites being the postero-medial cortex of the proximal tibia and in the 2nd metatarsal. There is usually associated cortical thickening (fig 19.9).

This pattern of periosteal reaction can sometimes be seen in early acute osteomyelitis and there will be associated destructive lytic changes in the adjacent bone. At later stages, the periosteal reaction may become more lamellar in appearance and extend parallel to the shaft of the bone (fig 19.10).

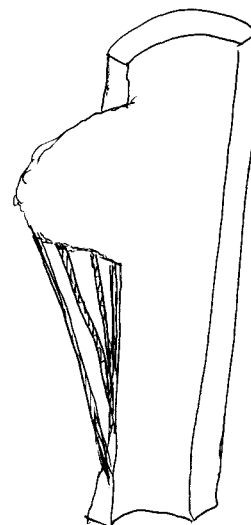


Diagram 19G

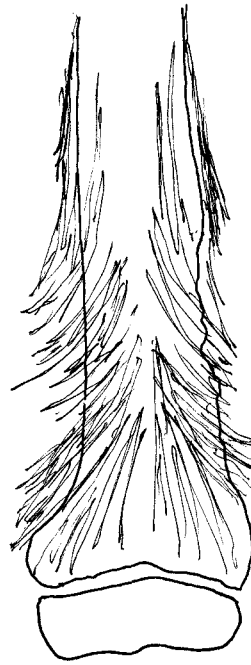
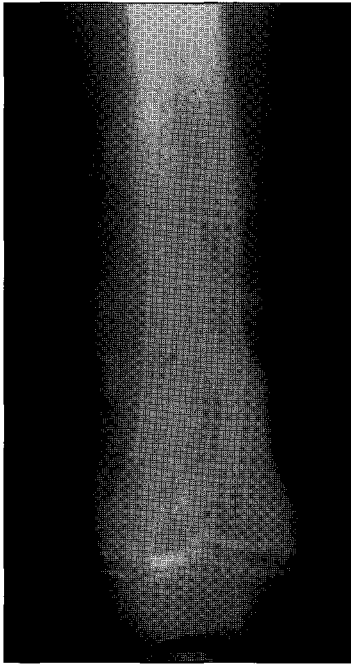


Fig 19.8
"Sun burst"
periosteal reaction
due to
osteosarcoma of
the distal femoral
metaphysis.

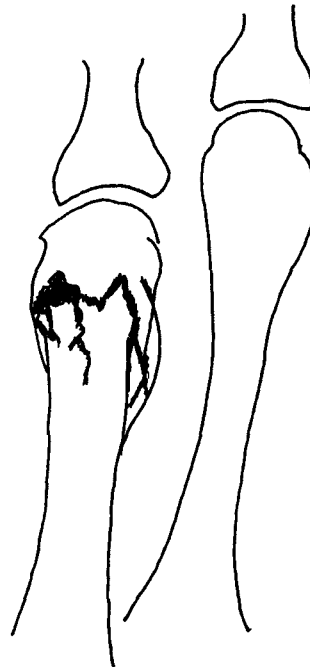
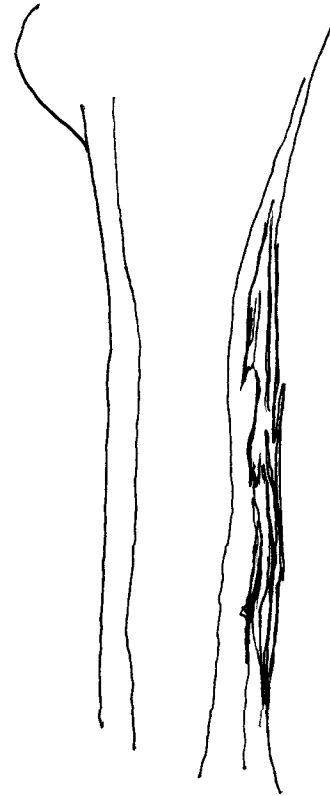
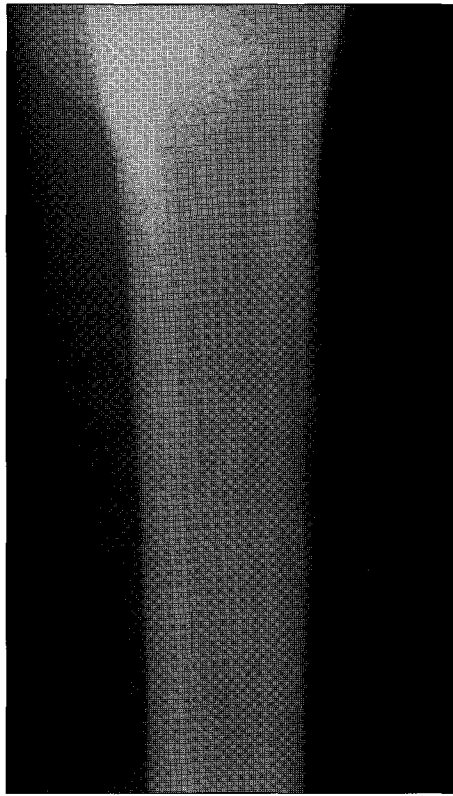


Fig 19.9
*Healing fracture of
the 2nd metatarsal
with surrounding
callus.*

Fig 19.10
 Patient with acute
 osteomyelitis of the
 proximal femur
 demonstrates a
 fluffy irregular
 periosteal reaction.



LEARNING POINTS: PERIOSTEAL REACTIONS

- Periosteal reactions are result of bone reacting to various insults. The same disease may produce several patterns of periosteal reaction.
- An aggressive lesion will usually be associated with destruction of the adjacent bone.
- Bilateral periosteal reactions are usually due to systemic diseases or syndromes.
- Obliteration of the soft tissue planes tends to favour an infective process.
- Looking at the underlying bone for an expansile mass, destruction, bone mineralisation and fracture will give important clues for diagnosis

CHAPTER 20

Extremities trauma

Siew-Kune Wong & Wilfred C.G. Peh

Introduction

Importance of radiographs

The primary aim is to diagnose the presence of a fracture or dislocation. It is also important to assess the position of the bone ends before and after treatment. Follow-up radiographs are subsequently needed for bony union and complications.

Principles of radiographic examination

- It is essential to take radiographs in at least 2 planes, preferably at right angles to each other. This will ensure that a fracture will not be missed and the bony alignment can be accurately assessed.
- The joint above and below the fracture should be included in the radiograph. This is to assess for associated dislocation especially in paired bones such as those in the forearm and leg.
- Due to bone resorption, a fracture line will become more visible about 2 weeks after an injury. Callus formation may also be present. Hence serial examinations may be required if a fracture is clinically suspected but is not visible immediately after injury (fig 20.1).

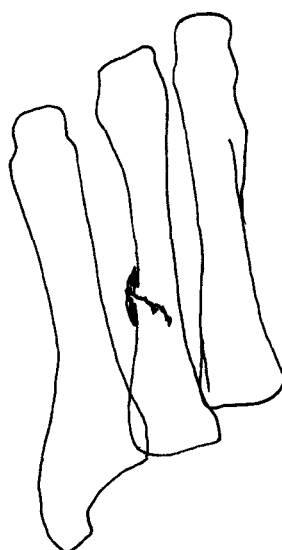


Fig 20.1
Callus formation is seen around a stress fracture of the 4th metatarsal bone.

- d. Comparison views of the opposite limb may be required in the immature skeleton before epiphyseal closure. This will help to confirm if a bony fragment is an accessory ossicle, unfused ossified epiphysis, or a fracture.
- e. Stress views are useful to assess for ligamentous injury, especially to the ankle and knees. These views help to accentuate the abnormal widening of the joint space associated with laxity or injury to the supporting ligaments (figs 20.2a & 20.2b).

Fig 20.2
Neutral (a) and
inversion (b) views
of the ankle
demonstrate a
lateral ligament
injury.

